ESCUELA TÉCNICA SUPERIOR DE INGENIERÍA DE TELECOMUNICACIÓN

Análisis y diseño de multiplexores espaciales cuasi-ópticos basados en antenas en tecnología SIW (Substrate Integrate Waveguide)

Autor: Salvador Mercader Pellicer
Director: José Luis Gómez Tornero, Ph.D.
Co-director: Alejandro Javier Martínez Ros

September 23, 2013

RESUMEN

Planteamiento inicial del proyecto:

- Usar las mejoras en calidad de ciertos parámetros, precio y peso que introduce la tecnología SIW en la construcción de un dispositivo real como es un multiplexor espacial.
- Familiarizarse con antenas construidas en tecnología SIW y multiplexores espaciales para unir estos dos conceptos.
- Elección de la antena que será usada en el desarrollo del proyecto.

Objetivos del proyecto:

- Conocer a fondo una tecnología puntera para diseño de antenas y dispositivos para circuitos de microondas como es la tecnología SIW.
- Conocer y adquirir destreza en el uso de un simulador comercial de estructuras electromagnéticas como es HFSS.
- Diseñar un prototipo final de un multiplexor espacial cuasi-óptico basado en tecnología SIW.

Fases del proyecto:

(1) Puesta a punto en los conocimientos de la tecnología SIW y del simulador HFSS.

(2) Definición de la antena en tecnología SIW a usar en el proyecto así como la ubicación de sus focos.

(3) Diseño de los puertos de salida del multiplexor, usando paredes PEC para una mayor sencillez en el diseño.

(4) Diseño de los puertos reales de entrada/salida en tecnología microstrip.

(5) Sustitución de las paredes PEC por cilindros periódicos y comprobación de semejanza de resultados.

(6) Introducción de pérdidas en la simulación.

(7) Estratificación en capas del dispositivo.

Los puntos (1) y (2) corresponderían a los capítulos del proyecto 1, 2 y 3. Hay infinidad de multiplexores diseñados en múltiples tecnologías, como los OMUX en banda Ku, usados en comunicaciones por satélite. Respecto a estos, se lleva ya tiempo buscando tecnologías alternativas para diseño de multiplexores que palien

desventajas de estos, como las pérdidas producidas a altas frecuencias debido a las resonancias que tienen lugar en estas cavidades. Desde hace años se están investigando multiplexores en otras tecnologías, como rejillas periódicas en líneas de transmisión hiperbólicas, metamateriales o prismas eléctricos, que en parte mejoran las cualidades de los multiplexores usados hasta ahora. Sin embargo, uno de los puntos flacos de todas estas tecnologías es la complejidad de estas.

En este proyecto queremos introducir una tecnología nueva, que está siendo usada cada vez con más frecuencia en el mercado, como son las guías-onda integradas en substrato (SIW), para el diseño de un nuevo multiplexor.

La tecnología SIW introduce numerosas ventajas respecto a las tecnologías hasta ahora mencionadas, como un alto factor Q, alta capacidad de pontencia, bajo coste, bajo peso o producción en masa. Una SIW rectangular típica está formada por dos líneas de postes de diámetro d, con una separación P entre postes. Ambos parámetros deben ser tales que no haya escape de energía. La energía se transmite por la cavidad formada por ambos postes.

Dentro de estas guías podemos distinguir las Leaky-Wave Antennas (LWA). En estos dispositivos se modifica el principio de no dejar escapar energía para conseguir precisamente el efecto contrario en una de las líneas de postes, y conseguir así una antena radiando un modo llamado "de fuga" que normalmente suele ser el fundamental, TE_{01}. Jugando con los diferentes parámetros de la antena se pueden conseguir diferentes funciones de distribución, así como en función de la frecuencia, enfocar la energía a un foco concreto. Este concepto se denomida focusing, y es el tipo de propiedad que queremos para nuestro multiplexor. La siguiente imagen muestra el diseÃśo de antena buscado:

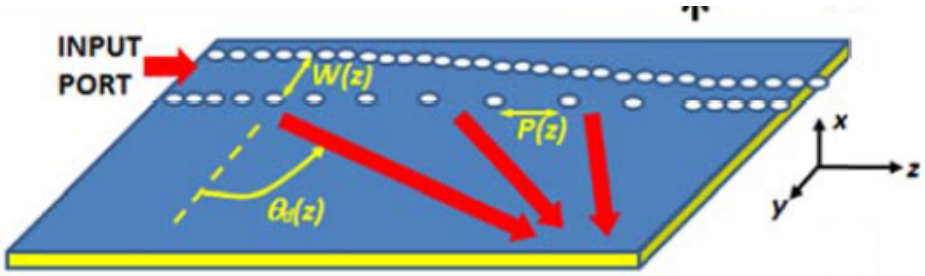

Donde *W(z)* es la anchura de la antena en función del eje z, *P(z)* es la mencionada separación entre postes pero en función del eje z, y $\Theta_d(z)$ es el ángulo de inclinación del haz respecto de la perpendicular a la antena.

La antena resultante es la proporcionada por los directores del proyecto, en la que se ha decido trabajar con frecuencias iguales o mayores que 11GHz, ya que por debajo el foco queda pobremente definido debido a que la antena está radiando en su dirección broadside. Por otro lado, se ha decidido como frecuencia mayor 15GHz, ya que por encima el foco comienza a estar un poco lejos y a quedar por tanto más débil, además de que estas frecuencias se encuentran muy juntas para este diseño y

por tanto sería complicado emplazar puertos reales:

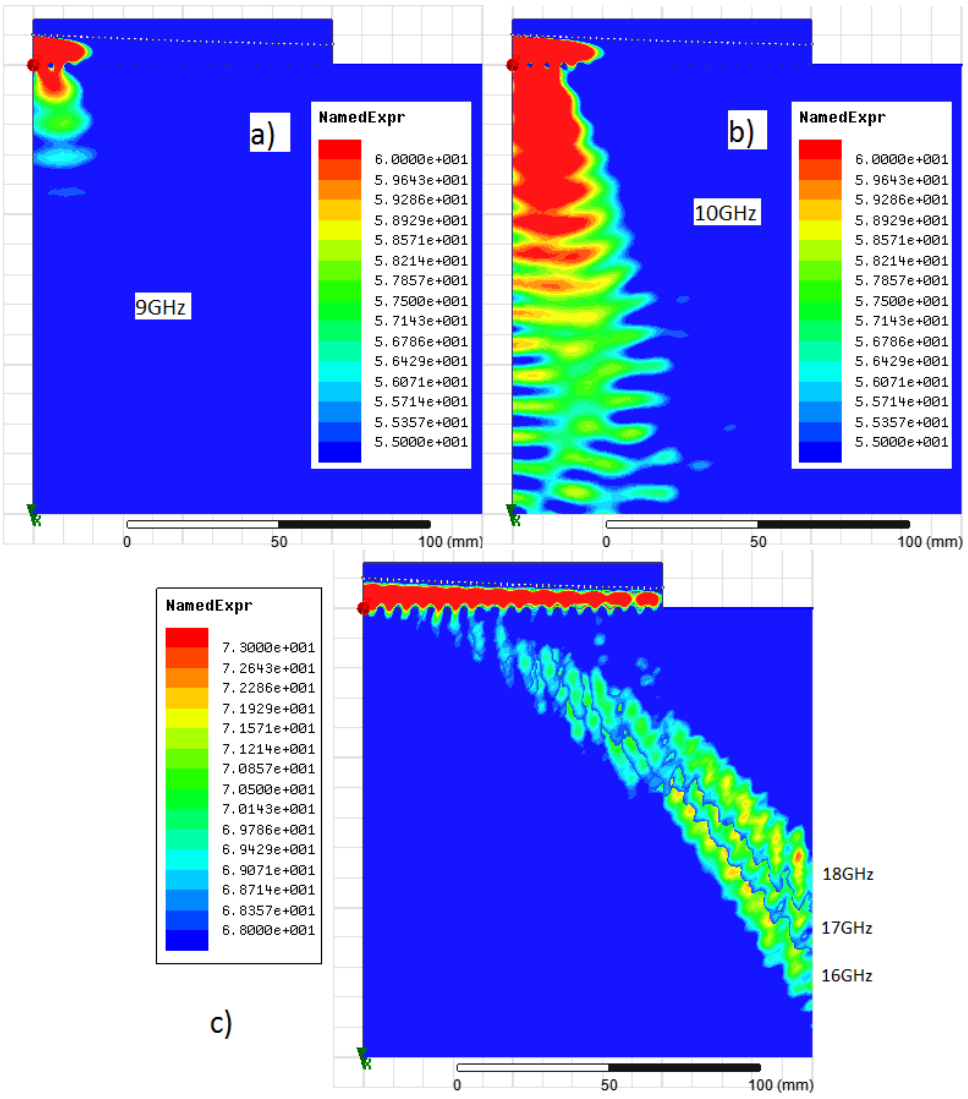

Por esta misma razón del emplazamiento de puertos se decide trabajar con 5 frecuencias: 11GHz, 12GHz, 13GHz, 14GHz y 15GHz. En cuanto a la elección de la función de distribución se decide trabajar con la uniforme ya que consigue minimizar respecto a la de seno y seno^2 el nivel de lóbulos secundarios y la anchura del foco. En cuanto a la altura se decide trabajar con una altura de 1.57mm.

Los parámetros con los que definimos un foco concreto son 3: la posición del foco (Y_F,X_F), el ángulo de inclinación del foco respecto del eje X α, y el ancho a 5dB del foco ΔW_{5dB}:

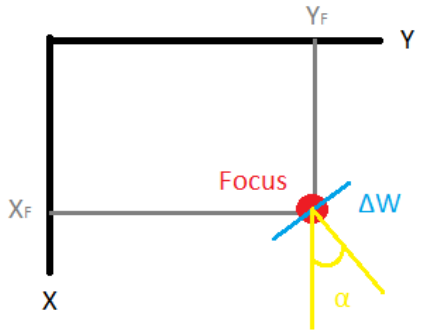

Los valores de la antena para estos parámetros quedan resumidos en la siguiente tabla:

f(GHz)	Y_F (mm)	X_F (mm)	ΔW_{5dB} (mm)	α(deg)
11	19	13	18.25	8.75
12	38	26	13.35	15.07
13	61	50	15.53	18.78
14	81	58	15.24	24.14
15	106	78	16.13	30.53

Como primer diseño para los puertos de salida (3) se pensó en cables coaxiales 4, en 2 configuraciones: posicionados en el foco de cada frecuencia o a lo largo de una línea paralela al eje transversal de la antena (eje y a lo largo del proyecto), situada a 60mm. Los diseños quedan:

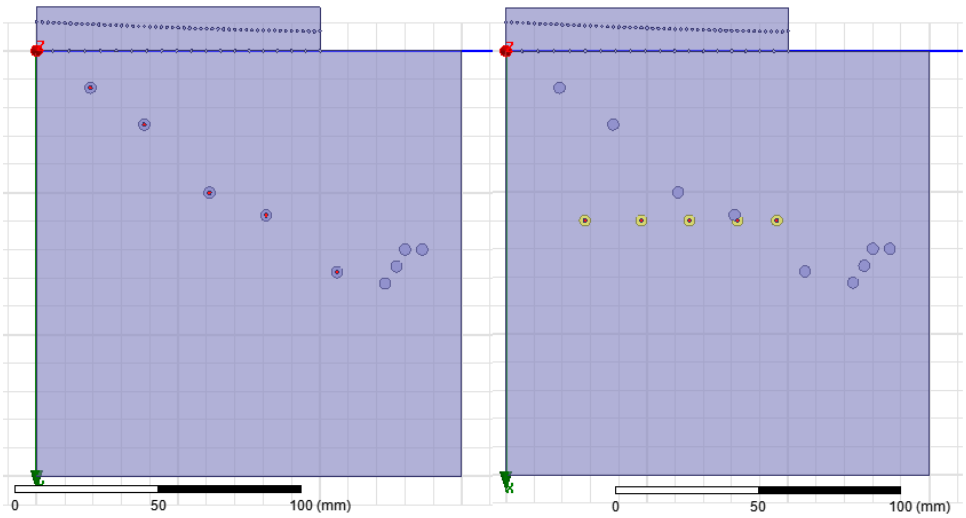

En las paredes se añaden condiciones de PML para que la energía sobrante sea

abosrvida en su mayor parte. Como comprobación de resultados se representan los parámetros S de ambas estructuras:

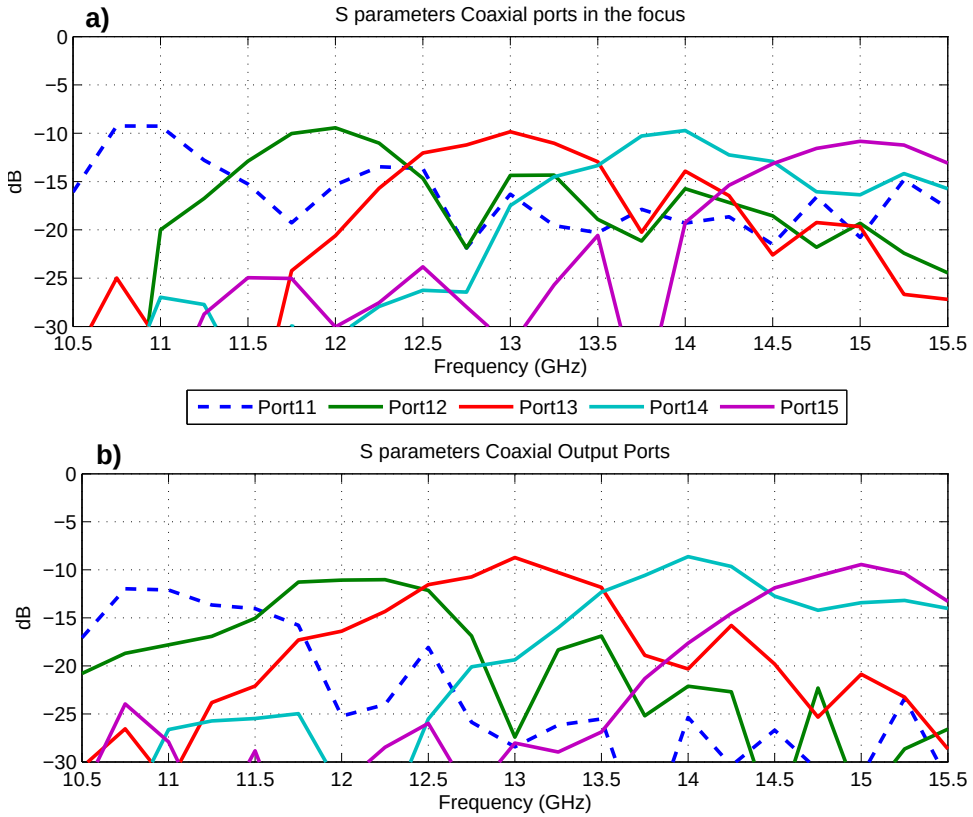

Primer punto importante: la idea buscada funciona. Para cada frecuencia se tiene un canal bien definido, pero con anchos de banda grandes y con niveles bajos. Entre ambas representaciones se aprecia que para frecuencias bajas (11GHz y 12GHz) se obtienen niveles superiores para el caso del emplazamiento en cada foco (a)), mientras que para el resto no ocurre así, sino que el emplazamiento en la misma línea obtiene mejores resultados, a pesar de estar estos puertos más lejos de sus respectivos focos. Esto debe ser debido a la sombra creada por los puertos que se sitúan más cerca de la antena. No se realizaron más pruebas con coaxiales ya que se prefirió trabajar con puertos SIW-microstrip.

Otro diseño probado fue usar puertos SIW alineados en la misma línea a 60mm. Se probaron 3 diseños 5: puertos pared con pared, con anchura de puertos para conseguir 1GHz de ancho de banda, y con anchura para conseguir 0.5GHz:

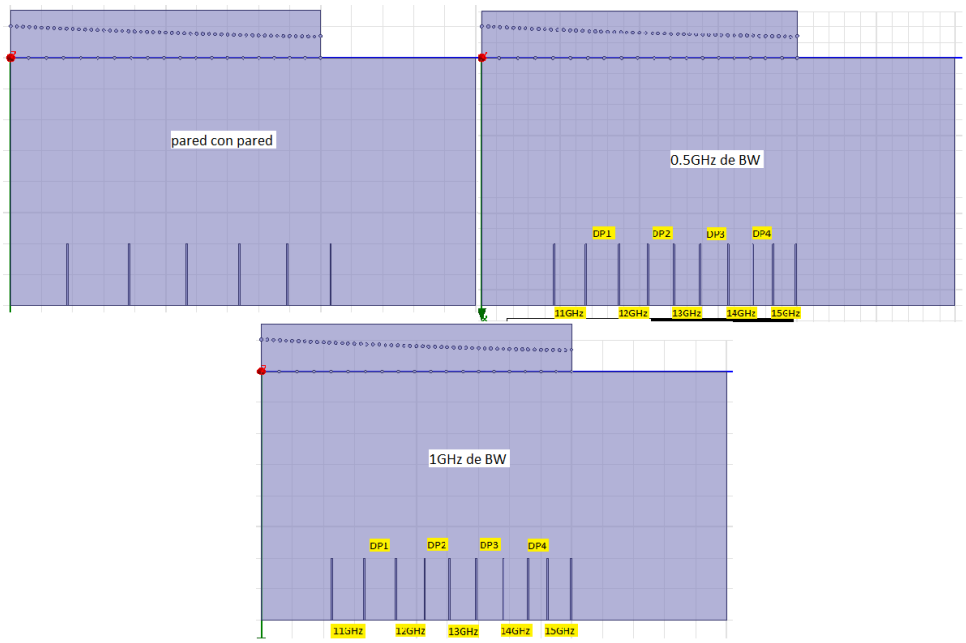

Los DP son los llamados Dummy Ports, y son puertos que sólo sirven para captar la energía sobrante, ya que de otra forma la energía que los puertos no son capaces de captar quedaría sufriendo reflexiones por el substrato sin control. Los parámetros S quedan:

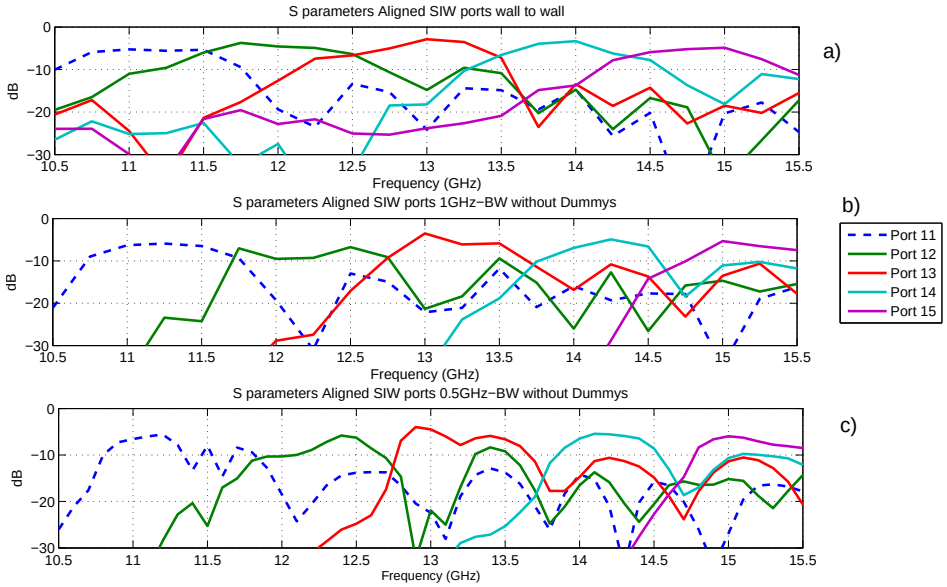

Se consigue el resultado esperado: se van obteniendo anchos de banda más pe-

queños. Aún así, hay que intentar conseguir niveles superiores. Y para ello, vamos a cambiar de diseño para intentar emplazar los puertos lo más cerca posible de sus respectivos focos 6.

Antes de comenzar el diseño hay que tener claro al igual que antes los parámetros de diseño de los puertos: el ángulo α(mismo de antes), anchura de entrada del puerto WINPUT, longitud del puerto LOUTPUT, anchura de salida del puerto WOUTPUT y distancia del puerto al foco SF:

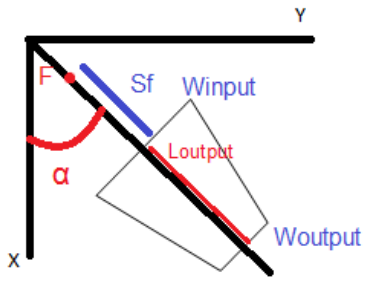

Después de algunos cambios en algunos parámetros podemos resumir los parámetros útiles de la estructura en la siguiente tabla, además de ver en la siguiente imagen cómo queda la estructura:

Port	ΔW_{5dB} (mm)	WINPUT (mm)	LOUTPUT (mm)	WOUTPUT (mm)	SF (mm)
11	18.25	17	18.39	13.61	21.29
12	13.35	20.13	16.85	12.49	21.036
13	15.53	17.62	15.56	11.53	8.96
14	15.24	17.8	14.45	10.72	13.108
15	16.13	18.28	13.5	10.01	-3.2

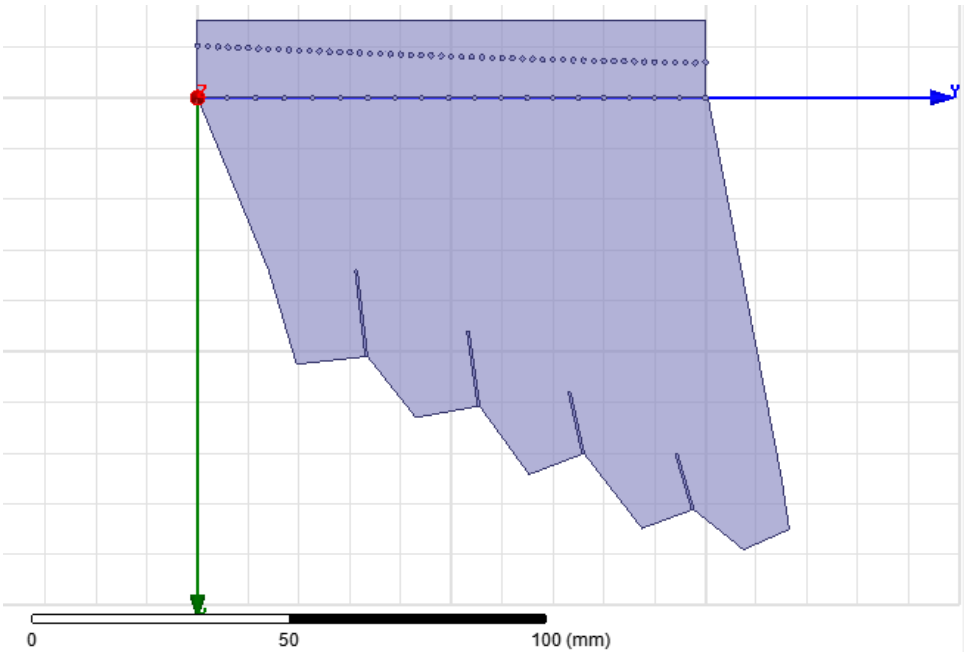

La siguiente figura muestra los parámetros S. Se observan las mejoras, tanto en los niveles superiores a -5dB, como en los anchos de banda, más estrechos y mejor definidos.

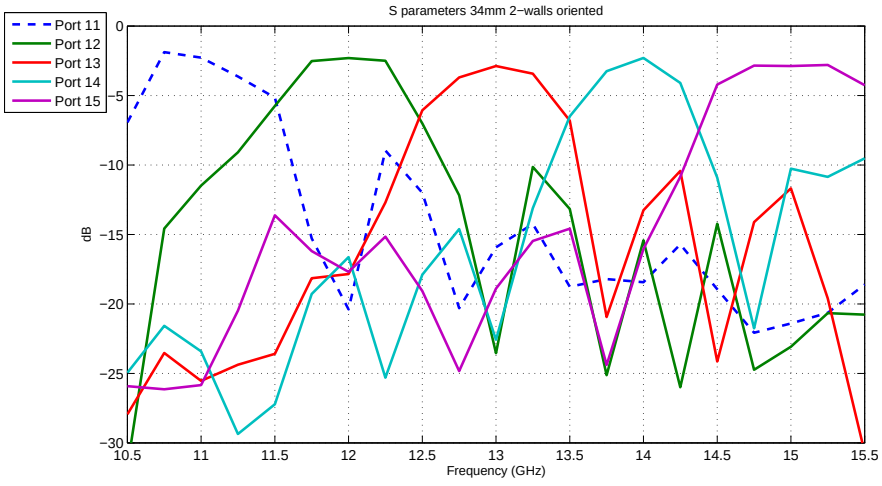

El siguiente paso es sustituir los PMLs por Dummy Ports para tener una forma real de absorción de energía sobrante. En las dos siguientes figuras podemos ver el diseño, así como los parámetros S:

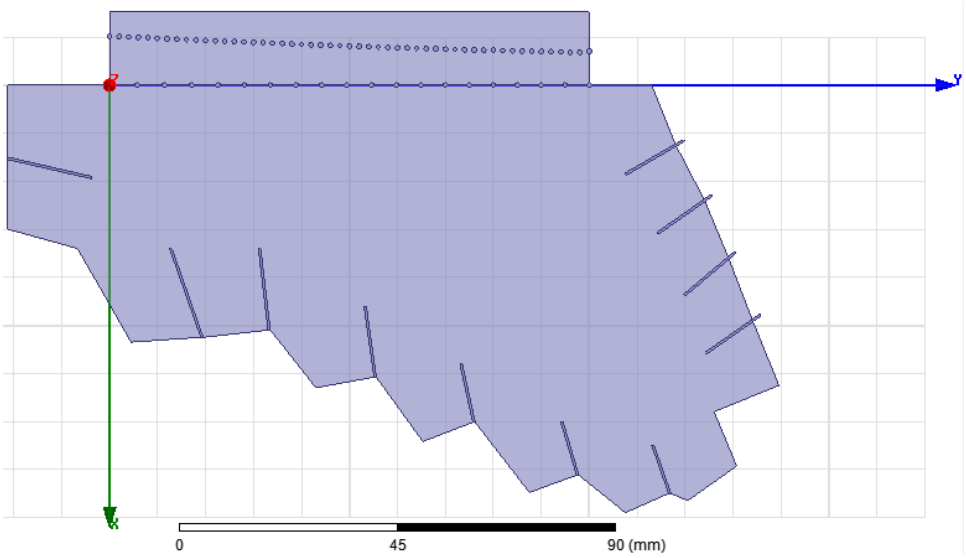

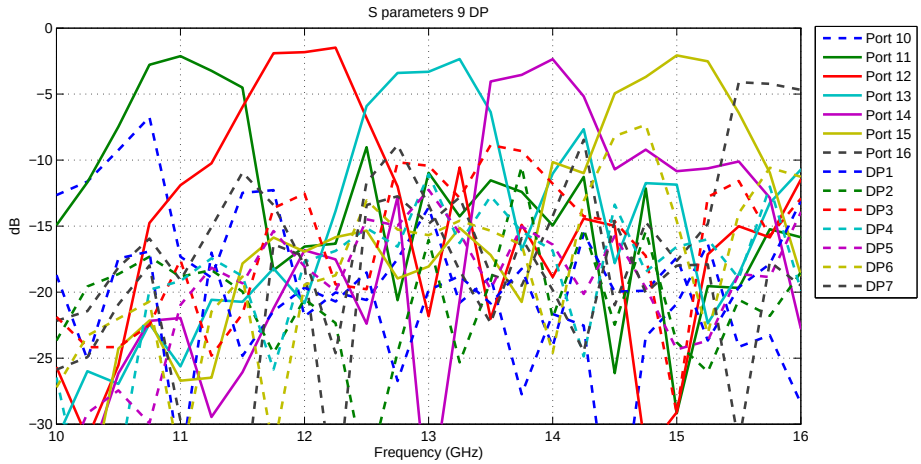

Hemos conseguido tener unos resultados bastante parecidos al caso con PMLs. Llegados a este punto se puede afirmar que hemos acabado el diseño del multiplexor en sí. El siguiente paso es diseñar los puertos microstrip (4) 7 para seguir avanzando hacia un modelo real, usando el software TXLINE para las anchuras de la línea microstrip w_0, y un barrido paramétrico para la anchura y la longitud w y l para el taper. La longitud de la línea microstrip l_u queda fijada a 5mm para que coja el conector. Y por último, para evitar que la anchura de salida w_0 sea mayor que un cuarto de la longitud de onda (frecuencia de diseño escogida: 15Ghz, por ser la menor longitud de onda), se ha modificado la altura de la estructura de 1.57mm a 0.787mm. Valores resumidos:

- w = 6mm.
- wo = 2.4415mm.
- l = 11mm.
- lu = 5mm.
- h = 0.787mm.

Terminado este punto queda substituir las paredes PEC por via-holes (5) 8 para tener toda la estructura en tecnología SIW. Y tras esto, introducir pérdidas (6) 9 para tener el máximo parecido a un modelo real. Por último, queda separar la estructura en capas (7) 10 para una clara diferenciación, así como para tener la estructura lista para ser fabricada. Las siguientes figuras muestran, por orden, la estructura final (el substrato resaltado para que se aprecien los via-holes, y la estructura entera vista desde arriba), los parámetros S y los campos representados para cada frecuencia:

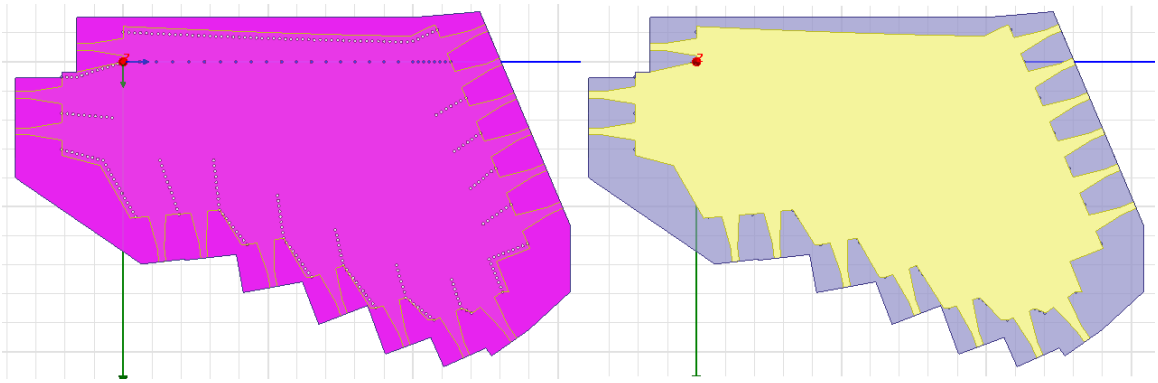

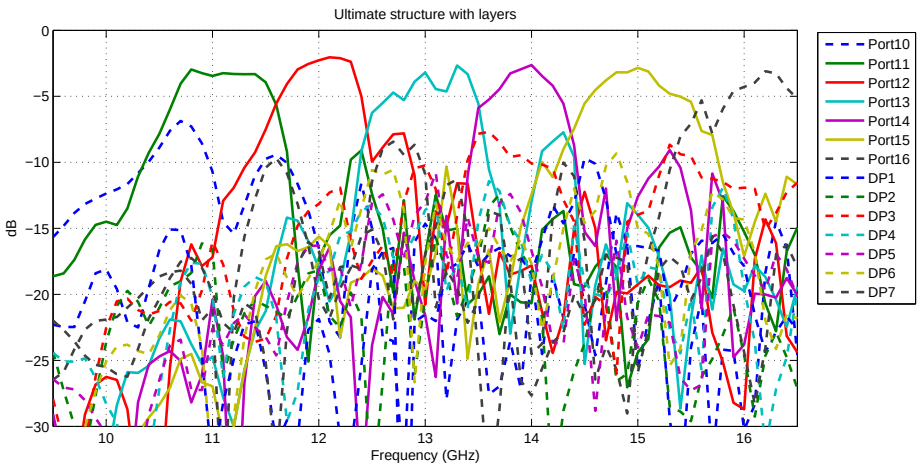

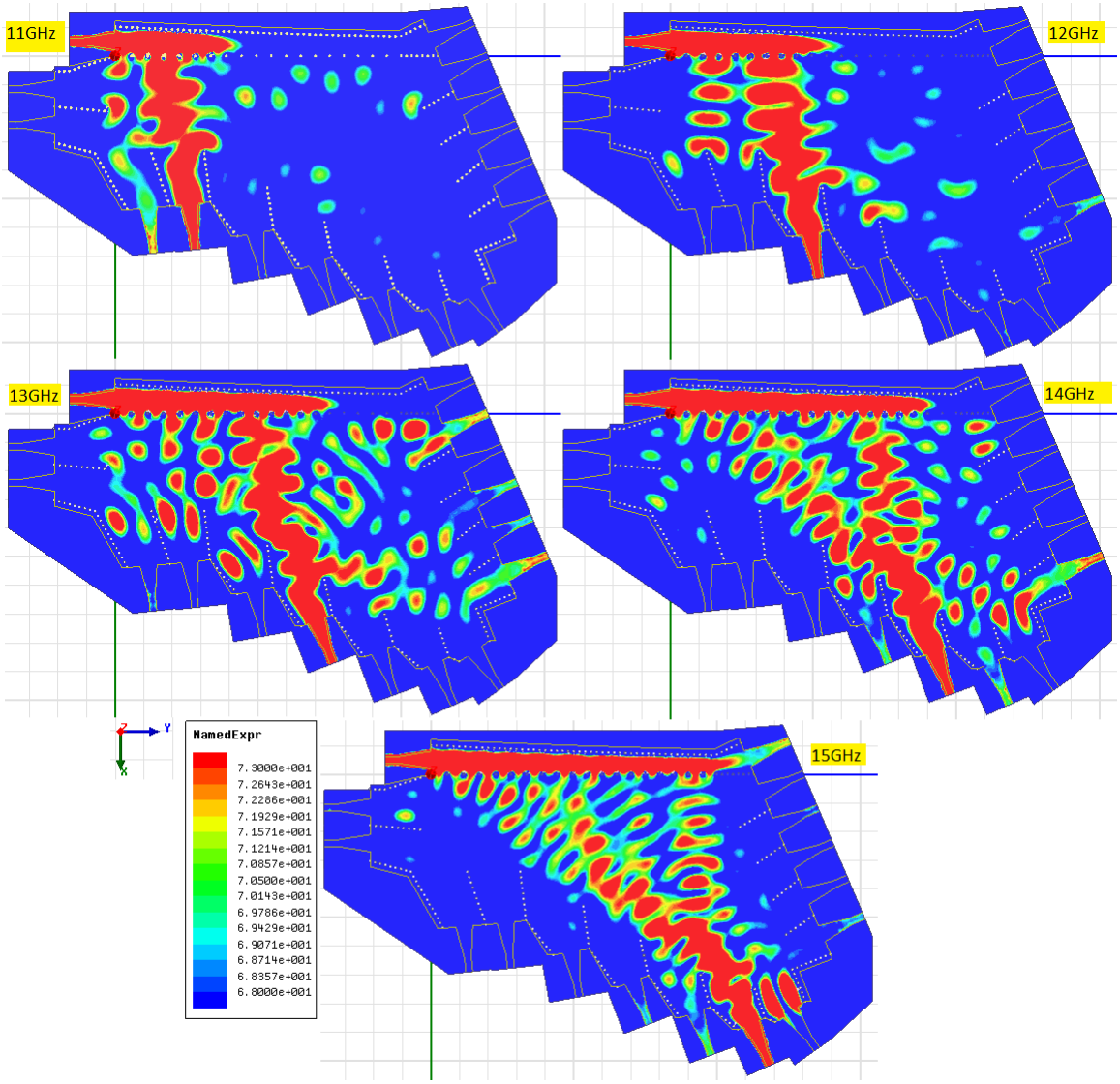

Ya hemos llegado a una estructura final lista para fabricar. Hay puntos mejorables, que son discutidos en el punto de línas futuras 11, como conseguir más puertos de salida, o disminuir el ancho de banda. Estas mejoras se podrían conseguir con el estudio del ancho a 5dB ΔW_{5dB} y el Scanning Ratio SR, relacionados con el ancho de banda mediante la fórmula: $BW = W_{5dB}/SR$.

Analysis and design of quasi-optical space multiplexer based on substrate-integrated waveguide antennas

Contents

List of Figures

Chapter 1

Initial approach and Project's Objectives and Phases

1.1 Initial approach

Over the past few years the Substrate Integrated Waveguide (SIW) has been replacing Rectangular Waveguide for multiple tasks because it preserves the well-known advantages of this conventional device, namely, high-Q factor and high power capacity [1], but it introduces the characteristics of the microstrip technology: low cost, mass production and low weight.

Therefore, there are a huge number of devices built in other technologies that could be enhanced in one or several characteristics (weight, high frequency, power capacity, cost,...) with SIW technology. For this project, we are interested in spatial multiplexers, which, depending on the input frequency they obtain the output in a concrete port, spatially separated from the others.

Microwave frequency division multiplexers are normally based on coupled-cavity resonators 1.1. As frequency increases, resonant elements become more lossy, so that novel low-loss filtering/multiplexing techniques are being investigated for millimeter and sub millimeter wave applications. Recently, increased interest is being given to the study of the inherent spatial-spectral decomposition obtained from artificial dispersion-engineered 1D and 2D transmission mediums to obtain diplexing/multiplexing responses with application to analog signal processing as Fourier transform or real-time spectrum analyzer. In all these cases, it is obtained a non-resonant spatial filtering response in which different frequencies are routed to different spatial direction as a result of the dispersion of the proposed transmission line. Another well-known non-resonant spatial multiplexing mechanism is the one based on diffraction gratings, usually used in optics but also applied to microwaves and millimeter waves.

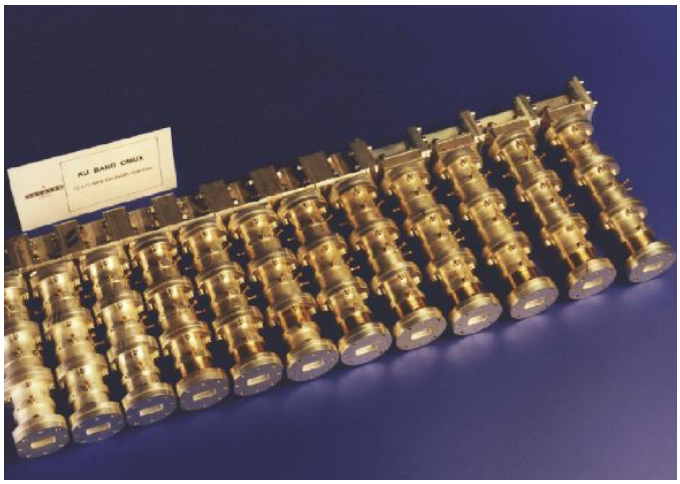

Figure 1.1: Ku-band OMUX.

We can see some graphic examples, such as hyperbolic transmission line (TL) periodic grids [2] 1.2 a), planar anisotropic transmission-line metamaterials [3] 1.2 b) or electrical prisms [4] 1.2 c).

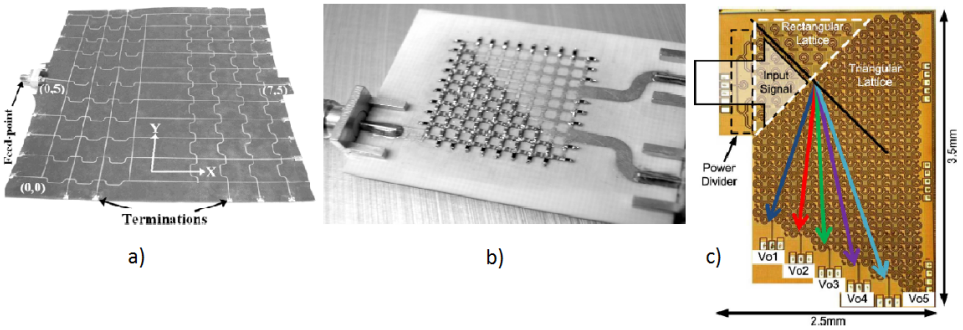

Figure 1.2: (a) TL periodic grids, (b) TL metamaterials and (c) Electrical prisms.

In this project we propose a new quasi-optical (non resonant) spatial multiplexing device, which is based on the spatial-spectral dispersion properties of an engineered substrate integrated waveguide (SIW). It presents a low-profile structure embedded in a shielded dielectric substrate, thus reducing the volume and complexity compared to spatial multiplexers operating in free space. Compared to recently proposed electrical prisms 1.2 c), which are based on anisotropic 2D lattices, this devices presents a much simpler topology. Certainly, its final structure is comprised only of a two-sides metallized dielectric substrate which must be conveniently perforated by conducting vias, thus having all the manufacturing and low-loss advantages of SIW technology.

We obtain, therefore, a simplification in the design, obtaining the multiplexed

focus by setting some simple parameters [5], such as the period of the cylinders P, their diameter d, the antenna's width W or the antenna's length L_A 1.3 .

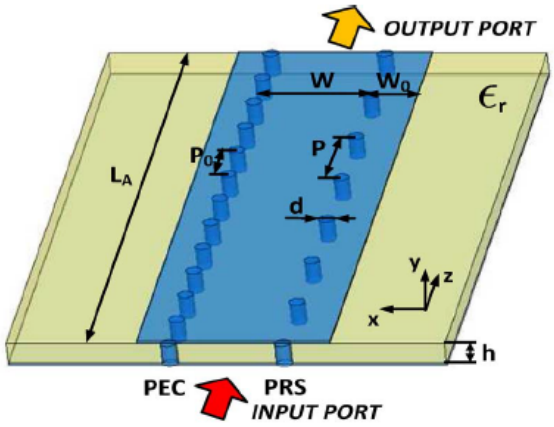

Figure 1.3: Antenna parameters.

As a last initial approach we need to choose some particular design for the antenna to obtain the focus of interest.

1.2 Project's Objectives

Firstly, from a theoretical point of view we have to familiarize with the technology of interest, its characteristics, parameters and applications.

For the development of this project we need a simulator to implement and to simulate the different designs. We have chosen the software *Ansoft HFSS* because its broadly use in the electromagnetic devices simulation and its easy handling.

And, obviously, the third and most important objective is to reach a final design of a spatial multiplexer and try to obtain a manufacturable device.

1.3 Project's phases

We can summarize the phases of this project to:

- SIW technology and HFSS software familiarization: chapters 2 and 3.
- Election of the antenna and definition of its focus location: chapter 3.
- Design of the multiplexer's output ports using PEC walls for an easiest verification: chapters 5, 6 and 7 (an introduction to a coaxial design is presented in 4).
- PEC walls substitution by via-holes and results verification: chapter 8.

- Losses insertion: chapter 9.

In chapter 10 we present the design in layers to its possible manufacture, and in chapter 11 we present some possible future lines of work.

Chapter 2

Introduction to the SIW technology

2.1 Substrate Integrated Waveguide

The substrate integrated waveguide (SIW) technology represents a promising candidate for a variety of circuits and components operating in the microwave, millimeter-wave and terahertz region, which belongs to the family of substrate integrated circuits (SICs) [6]. The fundamental of these SICs is to synthesize non-planar structure with a dielectric substrate and make it in planar form, which is completely compatible with other planar structures, and will have much better loss characteristics than planar counterparts, allowing for the design of millimeter wave high-Q filters, diplexers, resonators and other circuits using a low-cost fabrication technique [7].

A rectangular SIW is synthesized by placing two rows of metallized holes in the substrate, as in 2.1 . As we said in the Initial Approach, the parameters of the guide are: the diameter d of the holes, the spacing P between two rows, the hight h of the substrate, the real width W, the effective width $Weff$ and the length L_A of the guide (non represented here).

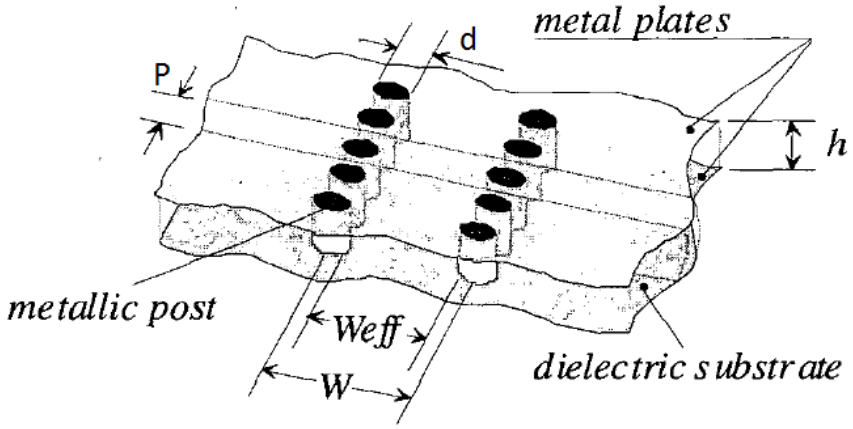

Figure 2.1: Topology of a SIW guide realized on a dielectric substrate.

One side of the SIW presents sparse vias to allow coupling to the TE surface wave (SW) which can propagate inside the shielded substrate, which acts as a dielectric-filled parallel-plate medium.

The separation between the sparse vias P and the width of the SIW W can be adequately modulated along the SIW propagating direction z, in order to shape the TE SW fields inside the substrate. Here this modulated SIW technology is applied for the first time to the synthesis of frequency dependent near-field focusing patterns inside the host dielectric substrate by modulating the complex coupling with a surface wave (SW).

The period P must be kept small to reduce the leakage loss between adjacent posts. However, the post diameter d is also subject to the loss problem. As a result, the ratio d/P is considered to be more critical than the post period because the post diameter and the post period are interrelated. The post diameter may significantly affect the return loss of the waveguide section in view of its input port. There are two design rules related to the posts diameter and period that are used to neglect the radiation loss. These two rules have been deducted from simulation results of different SIW geometries:

$$d < \lambda_g/5 \tag{2.1}$$

$$P \leq 2d \tag{2.2}$$

2.2 Leaky Wave Antennas

Leaky-wave antennas (LWAs) are based on the use of a tapered leaky-wave mode, where the complex propagation wavenumber (phase constant β and leakage rate α)

is varied along the LWA longitudinal axis, z [8].

$$k(z) = \beta(z) - j\alpha(z) \tag{2.3}$$

In the SIW LWAs the leaks are obtained with the variation of the distance between posts P (breaking condition of (2.2) equation). This radiation is in the form of a TE surface leaky-wave which propagates through the dielectric substrate at a given angle Θ_D (given by $\beta/k_d = sin(\theta_d)$ where k_d=$k_0\sqrt{\epsilon_r}$ is the substrate wavenumber and β is the leaky-mode phase constant along the z-axis), and with a given leakage rate α(nep/m) [11].

The simultaneous control of Θ_D and α are achieved by the variation of the SIW width W and posts distance P, thus allowing flexible design of the far-field radiation pattern. In figure 2.2 it can be seen two examples: a) uniform SIW and b) modulated SIW with near-field focusing.

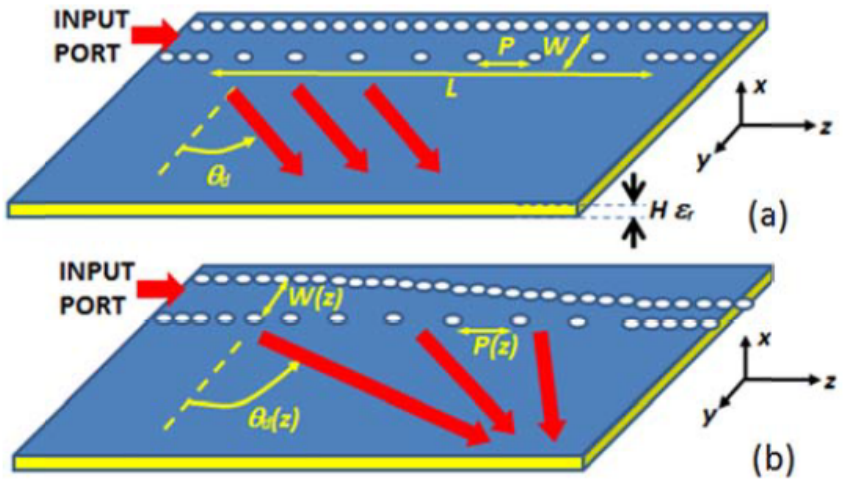

Figure 2.2: Scheme of leaky SIW radiating inside the integrated substrate a) uniform SIW and b) modulated SIW with near-field focusing.

The multiplexer performance and focusing can be obtained by modulating the SIW width *W(z)* and posts distance *P(z)* along the leaky SIW length. And of course, given these two parameters we can design the antenna for a chosen distribution function.

Chapter 3

Election of the antenna

The first step is to choose a specific antenna for this project. Some points of this chapter are previous to the project per se, because the antenna has been provided by the project's directors, but we have to understand why we choose this one and not another.

3.1 Design of a SIW SW launcher focused inside substrate

The design of the multiplexer starts with the definition of the focal point for a given frequency (which in our case is z_F=120mm, y_F=100mm at 15GHz) and the radiating length of the modulated SIW line (L=100mm). Following a similar procedure to the one described in [8] for near-field focused leaky waves, one can obtain the electrical modulation of the SW complex propagation constant. Two main parameters must be locally modulated to efficiently couple the energy to the substrate TE SW and to create a focusing pattern at the desired focal point. First, the equivalent SW propagating angle inside the substrate (Θ_D measured from the perpendicular direction in 2.2 b)) must be decreased along the SIW to create a SW wavefront converging at the desired focal point. Second, the coupling rate α_D (which measures the decay of guided signal along the SIW length in nep/m due to SW coupling), must be adequately modulated to keep uniform coupled power per unit of length and thus optimize the focusing efficiency. The resulting functions $\Theta_D(z)$ and $\alpha_D(z)$ are plotted in 3.1.

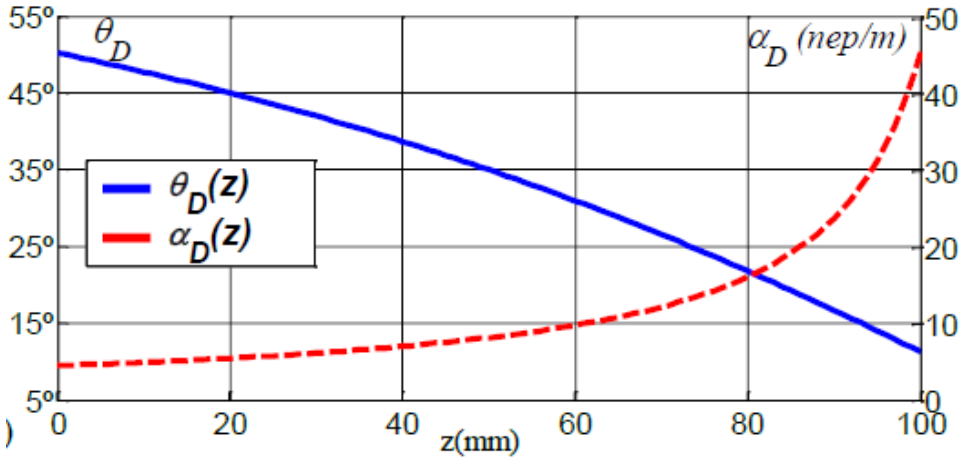

Figure 3.1: Modulated surface-wave (SW) coupling functions.

Then, one needs to transform these SW electrical functions into geometrical modulations functions over the SIW width W and distance between coupling posts P. For this purpose, a dispersion analysis must be performed to obtain the dependence of $\Theta_D(z)$ and $\alpha_D(z)$ with W and P. This can be efficiently done by using a simple Transverse Equivalent Network (TEN in the y-direction) as the one proposed in [9] for the analysis of leaky waves radiating from a SIW into free space. This TEN is here modified as represented in 3.2 to study the dispersion of SIW-to-SW coupling inside the dielectric substrate.

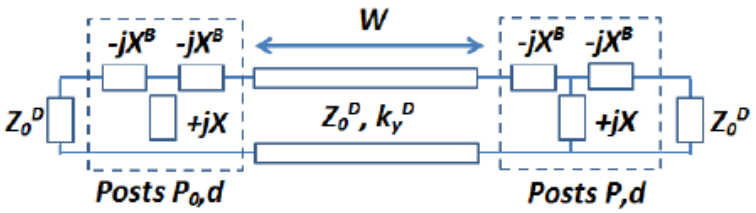

Figure 3.2: Transverse Equivalent Network of SIW coupling to SW inside substrate along y direction.

The SIW line is represented in the transverse y-direction by a dielectric-filled parallel-plate transmission line of length W, with characteristic impedance Z_0^D, and transverse complex wavenumber k_y^D. At the right side, a T-junction equivalent circuit models the vias with period P which allow the coupling from the SIW to the SW by the right side. It can be noticed the termination with the characteristic impedance Z_0^D which models the dielectric-filled parallel-plate where the SW can propagate. The same equivalent circuit is used to model the row of vias at the left

side, which must be located in close proximity to avoid SW coupling by this side (normally $P_0/d>3$, where P_0 is the distance between vias and d is their diameter [1]).

By solving the Transverse Resonance Equation, the unknown transverse wavenumber $k_y{}^D$ for the main TE mode propagating along the SIW can be obtained as a function of frequency, and for the any values of W and P. Then, the corresponding SIW-to-SW coupling factor α_D and SW propagating angle Θ_D can be obtained as:

$$\alpha_D = imag\sqrt{k_0^2\epsilon_r - (k_y^D)^2} \tag{3.1}$$

$$\theta_D = \frac{real\sqrt{k_0^2\epsilon_r - (k_y^D)^2}}{k_0\sqrt{\epsilon_r}} \tag{3.2}$$

For our design, we use a substrate with ε_r=2.2 and thickness H=1.57mm, and all vias have a diameter d=1mm (the close vias modeled on the left side of the TEN have a period P_0=2mm so that P/d=2 is satisfied to create a reflecting wall). The resulting modulation functions for the SIW dimensions $W(z)$ and $P(z)$ are represented in 3.3. The width must be decreased from W=10.2mm to W=6.8mm along the SIW of length L=100mm, while the distance between coupling post is decreased from P=5.7mm to P=5.0mm.

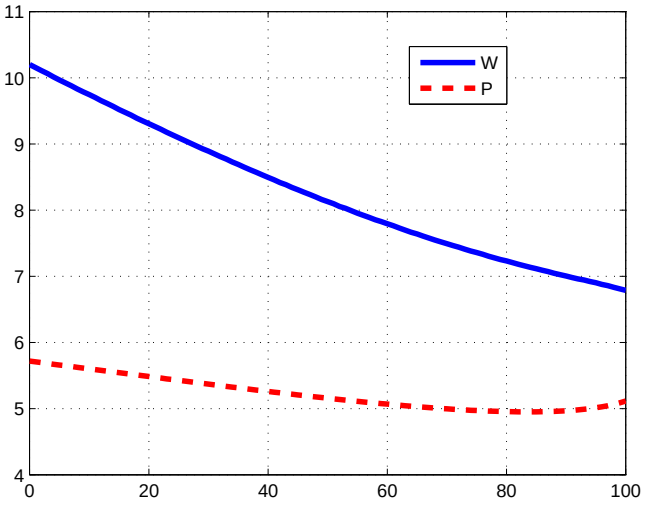

Figure 3.3: Modulated dimensions of SIW.

The theoretical nearfield focused distribution across the ZY plane is represented in 3.4 a) with -10dB scale. Full-wave results of the fields guided along the modulated

SIW and coupling into the substrate at 15GHz are obtained from HFSS, and they are represented in 3.4 b).

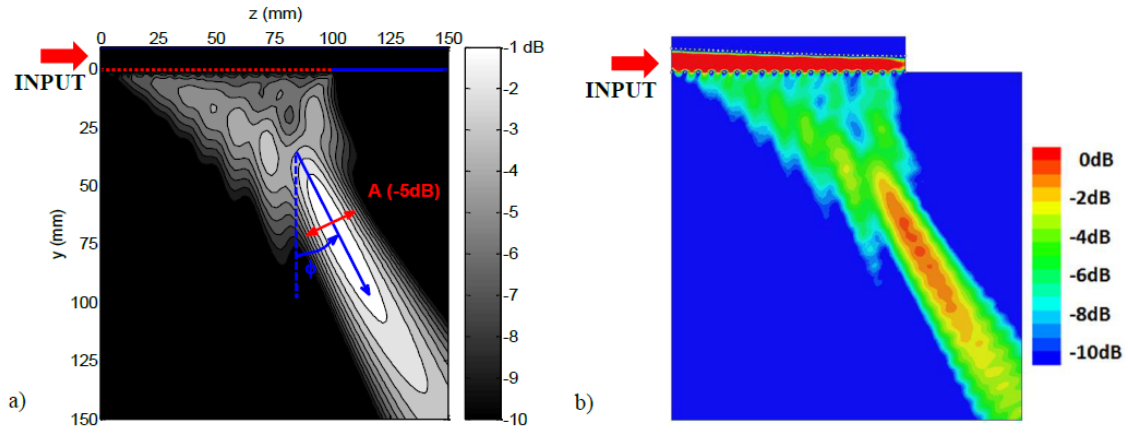

Figure 3.4: a) Theoretical and b) HFSS simulated 2D surface-wave focusing pattern inside the substrate at 15GHz.

It is demonstrated the launching of a surface wave inside the substrate which synthesizes a focusing pattern around the desired focal point z_F=120mm, y_F=100mm at 15GHz. The maximum of power density is located at the point (z_0=106mm, y_0=78mm), which is closer to the SIW aperture than the focal point due to the well-known focal shift phenomenon [10]. A longitudinal field-cut along the z-direction at a distance y=y_0=78mm from the SIW aperture is analyzed in 3.5 to compare theoretical and full-wave HFSS results, showing good agreement. The focal region is ellipsoidal and tilted as it propagates towards a scanning direction given by the angle Φ along the ellipse principal axis in 3.4 a).

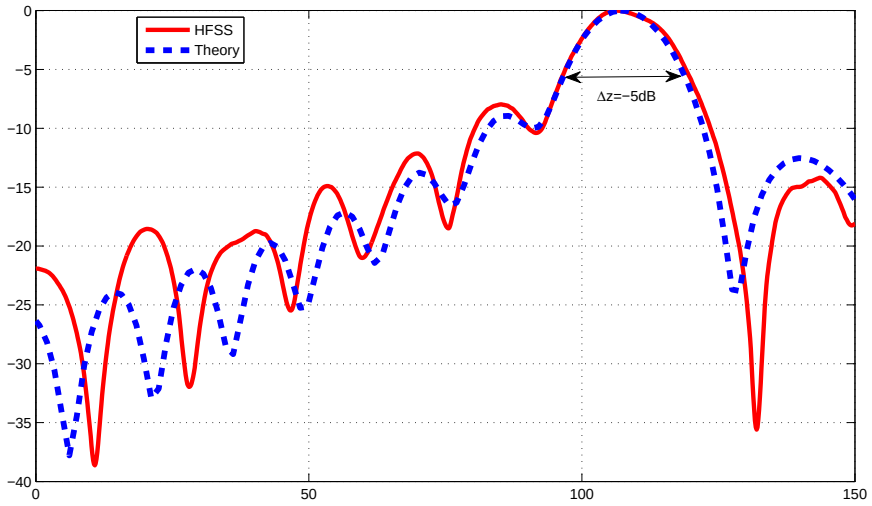

Figure 3.5: Cut along the z-direction at a distance y=y0=78mm from the SIW aperture.

Also, it is defined the effective focal width A, such that the field intensity decays -5dB w.r.t. the maximum level and 70% of the SW power density travels through this width. The studied focusing pattern presents a direction Φ=30deg and a 5dB focal width A=16mm. The projection of this focal width along the z-cut (Δ_z -5dB), is represented in 3.5.

3.2 Frequency range

The frequency band usually used by this kind of devices are the microwaves, i.e. from 300MHz to 300GHz. The antenna provided by the directors has been designed for a approximated range of 10-16GHz. For values equal or less than 10GHz the focus is poorly defined. In fact, for 10GHz the antenna is closed to radiate in the broadside position, and the focus is too near to the antenna with a weak signal 3.6 a), b). The scale, 55-60dB (always 5dB wide), is smaller than the other, 68-73dB (used in 3.6 c)), to see both frequencies. With this diminution of the frequency we are approaching the antenna's cut-off frequency, and this is the reason both frequencies are radiating in the same position but with less energy. So we should choose a higher frequency for the multiplexer's first output port.

For values equal and greater than 16GHz the antenna is closed to radiate in the endfire position and the focus is too far from the antenna 3.6 c). This is the scale we will usually use, but for these frequencies it seems too high. It can be seen also the proximity between them. Even with 1GHz-steps it is not possible to design the

multiplexer including these frequencies. So, as in the previous case, we should choose a lower frequency for the multiplexer's last output port.

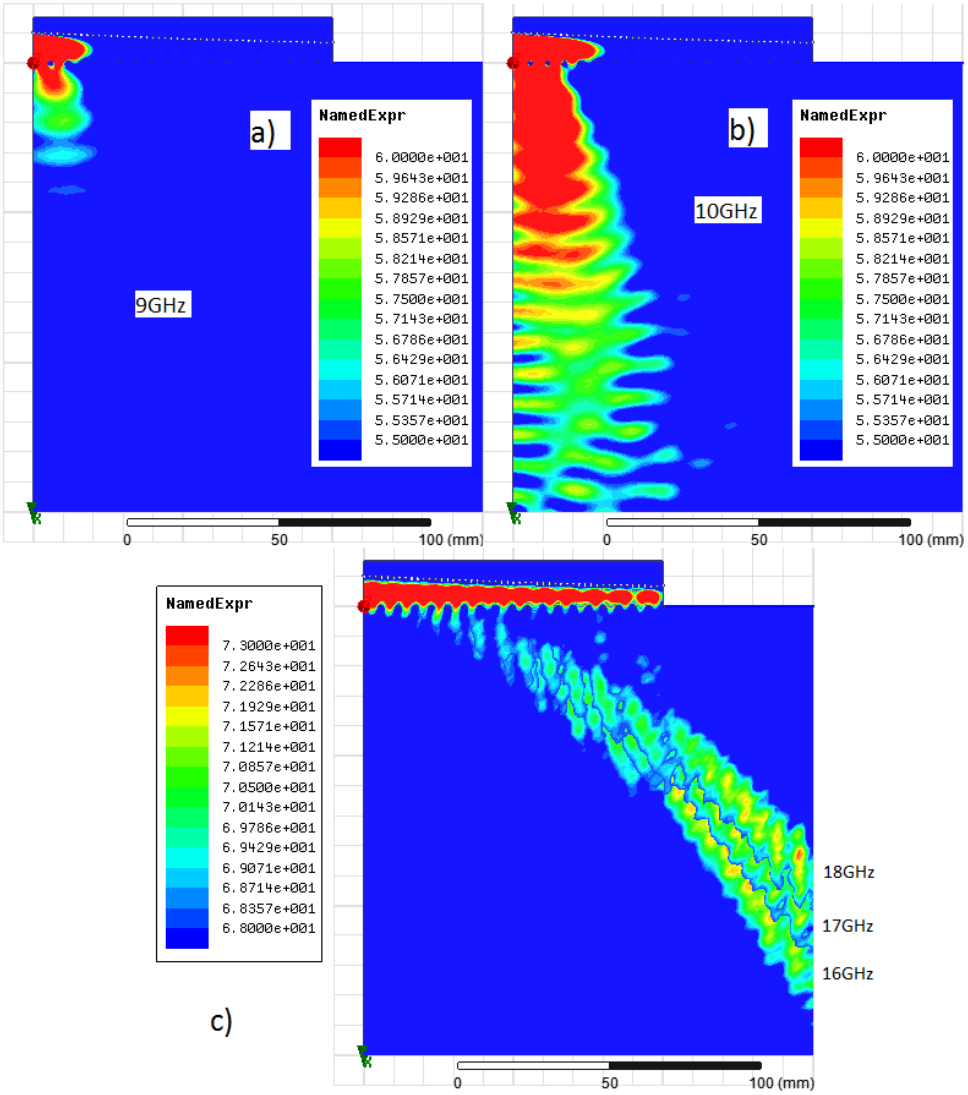

Figure 3.6: a) 9GHz, b) 10GHz, c) 16GHz, 17GHz and 18GHz.

For all these reasons we are going to choose frequencies between 11GHz and 15GHz. Seeing the next figure 3.7 it can be seen that with a 1GHz-step, i.e. 5 ports, there is already some overlap between ports. But with less ports we waste useful frequencies because even with the tiny overlap there are space to design the output ports.

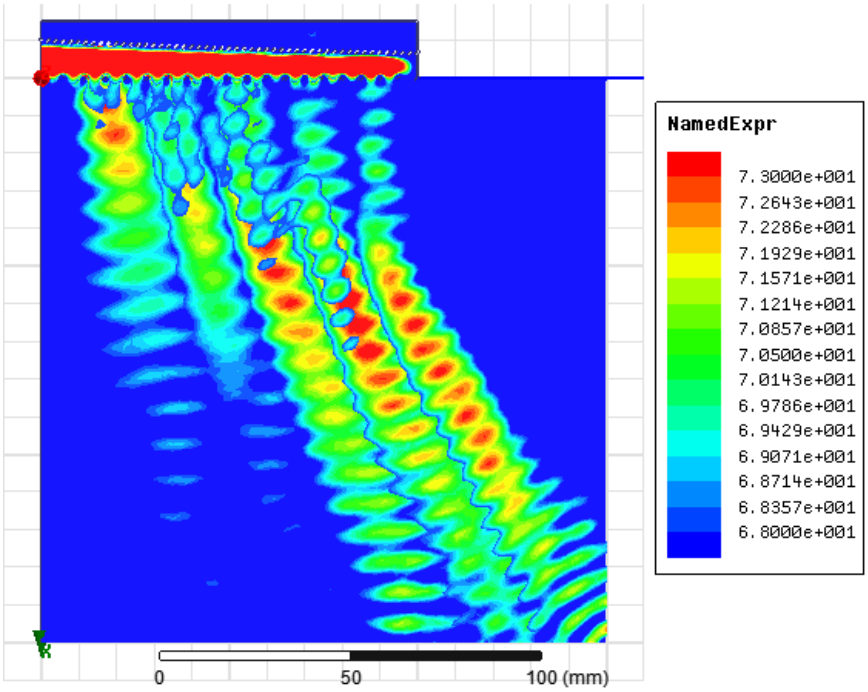

Figure 3.7: 5 useful frequencies (ports): 11GHz, 12GHz, 13GHz, 14GHz and 15GHz

As it is known, the beams width is one that ensure that the power only decays 5dB, i.e., the 70% of the energy is in the footprint. As figure 3.7 shows, also with this value we achieve a minimum overlap. So the final solution is:

- 5 ports: 11GHz, 12GHz, 13GHz, 14GHz and 15GHz.

3.3 Election of the distribution function

In this project we will try to design a space multiplexer, so from the beginning we need a modulated SIW with near-field focusing like in 2.2 b). But, which distribution should we use? Uniform, Sine, Sine^2 3.8 ? We have to choose based on this two options:

- Minimize secondary lobes
- Minimize the width of the focus

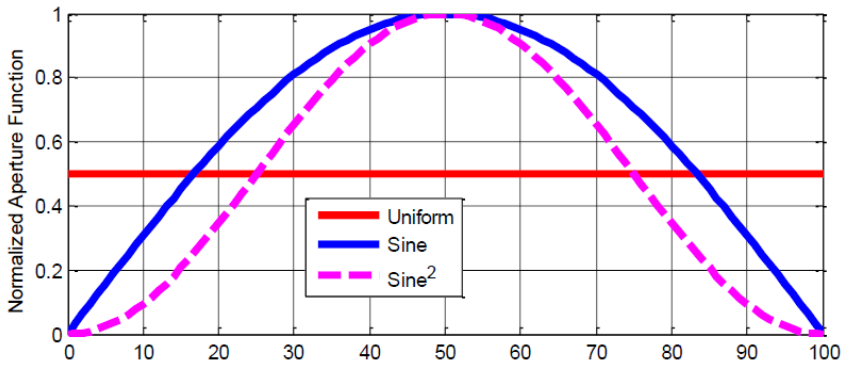

Figure 3.8: Normalize aperture functions.

In the next figure 3.9 it can be seen a field representation for the three distribution functions. The function with bigger secondary lobes is the Uniform, but on the contrary, it is the one with the narrowest main lobe.

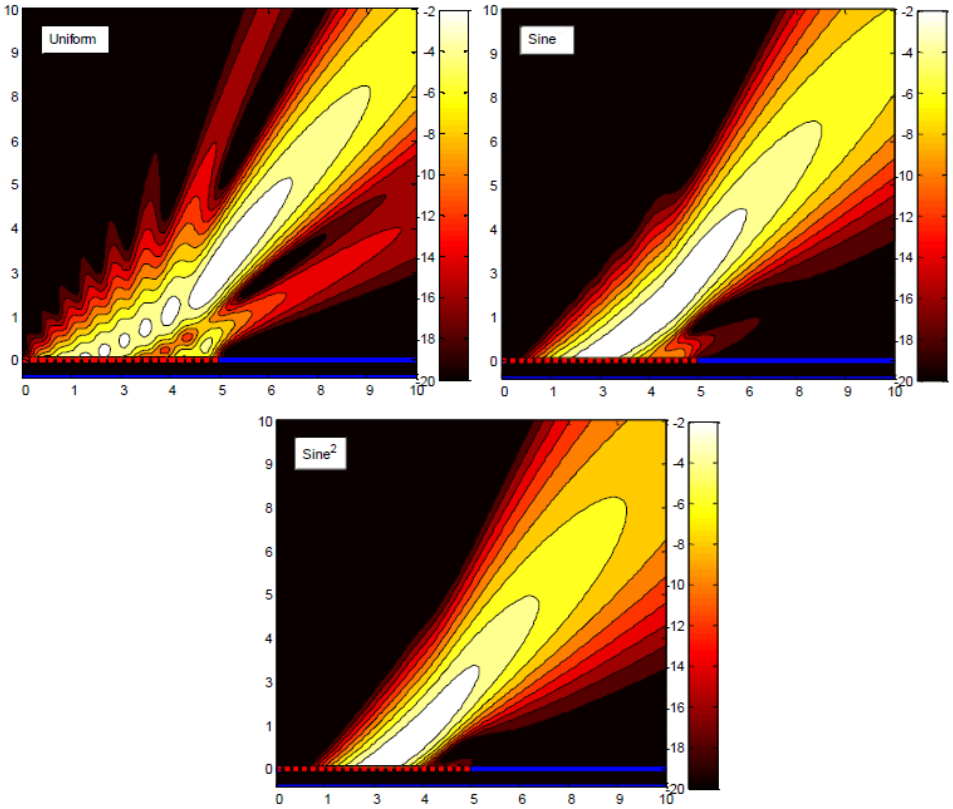

Figure 3.9: Field distribution functions.

We can see an example. The directors provided with other antenna equally in dimensions, but with the design of a Cosine distribution 3.10 . As we said before each frequency's principal lobe are too wide and overlap with the next ones. The width represented is for 5dB again. But it isn't possible to locate physical ports to collect the energy.

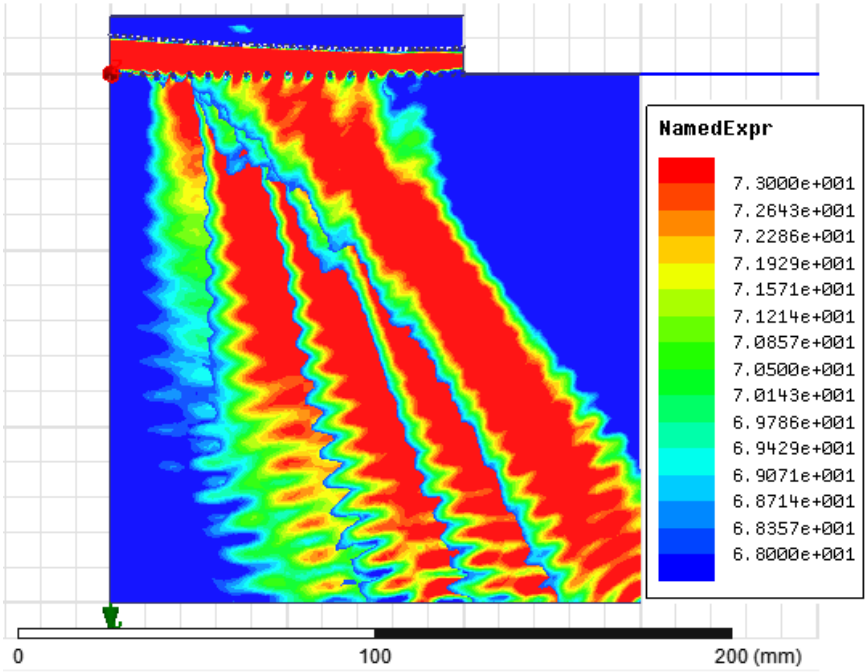

Figure 3.10: Cosine distribution.

For our device, at first, it is more restrictive the width of the central lobe than the second lobes levels because we will have a small range of frequencies in a small substrate. Anyway, there are ways to bring down the second lobes levels. This is why we use for this project an antenna with Uniform distribution function.

3.4 Changing Substrate Height

Firstly, it has to be clear if the field distribution changes with the substrate height h. Because the substrate's height changes, the Z-axis will be modified, and this will affect the energy density, considering that the same volts quantity have to distribute in a higher structure. But the energy distribution form will remain unchanged, so it can be use any usual height, for example: 0.508mm, 1.57mm or 3.175mm.

This can be seen with an example of two different heights: 1.57mm 3.11 and 3.175mm 3.12. It can be seen clearly how the energy density decreases with the higher height, but how the energy distribution remain unchanged.

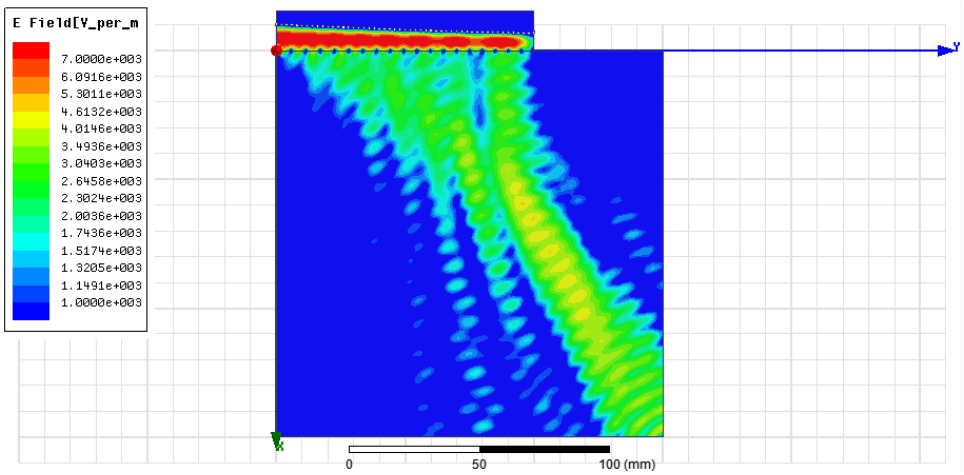

Figure 3.11: Original structure with 1.57mm of height.

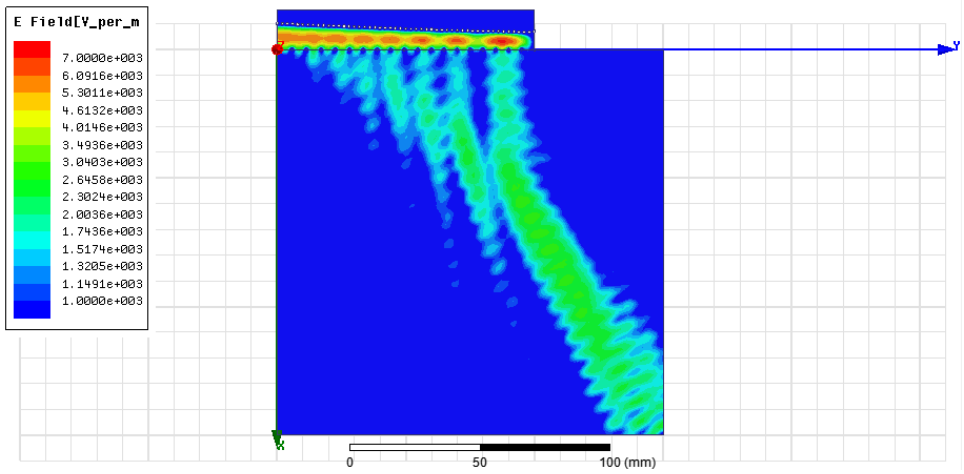

Figure 3.12: Original structure with 3.175mm of height.

So we can see how it remains the independence between the substrate height and the energy distribution. Now we have to decide which one better fulfils our necessities. Between 0.508mm and 1.57mm we choose 1.57mm because of:

1 The greater rigidity and strength in the connectors mounting

2 We must try to avoid bending

3 The greater facility in the adaptation with perpendicular coaxial connectors

4 Trying to extrapolate to millimetre bands, it is interesting to maintain the aspect relation between dimensions. For example, for a 60GHz frequency we are multiplying by 4, so we'll have to divide by 4 the dimensions. And it is less fragile a h/4=1.57/4=0.392mm substrate than a h/4=0.508/4=0.127mm

3.5 Chosen structure

To begin with the design of the structure we have:

- A modulated SIW with near-field focusing and a 150x150mm substrate
- Frequencies from 11GHz to 15GHz with 1GHz-steps
- Uniform distribution function
- Hight of the entire structure: 1.57mm

With the chosen structure defined, it is advisable to define some parameters to characterize the focus.

3.6 Antenna's parameters

To define a focus there are needed three parameters 3.13 : the position of the focus (Y_F, X_F), the inclination angle of the footprint α, and the 5dB-width ΔW_{5dB}.

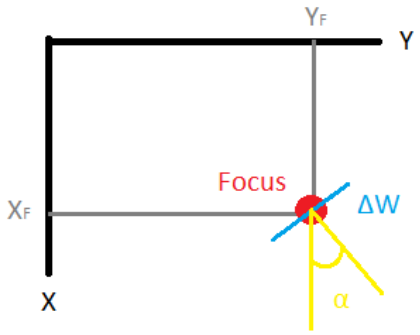

Figure 3.13: Antenna's parameters.

In the next figure 3.14 it can be seen circles positioned in each frequency's focus. The position of this 2D circles gives the parameter (Y_F, X_F).

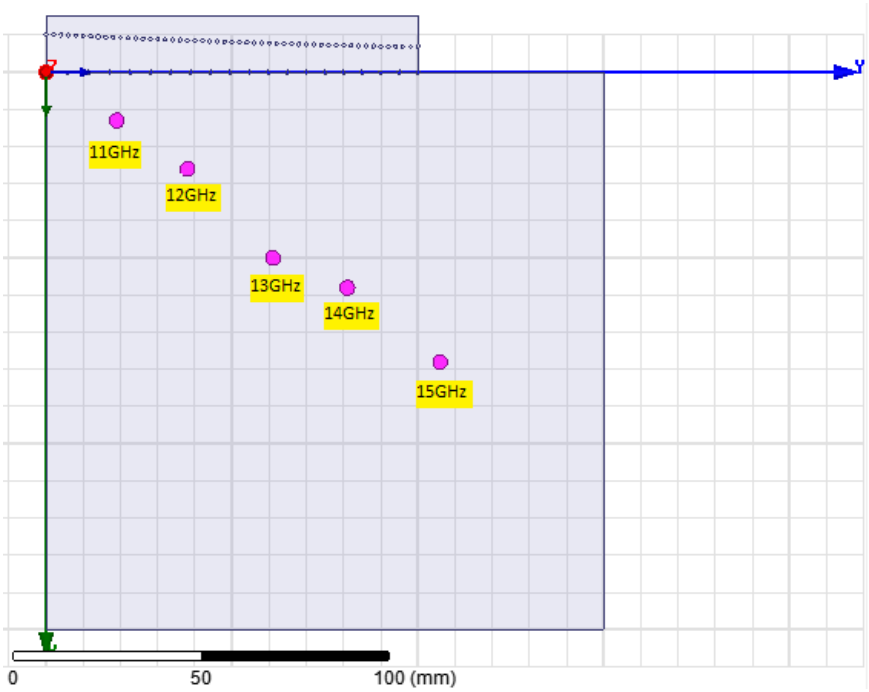

Figure 3.14: Frequencies focus position.

The angle α (before called Φ) is the angle formed by the perpendicular from the pulse's origin center and the line from this same point to the focus center (center line) 3.15 . It will increase with the frequency.

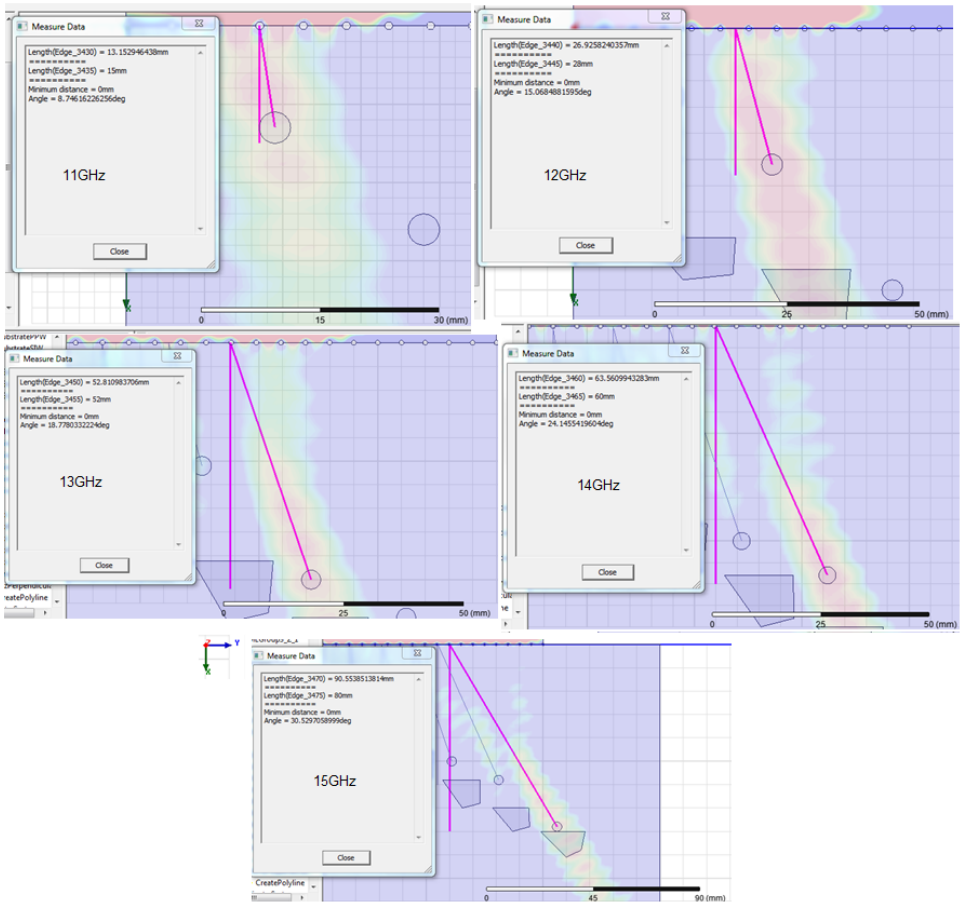

Figure 3.15: Angle for each frequency.

Figure 3.16 shows for each frequency the ΔW_{5dB} in accordance with each frequency's angle α, and figure 3.17 shows all together, demonstrating the tiny overlap between some ports, so as we said before, with the 5dB width we are already at the limit.

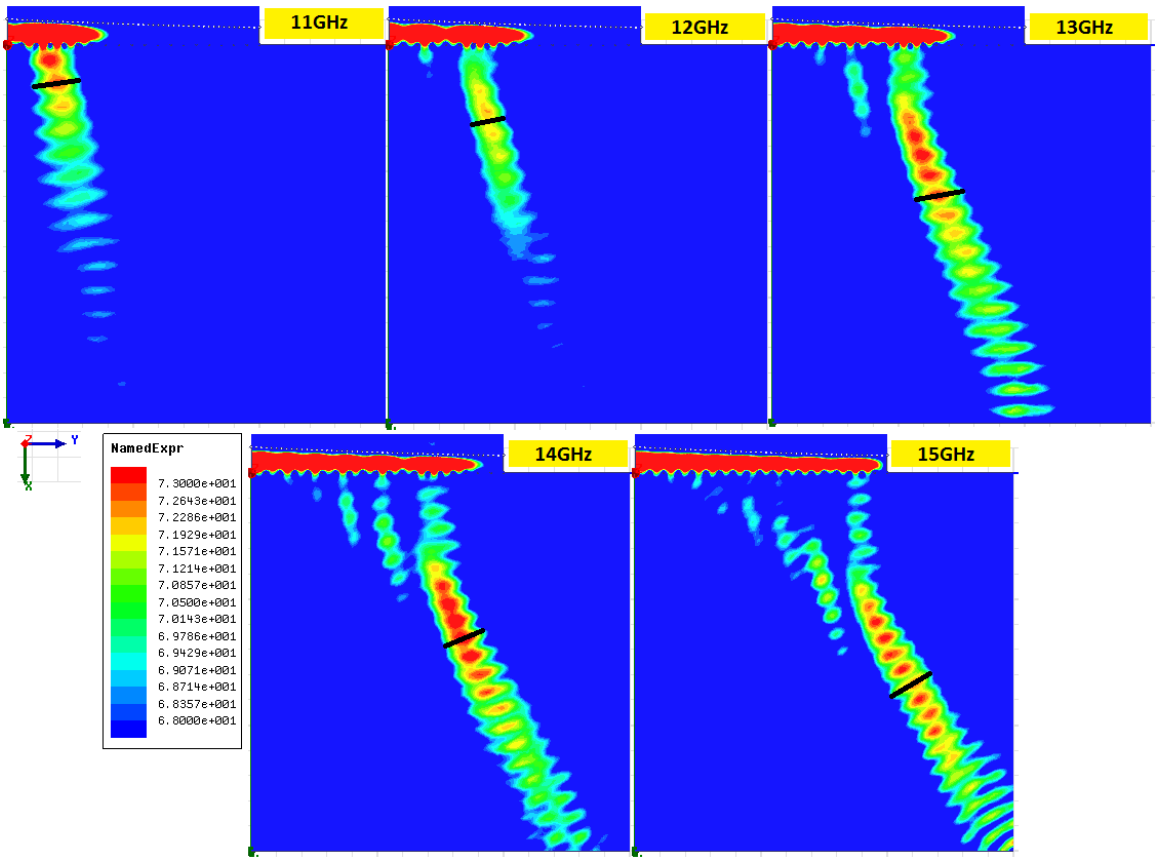

Figure 3.16: 5dB width for each frequency.

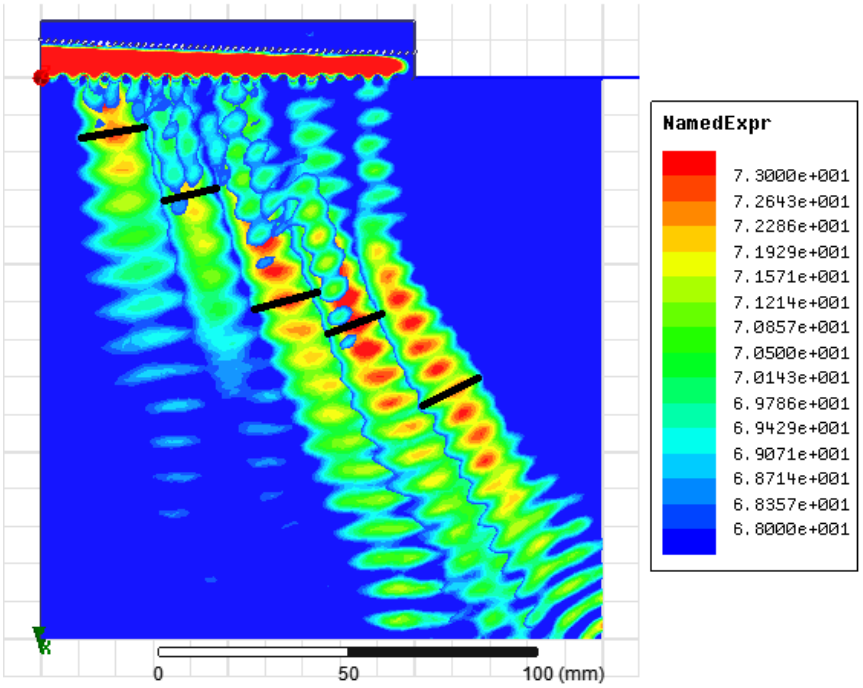

Figure 3.17: 5dB width.

For an easier overview we can present all the explained parameters in a table.

f(GHz)	Y_F (mm)	X_F (mm)	ΔW_{5dB} (mm)	α(deg)
11	19	13	18.25	8.75
12	38	26	13.35	15.07
13	61	50	15.53	18.78
14	81	58	15.24	24.14
15	106	78	16.13	30.53

Now we can start thinking in the best solution to extract the energy given the frequency with some output ports. We are going to use two technologies: coaxial ports and SIW ports. With the coaxial technology we will only reach to a initial design and the rest will remain as undo work to future projects. With the SIW technology we will try to reach to a manufacturable prototype.

Chapter 4

Coaxial Ports

One way to extract the output energy is to use coaxial ports. We put them in the vertical axis (Z-axis) 4.1 so that the coaxial core crosses through the substrate's height. The coaxial's dielectric is placed just below the substrate. This way we can study the quantity of energy the coaxial is capable to extract.

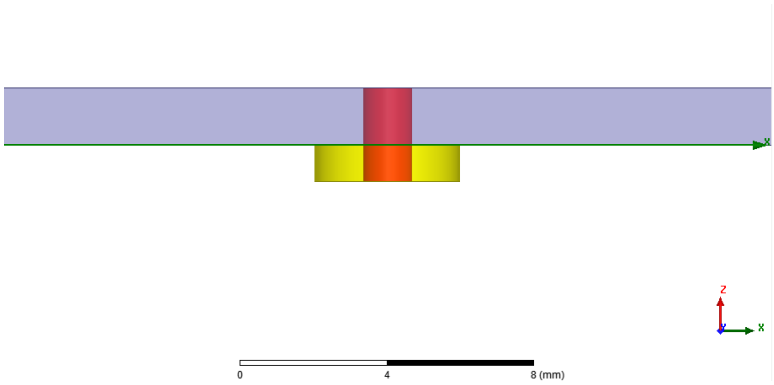

Figure 4.1: Coaxial port view.

The coaxial core is defined as PEC. For the dielectric we choose a different dielectric constant, 2.08 so we have a more lifelike case. The next step is to choose the place for the ports.

4.1 Coaxials in the focus

The first logical attempt is to locate them in the maximum energy point, the focus. Theoretically there are two focus: the maximum intensity focus and the maximum resolution focus. From now on we are interested in extract energy from the maximum resolution focus. Figure 4.2 shows this design.

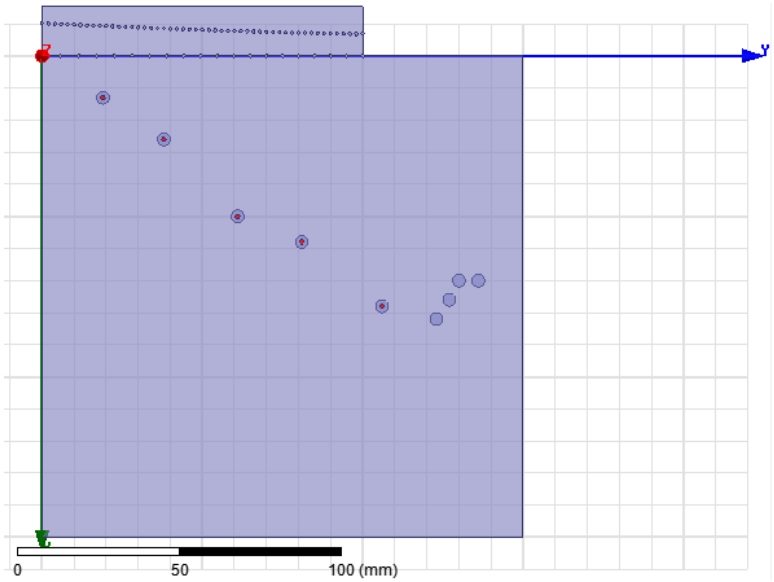

Figure 4.2: Coaxial in the focus.

The first five circles are the useful coaxial ports (11GHz, 12GHz, 13GHz, 14GHz and 15GHz). The others circles are the maximum focus for others frequencies. It is useful to represent 4.3 the E-field for each frequency.

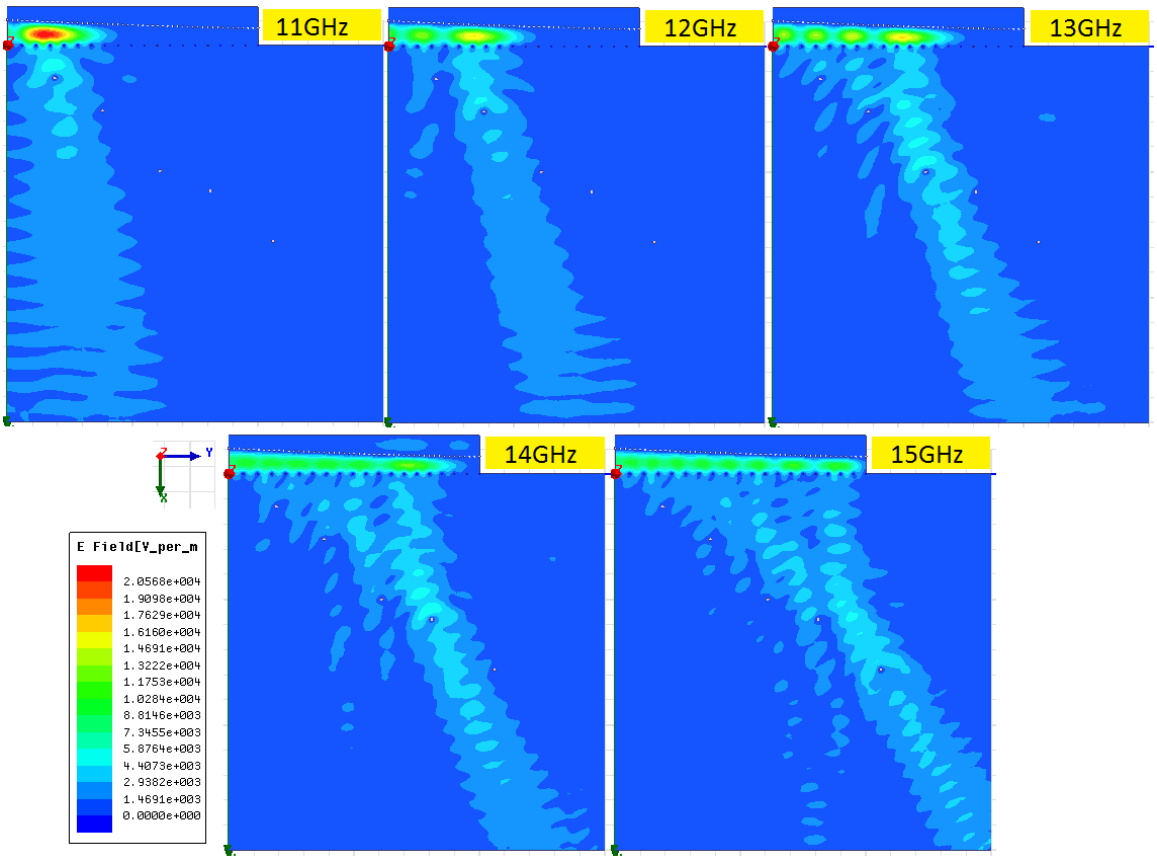

Figure 4.3: ComplexMag of E-field for focus coaxial output ports.

As we expected, the major quantity of energy reaches the coaxials. But there are a lot of wasted energy that goes through them a continue across the substrate. To improve this issue it would be useful to locate some reflectors after the ports to redirect the wasted energy to the ports again. And for the energy that still will remain free it is helpful to use some Dummy Ports to collect it. Besides, some ports overlap with others making shadowing.

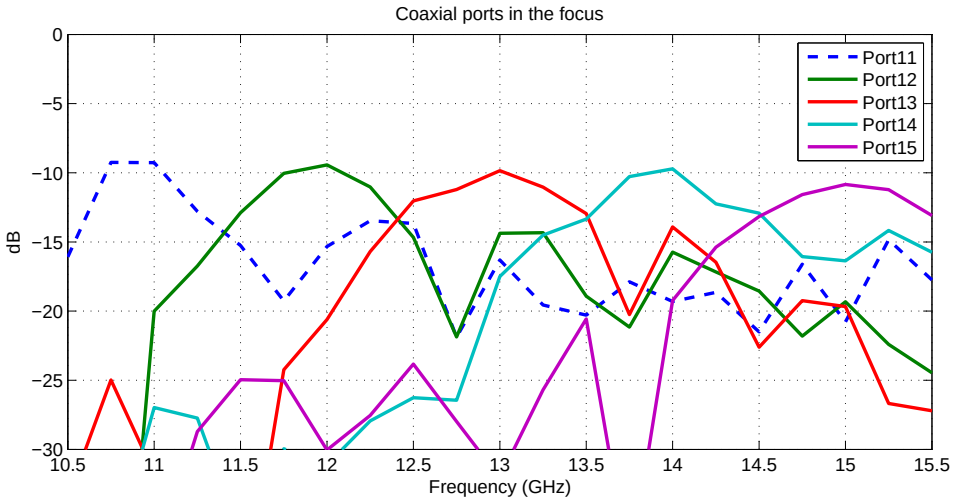

Figure 4.4: Coaxial ports in the focus S parameters.

From this S parameters representation 4.4 it can be seen that upper ports collect more energy, maybe due to the overlap between ports. Higher ports will suffer more overlap because they will have more ports causing shadows. Besides the low levels, it can be seen well defined bands for each frequency. It is indeed a good start.

4.2 Aligned coaxials

A second option is an aligned distribution such as in [11]. We use the same X-axis distance from the antenna: 60mm. And we place them in the maximum calculated in [11] (the Z-axis is here Y-axis) 4.5 .

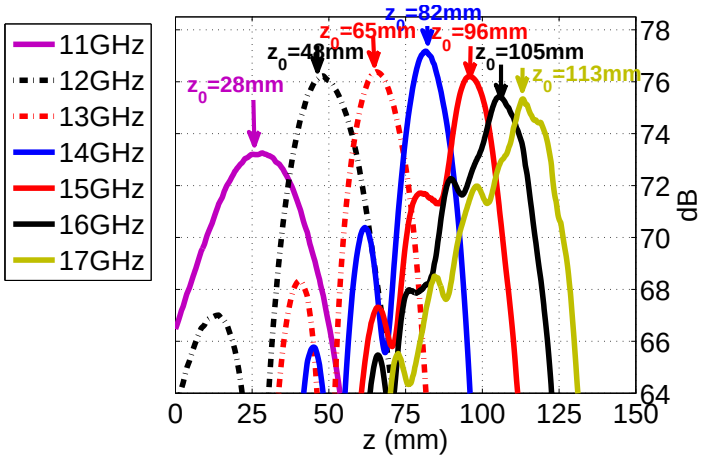

Figure 4.5: Y-axis ports position.

As we decided, we are going to use five ports, 11, 12, 13, 14 and 15GHz frequencies 4.6 . Along the 60mm X-axis distance we place the ports in each Y-axis point: 28, 48, 65, 82 and 96mm.

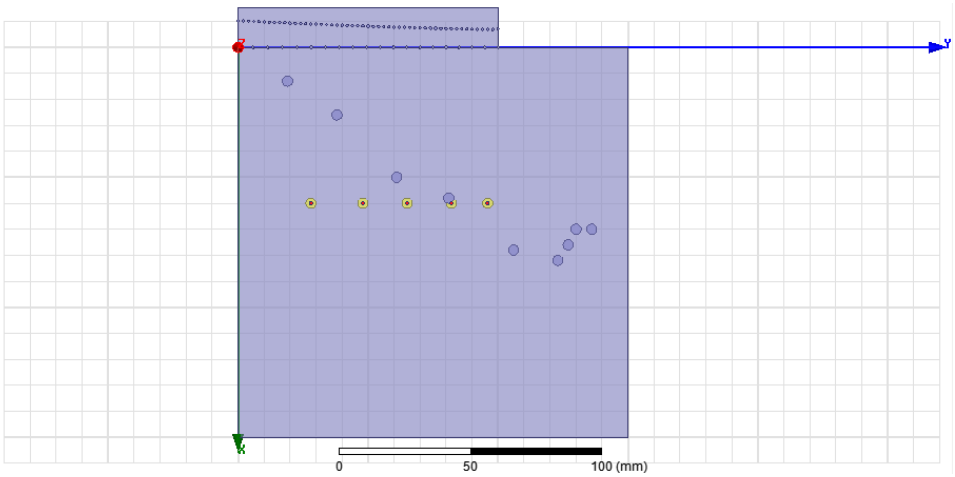

Figure 4.6: Coaxial output ports structure.

In the next figure we can see the complex magnitude of E-field for the frequencies 11GHz to 15GHz 4.7 , i.e., ports 11 to 15.

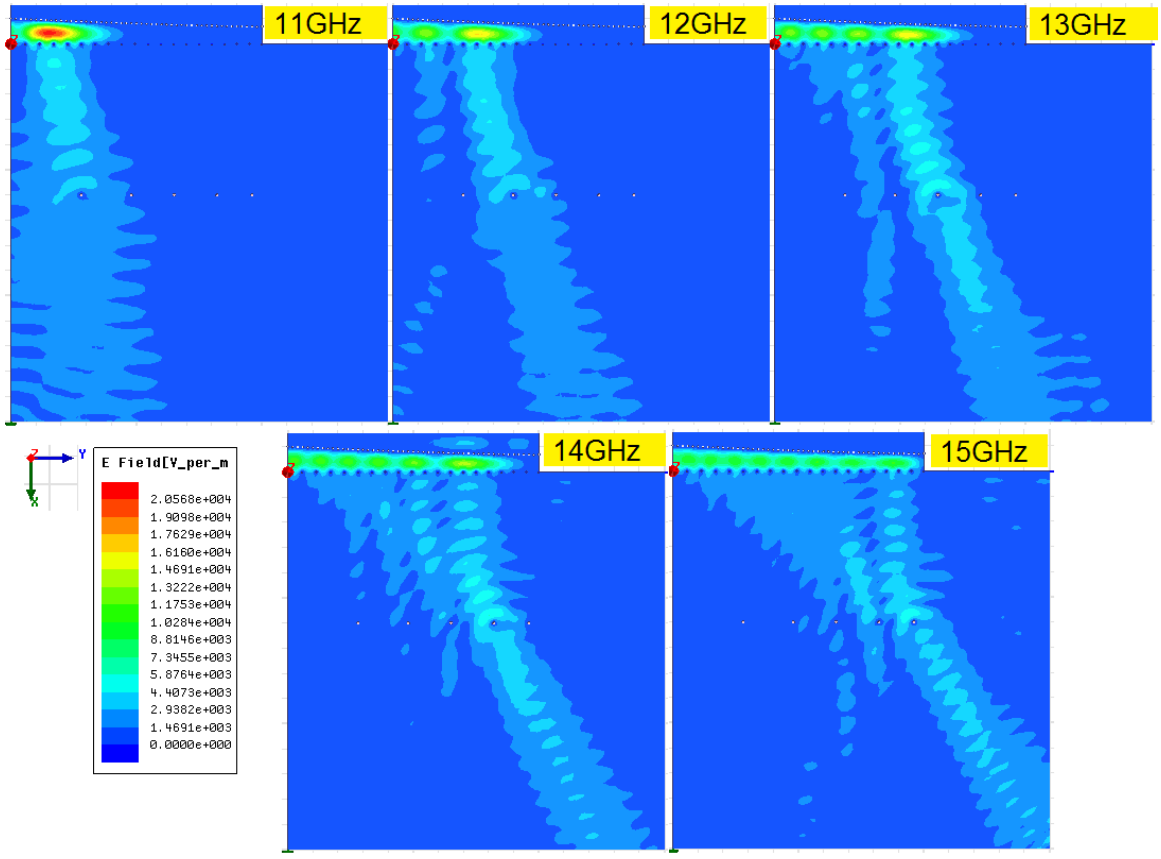

Figure 4.7: ComplexMag of E-field for aligned coaxial output ports.

It can be appreciated again the need to include some reflectors and Dummy ports to recollect all the wasted energy.

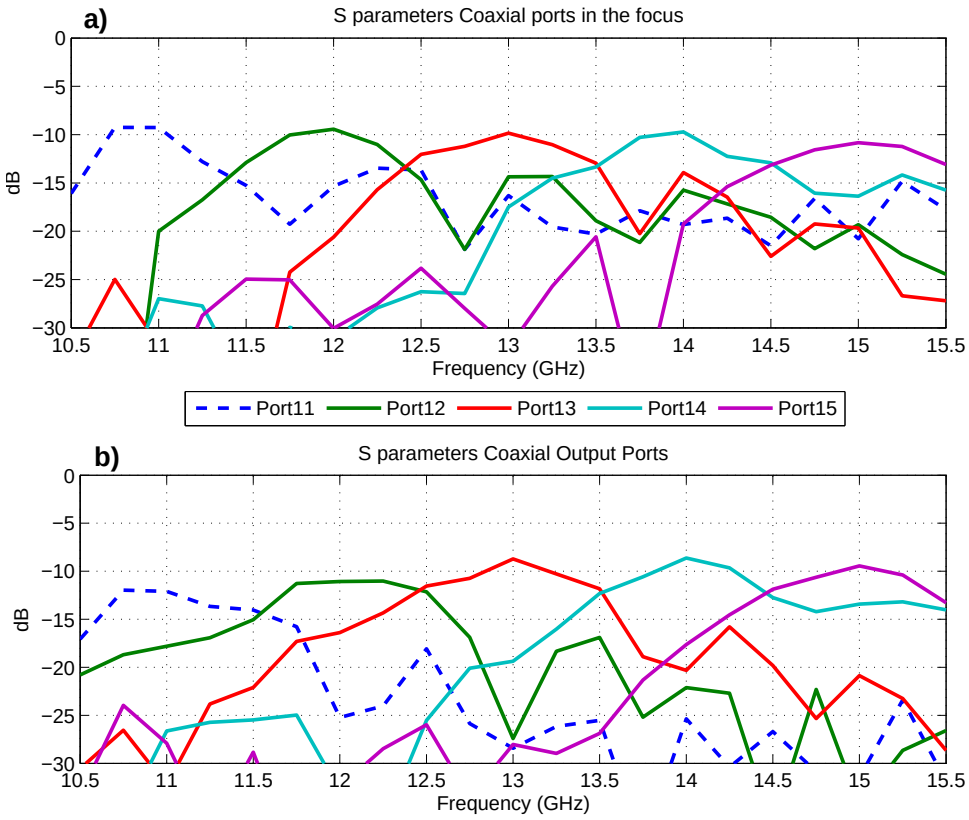

Figure 4.8: Aligned and focus coaxial output ports S parameters.

Figure 4.8 shows S parameters for both focus and aligned structures. For 11GHz and 12GHz ports the first structure gets better levels. This is due to the remoteness of these two ports to theirs focus for the second structure b). However, the other three ports are closer to theirs focus and they obtain better levels. The curious issue is that even not being exactly in the focus they obtain better levels that the focus-located structure. This has to be due to the non-overlapping between ports, thanks to the aligned design.

Now we have seen the idea works, we can start to think in some modifications. But due to time and space limitation this work remains as a future line of work.

Chapter 5

Aligned SIW Ports

Because we are using the leaky-wave technology for the antenna, it seems logical to use this same idea to the output ports. To make the design simpler we use from now on PEC walls. When we obtain a definitive design we'll replace the walls with via holes.

5.1 Aligned SIW Ports Wall To Wall

We use the same idea that in 4.2, in order to locate ports aligned at the same distance from the SIW aperture. But with the SIW technology for the ports, separated by PEC walls 5.1 . These walls have the same height than the substrate, d/2 (0.5mm) wide and 20mm long. The substrate is cut at this distance (60+20mm) to set the ports. Like in the coaxial definition, each port is centred in his frequency's focus, using the same five frequencies (five ports): 11, 12, 13, 14 and 15GHz. In this wall to wall case we put each wall in the middle point between two adjacent focuses. All output ports are defined as HFSS's wave ports.

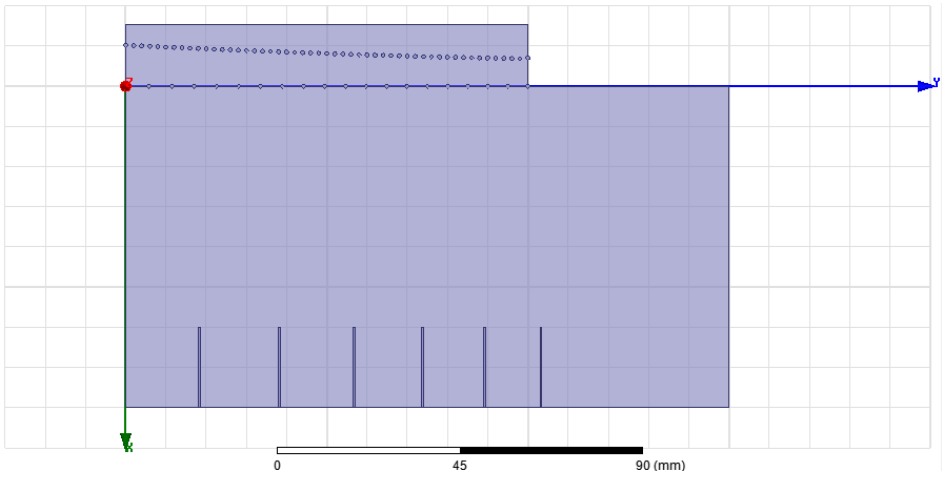

Figure 5.1: Aligned SIW ports wall to wall.

We use PML in all outer walls. We can see the complex magnitude of the E-field for all frequencies in 5.2 .

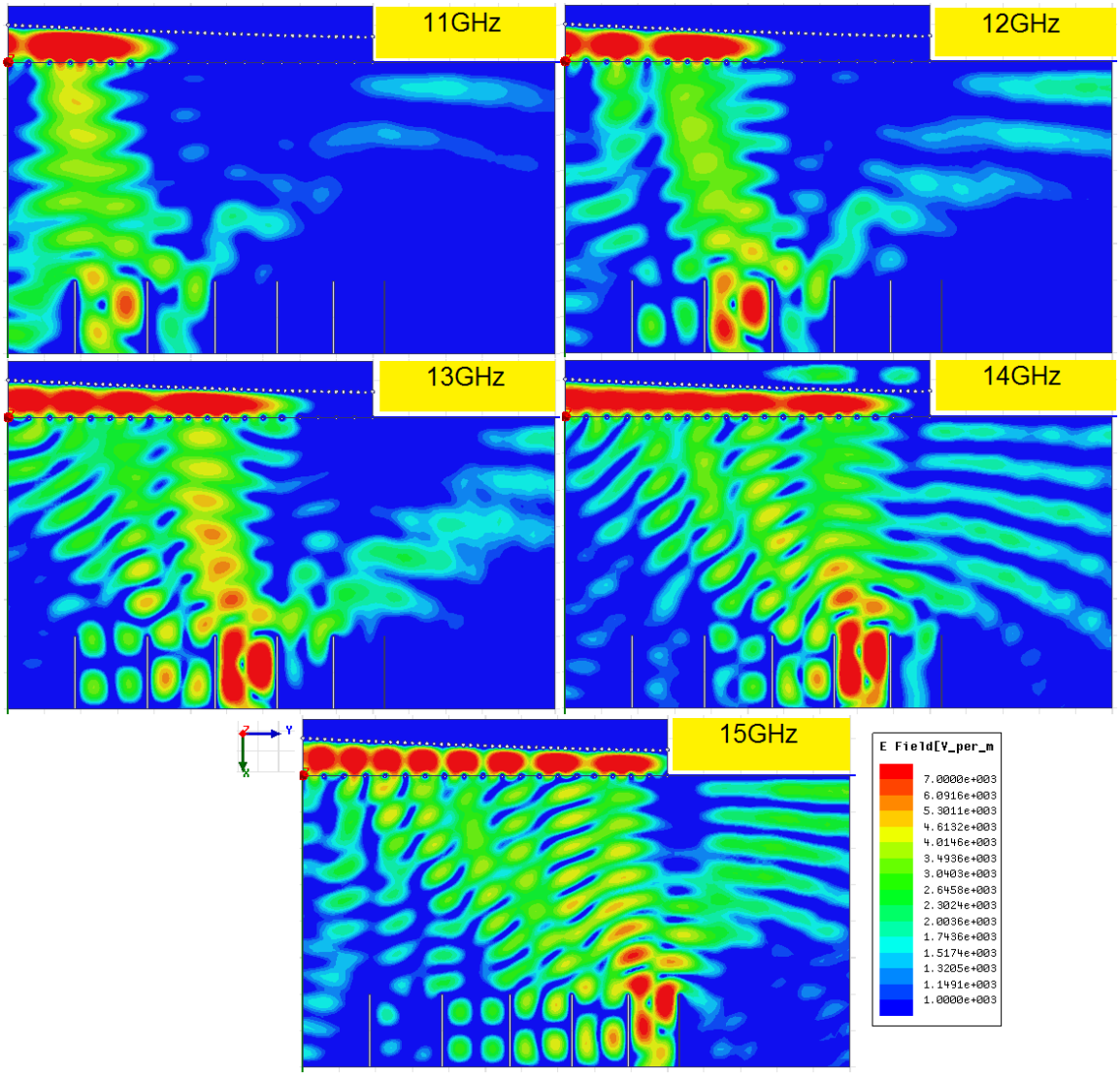

Figure 5.2: ComplexMag of E-field for aligned SIW ports wall to wall.

It can be seen a mayor quantity of energy going to the expected ports, although there is energy straining into other ports. There is also reflected energy addressing to the PML walls. Due to the chosen widths it seems all ports are collecting the TE_{20} mode.

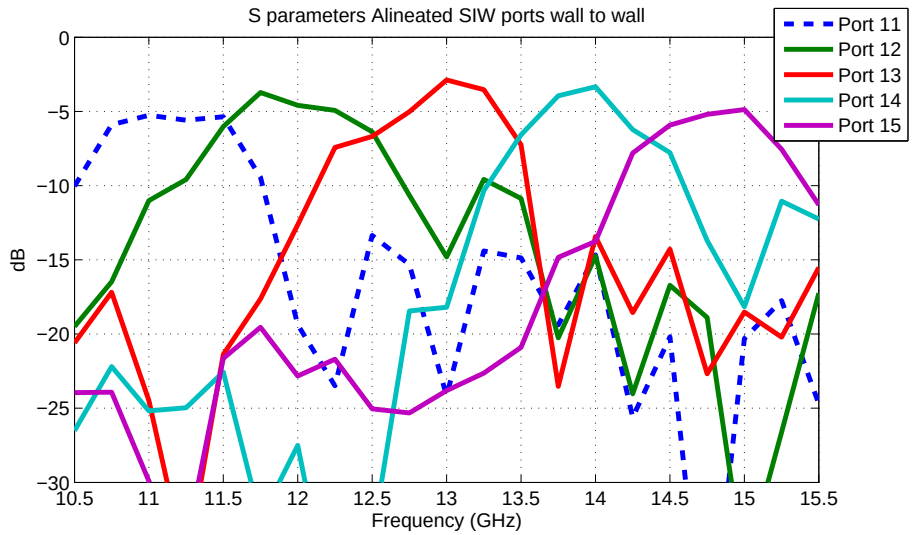

Figure 5.3: Aligned SIW ports wall to wall S parameters.

The S parameter representation 5.3 shows the same idea. It could be a bad response, but it can be seen the principal idea of the multiplexer: at the frequencies of interest we have the maximum captured energy and some rejection between ports.

The worst responses are port 11 and 15. At 11GHz the focus are near the antenna, but however, its port is at 80mm. At 15GHz, we have the real focus behind its port, so an important quantity of energy isn't yet addressing to the centre and it will exist important reflections in the walls.

5.2 Aligned SIW Ports With 1GHz Of Bandwidth

We may be interested in seeing the structure response for some given bandwidth, for example 1GHz. In the next table it is represented for each frequency the position each port occupies (focus), the minimum width they must present to have at least the fundamental mode out of cut-off and the width we are going to use. For example, for the 11GHz, we want frequencies from 10.5GHz to 11.5GHz, so we obtain the port width from it lower frequency (upper wavelength), 10.5GHz.

f(GHz)	y_0(mm)	$\lambda/2$ (mm)	Real width (mm)
11	28	9.2	9.63
12	48	8.4	8.79
13	65	7.8	8.09
14	82	7.2	7.49
15	96	6.7	6.97

Using this rule there will remain gaps between ports. We fill them with Dummy Ports 5.4 . With these ports we try to collect all the leftover energy. Therefore there are four Dummy Ports whose widths are presented in the next table.

Dummy Port	widht (mm)
1	9.787
2	7.558
3	8.209
4	5.767

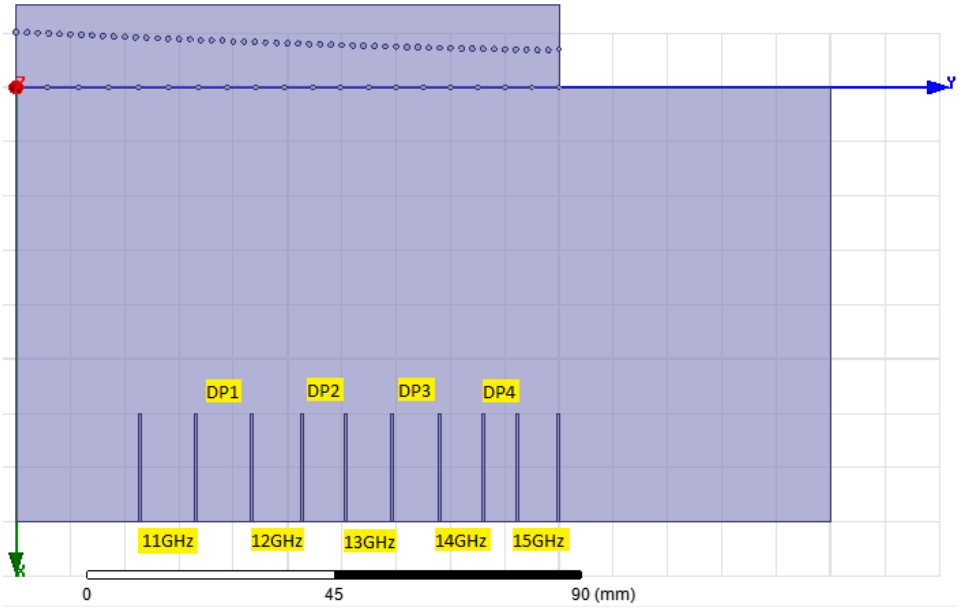

Figure 5.4: Aligned SIW ports 1GHz of Bandwidth.

The next figure shows the complex magnitude of E-field for all frequencies 5.5 .

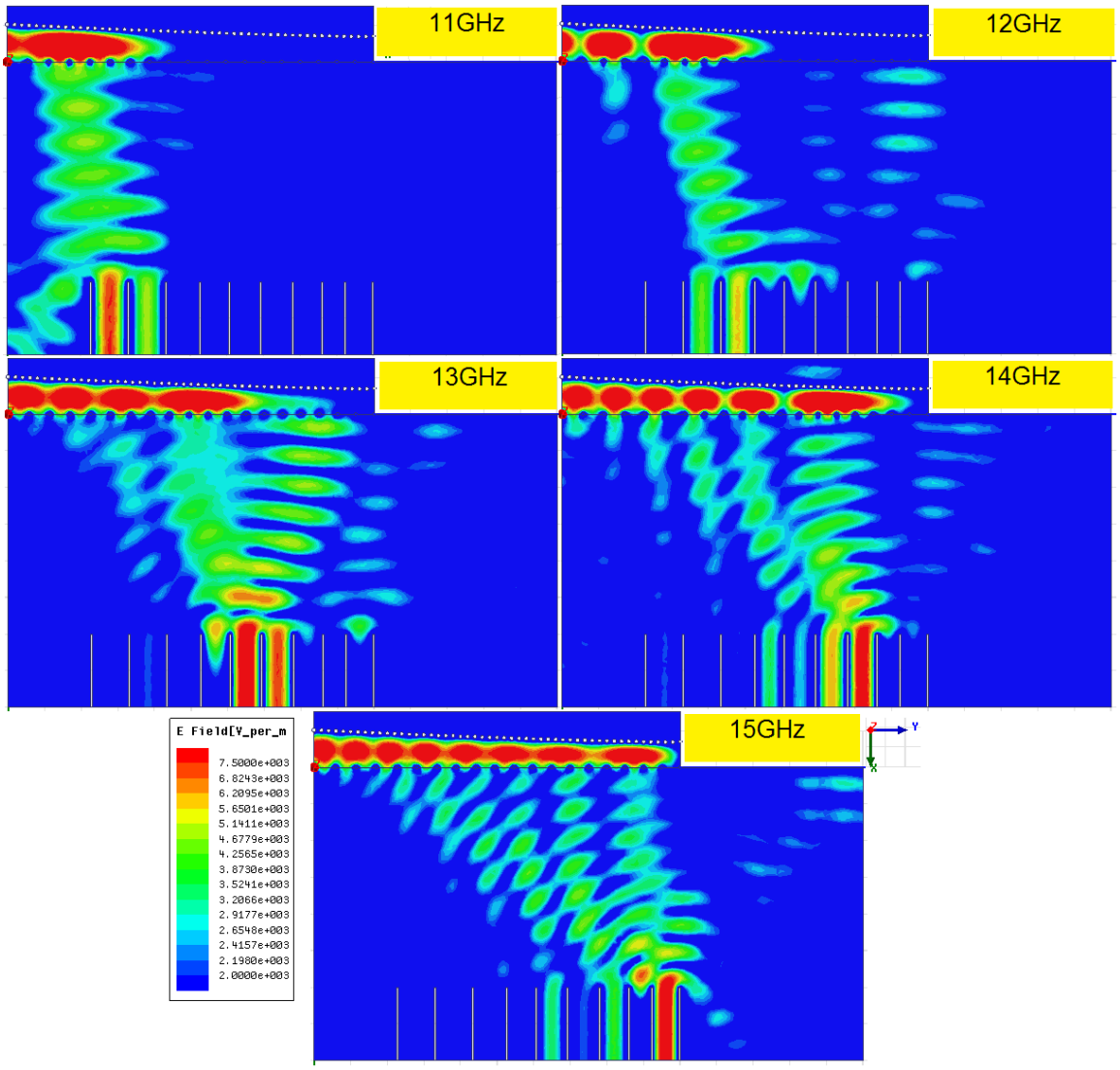

Figure 5.5: ComplexMag of E-field for aligned SIW ports 1GHz-BW.

We see how the Dummy ports certainly absorb energy. There is nevertheless one clear exception: the last Dummy before port 15 (DP4). The reason for this block could be that the port at this frequency is at cut-off. Its width (5.76mm) is actually smaller than 15GHz cut-off wavelength (6.74mm). In fact, if it is at cut-off for this frequency, it is for all the others because this is the highest frequency (smallest width). There is again energy straining other ports and reflected energy addressing the PML walls.

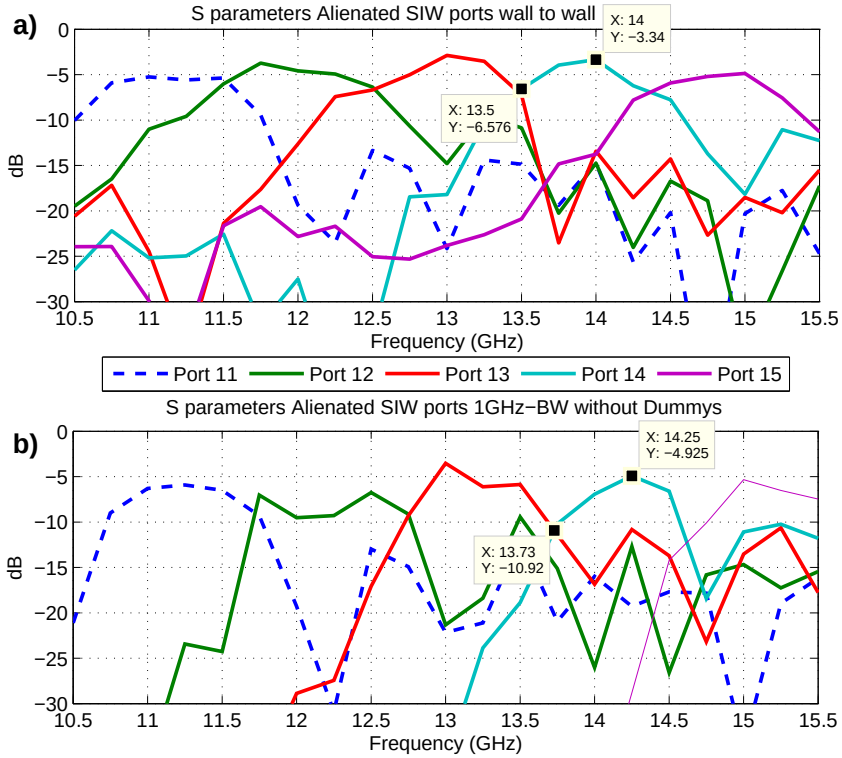

Figure 5.6: Aligned SIW S parameters with markers.

Figure 5.6 shows the S parameter representation for the wall to wall and for the 1GHz-BW structures, both with markers. It can be appreciate the increase in the ports rejection in b). It can be seen with the marked port, port 14. For the wall-to-wall structure a), the difference between the minimum and the maximum is 3.2dB, meanwhile, for the 1GHz-BW structure b) is 6dB. It has been increased therefore 3dB. Due to the Dummy Ports inclusion, the medium collected energy for all ports has been reduced. In the wall-to-wall case there were some levels above -5dB, but now only the port 13 is above this value. It can be also seen that the maximum for a given frequency is not centred in its frequency but shifted at upper frequencies. This may simply be due to we don't have any port in it real focus.

For figure 5.6 the Dummy Ports S parameters have not been represented. They all can be seen in the next figure 5.7, where it is shown the complete representation for the S parameters with all the Dummys, seeing this way how they absorb the middle energy, contributing to the increase in the ports rejection.

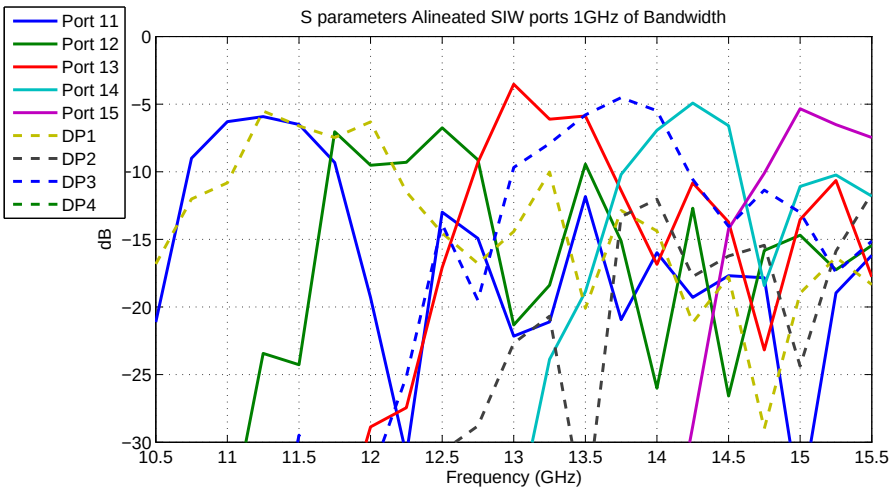

Figure 5.7: Aligned SIW ports 1GHz-BW S parameters.

5.3 Aligned SIW Ports With 0.5GHz Of Bandwidth

Now we can try to use a smaller bandwidth, 0.5GHz. This means that we will have narrower ports and wider dummy ports. Following the same steps, we firstly elaborated a table containing the ports location, the cut-off wavelengths for the TE_{10} modes and the ports width given the new 0.5GHz-BW.

f(GHz)	y_0(mm)	$\lambda/2$ (mm)	Real width (mm)
11	28	9.2	9.41
12	48	8.4	8.61
13	65	7.8	7.93
14	82	7.2	7.35
15	96	6.7	6.86

In this case we also have gaps for the Dummy Ports 5.8 . In fact, they will be wider due to the decrease in the ports, like the next table shows.

Dummy Port	widht (mm)
1	9.993
2	7.73
3	8.36
4	5.894

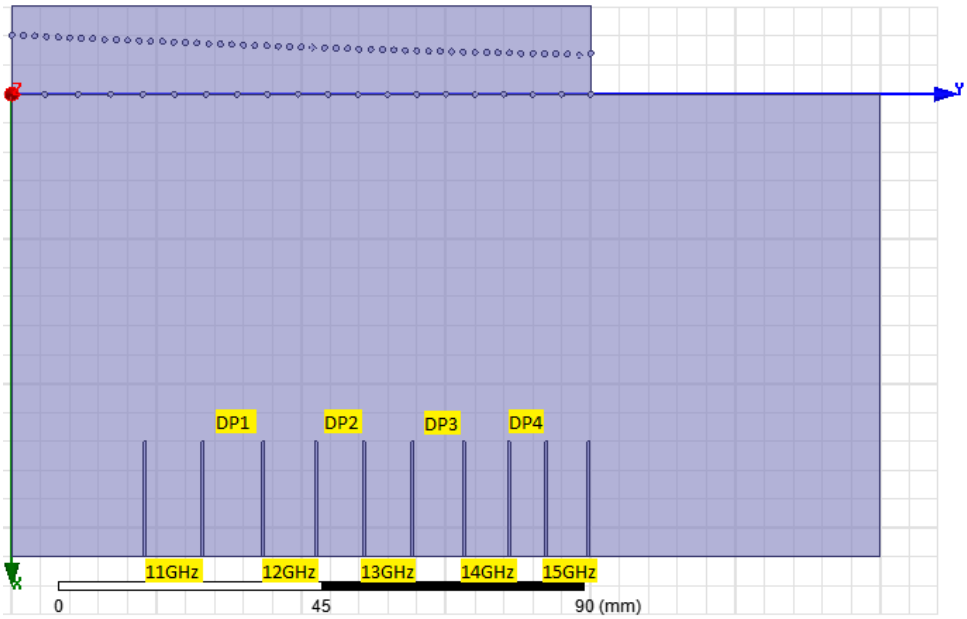

Figure 5.8: Aligned SIW ports 0.5GHz of Bandwidth.

We show again the complex magnitude of E-field for all frequencies 5.9 .

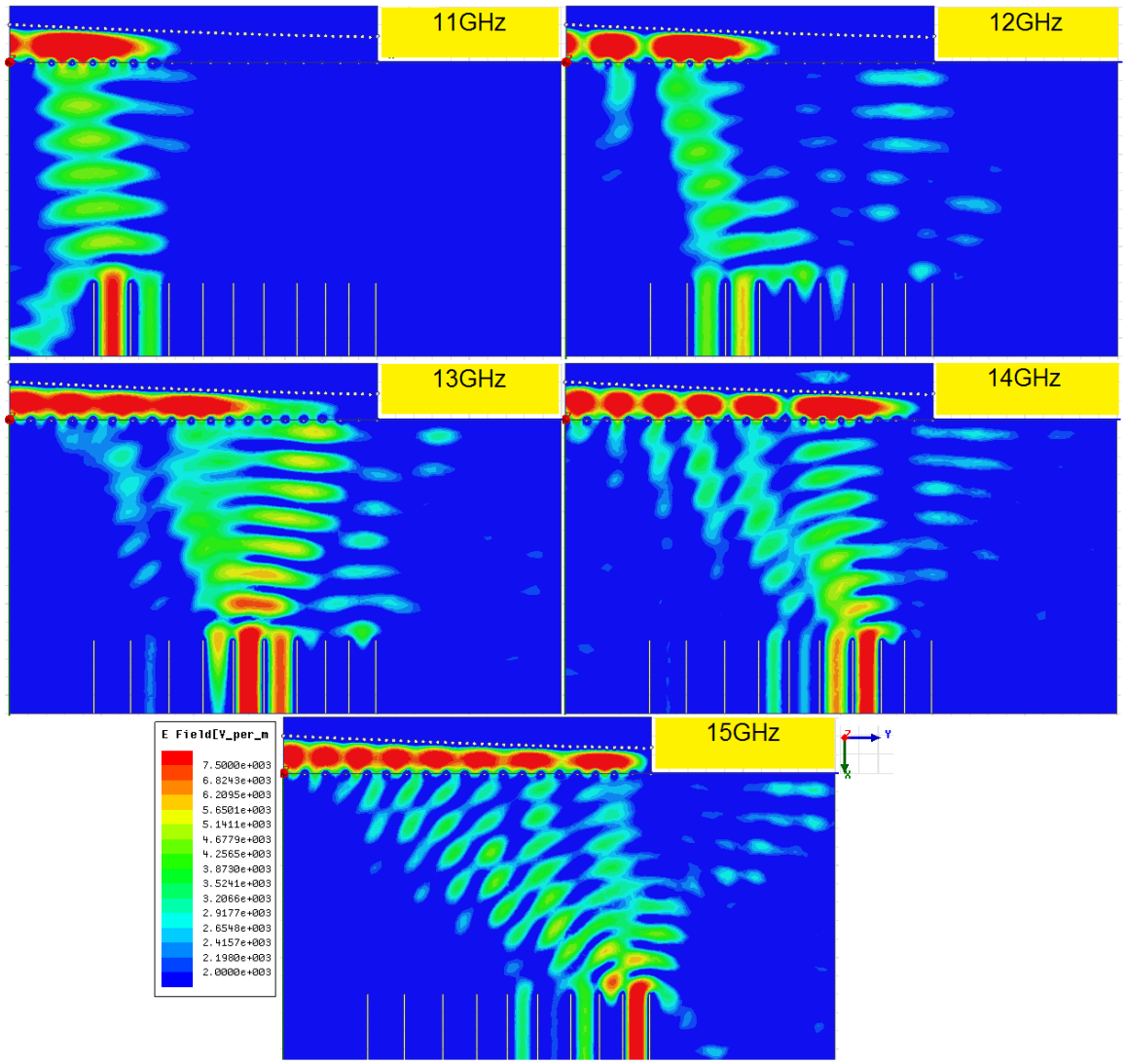

Figure 5.9: ComplexMag of E-field for aligned SIW ports 0.5GHz-BW.

In this case all ports are thinner, and because of that the Dummys collect more quantity of energy. For this reason there is more leftover energy addressing the PML walls. Although the Dummys are wider, the last one is at cut-off again because, even in this case (5.894mm) is lower than the 15GHz cut-off wavelength (6.74mm).

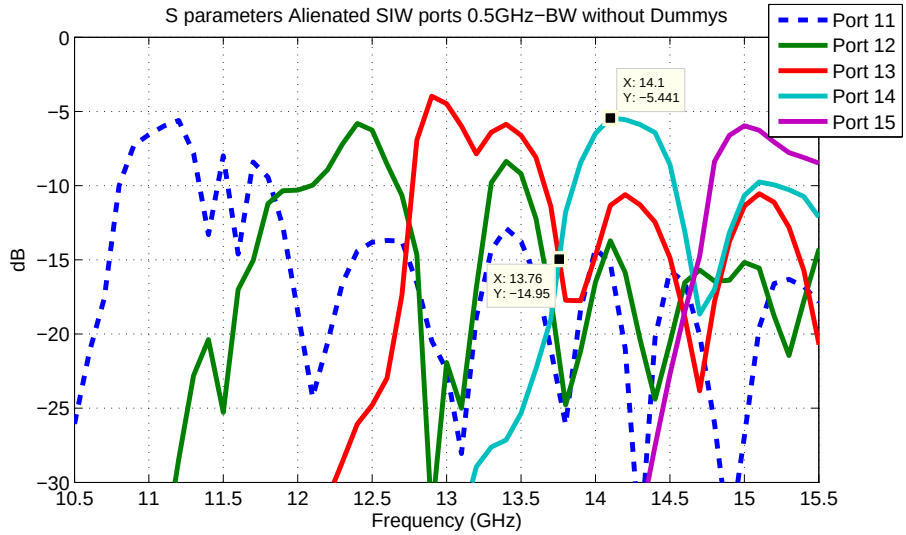

Figure 5.10: Aligned SIW ports 0.5GHz-BW S parameter with markers.

Figure 5.10 shows with markers, the rejection level for the port 14 like in the previous case. Theoretically, because we have reduced the ports width (increased the Dummys width), they should catch a lower level of energy (they are thinner; and the Dummys are wider so they collect more), and there should have more rejection between ports.

In comparison with the 1GHz-BW, the diminution in the absorb energy by the real ports is not so clear because there are some changes in the levels form. But the diminution has been less abrupt than in the previous case, so maybe this is not so easily visible. In the other hand, the rejection between ports has been clearly increased because of this diminution. For port 14, between the minimum and the maximum there is a 9.52dB separation, 3dB upper than the previous case.

Next figure 5.11 shows the complete S parameter representation with all the Dummy ports.

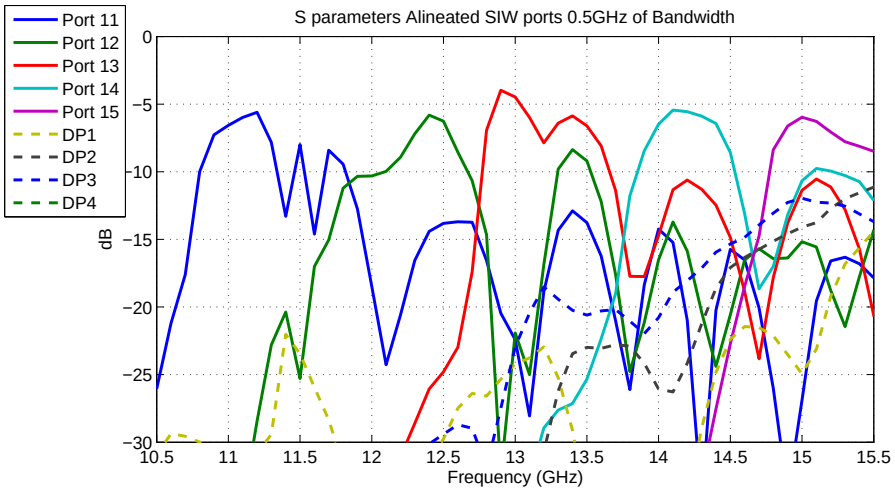

Figure 5.11: Aligned SIW ports 0.5GHz-BW S parameter.

Chapter 6

SIW Ports in the Frequencies focus

Until now we've been mainly using aligned ports, both for the coaxial and the SIW design. We have talked already about the principal disadvantage of this design: some ports are far from their energy focus. But it seems logical to benefit from the antenna focusing design. This means trying to set every port in its real energy focus (as it was done in 4.1). Doing this we make sure we are taking the maximum quantity of energy for each frequency (for the coaxial design we saw this is not so obvious). But firstly, we need to define some parameters that will help with the design.

6.1 Design Parameters

All the parameters 6.1 explained here will have strong influence in the final multiplexer frequency response:

- Central frequency of each channel
- Insertion losses of each channel
- Bandwidth of each channel
- Rejections between channels
- Ripple in the bandwidth

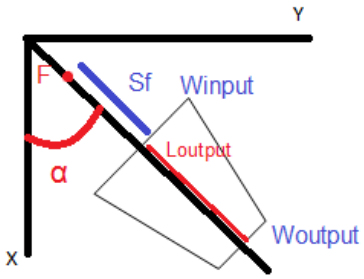

Figure 6.1: Design parameters.

6.1.1 Angle α

This is the parameter explained in 3.6.

6.1.2 WINPUT

This line is the superior face (the aperture) of the polyhedron 6.1 that forms the output port. It can be designed as the center line's perpendicular or just orientated in the X-axis. For convenience, we will use the X's orientation. For its optimal calculation it is very hard to use a numeric way. We pursuit to get as most energy as possible avoiding overlapping/shadowing. In theory, it has two limitations:

- The width of the concerned frequency pulse: for quality issue, we can choose a 5 dB focal width.
- The overlapping with the nearest frequencies: if the WINPUT parameter is too wide, it can take energy from the nearest frequencies, or, in other words, it can make shadows for the nearest frequencies (usually the next one).

It has to be chosen between the maximum aperture for the 5 dB even if we make shadow for the next one, not to make shadows even if we haven't the maximum aperture, or the middle point. It has been demonstrated that the best choice is the second one: it has to exist the minimum shadow.

6.1.3 LOUTPUT

This is the length of the polyhedron 6.1 , or, in other words, the line that separates the centers of WINPUT and WOUTPUT. It can be set as λ_0.

6.1.4 WOUTPUT

This is the inferior face of the polyhedron 6.1 and it has to be a perpendicular from the center line because this is the real output port. It has to be above $\lambda_0/2$ so that TE_{10} mode of the SIW is not below cut-off, and, it has to be below λ_0 so that TE_{20}

is below cut-off. The final width will change if we want some bandwidth limitation (1 GHz of BW, 0.5 GHz of BW, ...).

We suppose we have three frequencies: f_0, f_1 and f_2. f_0 represents the central frequency and the other two define the bandwidth ($f_1 < f_0 < f_2$). The minimum frequency gives us the biggest cut-wavelength (λ_1), so its $\lambda_1/2$ will be the minimum port length. On the contrary, the wavelength of the upper frequency (λ_2) will give us the maximum port length to only have the elemental modes. To use a safe value, we'll choose the midpoint between $\lambda_1/2$ and λ_2. We've used 1 GHz of bandwidth.

We can see an example: f_0=15GHz (λ_0=13.484mm). So, with a 1GHz-BW f_1=14.5GHz (λ_1=13.95mm) and f_2=15.5GHz (λ_2=13.049mm). So the real value for WOUTPUT will be the midpoint between $\lambda_1/2$=6.974mm and λ_2=13.049mm, i.e., 10.01mm.

Anyway, in the first design 6.2 it has been use other criterion. This one will be introduced in 6.3.1.

6.1.5 SF

The distance between the real focus and the center of WINPUT 6.1 . This parameter is one of the most critical. Theoretically, the port should be in the focus. But for all the limitations explained above, this is an impossible issue. So, with this parameter we measure the deviation from the focus. We'll have to think about these two issues about the ports:

- Having them as close as we can to their focus.
- Trying to avoid shadowing as much as we can.

6.2 First Design

As we said before, the ideal position for the ports would be their focus location, but this is going to be impossible to realize. So the first thing to decide is where we put them. The port that will suffer more because the shadowing will be the farthest, i.e., port 15. It is useful to draw a line 6.2 that helps us to know the minimum distance from the antenna.

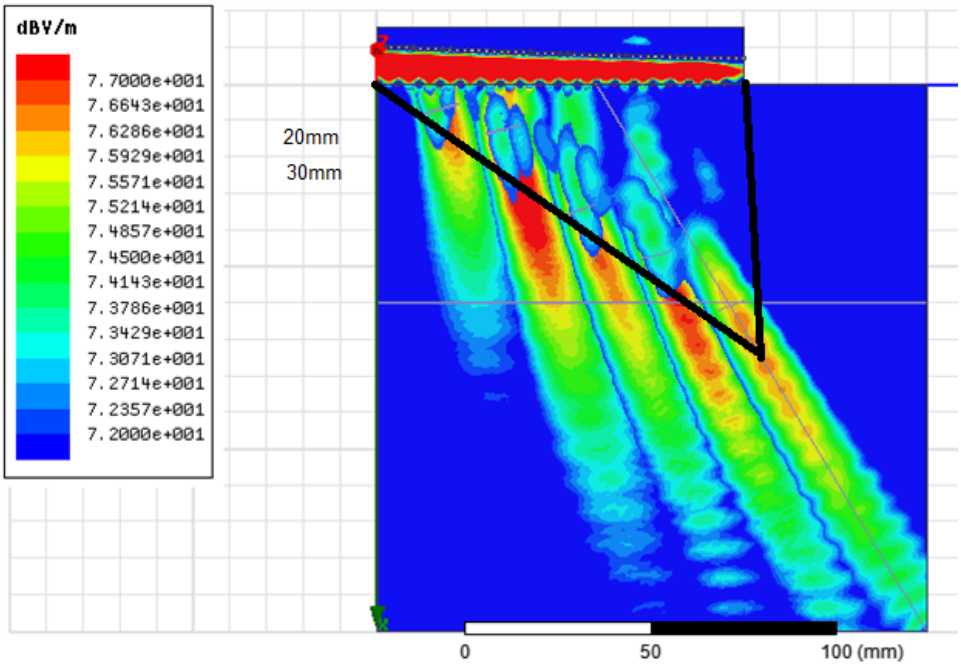

Figure 6.2: Drawn line to port 15's focus.

We know all ports have to be behind this line. And, of course, this is not an absolute rule; some energy may be behind this point, so it is advisable to let some margin. Anyway, the most critical port's distance to decide is port 11's, because it is the most advanced and it'll be the farther to its focus.

We can start by setting port 11 above 30mm, for example, 34mm. This means a distance separated from its focus of SF = 21.29mm. The LOUTPUT parameter will be, as we said before, for this port and for all the others λ(for each frequency). Other unchanged parameter is angle α, which will always be the same for each frequency, as the energy's direction is always the same. As we said in the WINPUT description, this parameter won't have a numeric value, due to its complexity. We try to set it not doing shadowing to the next port and, in a minor way, trying to collect the maximum quantity of energy 6.3 . For WOUTPUT parameter we set it as a value higher than frequency port's $\lambda_0/2$ and lower than width calculated in 5.2 6.3 . We do the same for all the other ports.

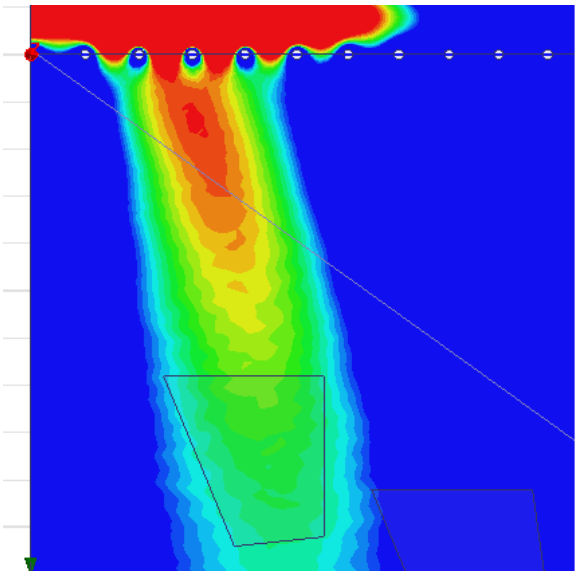

Figure 6.3: Example for polyhedron's port 11 orientation.

It can be seen that port 15's WINPUT is placed before its focus (negative sign). We can do this because this is the last port of interest, so it won't be able to make shadowing. As we can see in 6.4 , once we have all the polyhedrons defined, we eliminate all the leftover substrate and place all the "wave ports" for the output ports.

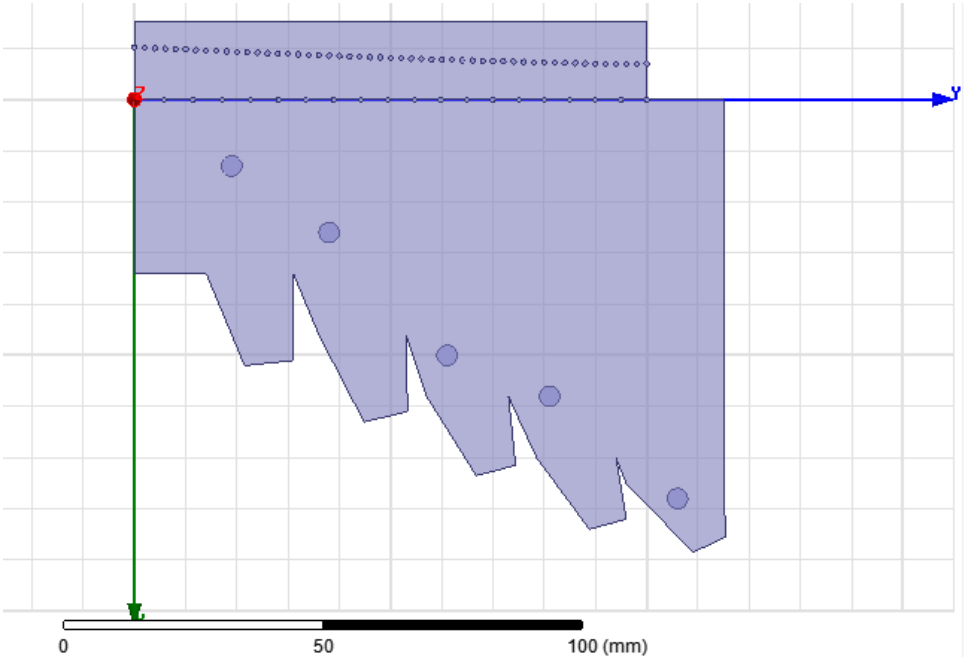

Figure 6.4: First design.

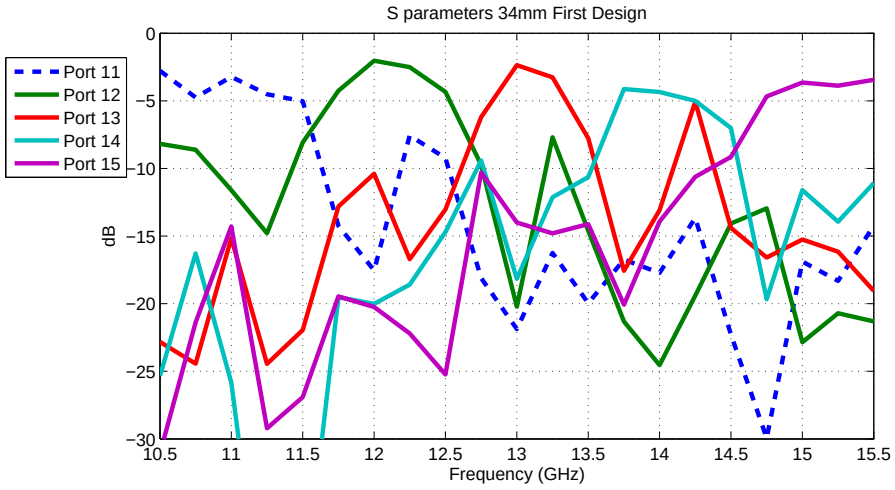

Figure 6.5: First design S parameters.

Figure 6.5 shows the S parameters for this first structure. They are not indeed bad results. We have some well defined bands. But we have to remember that we are using PML. And anyway, some ports have low levels or high secondary lobes. We have to make some changes to improve these results.

We can resume all the ports parameters in a table.

Port	α(deg)	ΔW5dB (mm)	WINPUT (mm)	LOUTPUT (mm)	WOUTPUT (mm)	SF (mm)
11	8.75	18.25	17	18.39	9.55	21.29
12	15.07	13.35	17	16.85	8.73	21.036
13	18.78	15.53	16	15.56	7.96	8.96
14	24.14	15.24	15.5	14.45	7.47	13.108
15	30.53	16.13	19	13.5	7.07	-3.2

Angle α remains unchanged. In fact, as we know, this is an antenna's parameter, so it will always have the same value. Comparing antenna's parameter ΔW_{5dB} and ports parameter WINPUT it can be seen some differences in some ports. All ports have been design, as we know, with the balance between overlapping and footprint's width, so in some cases WINPUT is wider, and in others it is narrower. LOUTPUT is each frequency's λ.

6.3 Changing the First Design

Now we are going to try to improve the first design adding changes to some of these parameters or to other parts of the design.

6.3.1 Changing the WOUTPUT parameter

In the first design we settled the WOUTPUT parameter to a value between $\lambda_0/2$ and length obtained in 5.2 . With this setting it's true that we have spreading the fundamental mode, and TE_{20} mode at cut-off. But until breaking this last cut-off we have some margin. And it is logical to think that if we have wider ports we'll be able to collect more energy. So, we can try to enlarge the ports's width to a value between $\lambda_1/2$ and λ_2, as explained before in 6.1.4 6.6 . In the next table we can see the new values.

Port	WOUTPUT (mm)
11	13.61
12	12.49
13	11.53
14	10.72
15	10.01

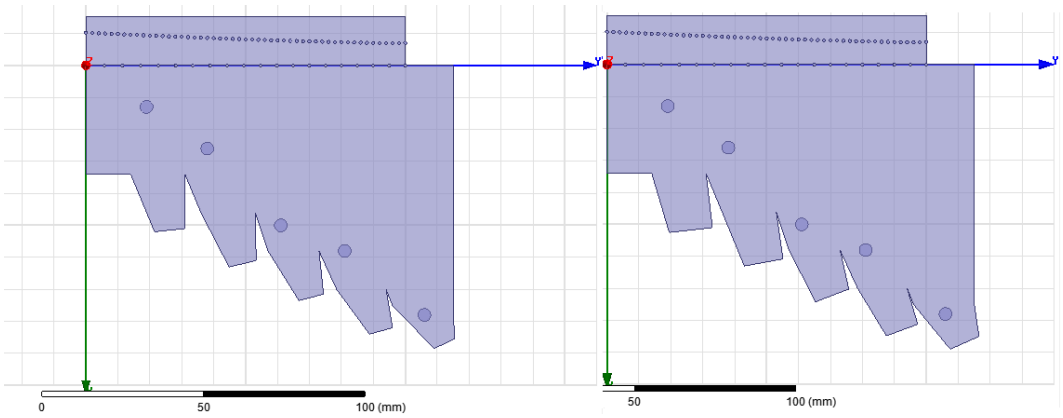

Figure 6.6: First and second designs.

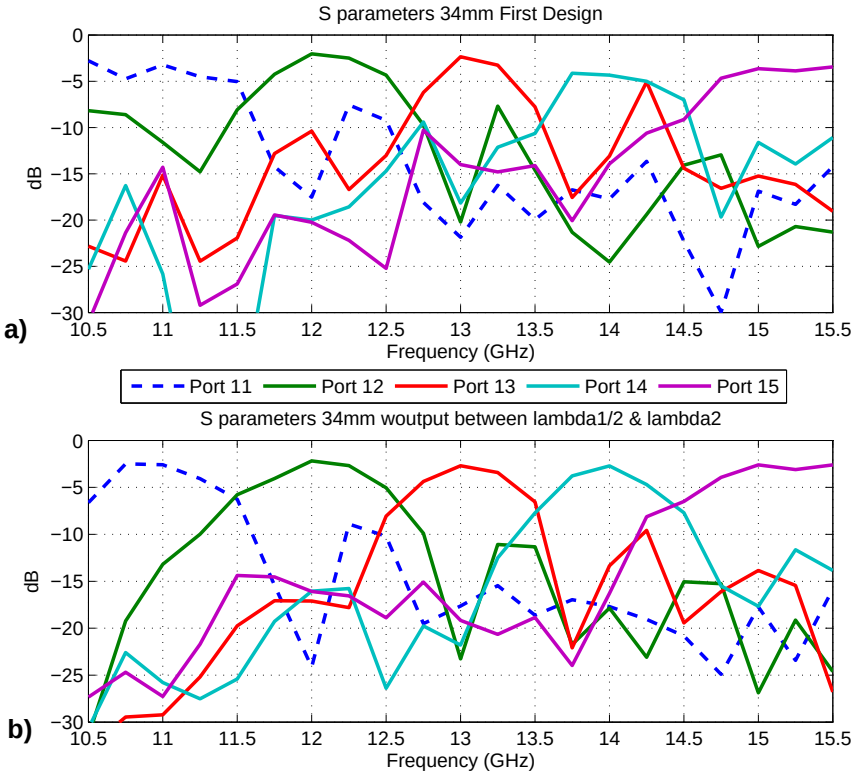

Figure 6.7: First and second designs S parameters.

We can obtain some conclusions comparing both S parameters representations 6.7 . The medium energy level for the five ports has been increased in b) because the ports are wider and we can capture more energy. The bandwidth of all ports has increased due to, now, more elementary modes of more frequencies are out of the cut-off.

In the future, we can be interested in having more selective bandwidths (or even less). The only thing to do is change values f_1 and f_2 to get the desired bandwidth. From now on we'll use this wide for the ports.

6.3.2 Changing the LOUTPUT parameter

At the moment of the parameters definition it was settled LOUTPUT to λ_0 for all the ports. It is probably, the minimum logical length to choose. But we don't know what happen if we make it higher. To be certain we choose the best option, we compare the LOUTPUT length used until now, with a length of $1.5*\lambda_0$ 6.8 , using all the improvement achieved till now.

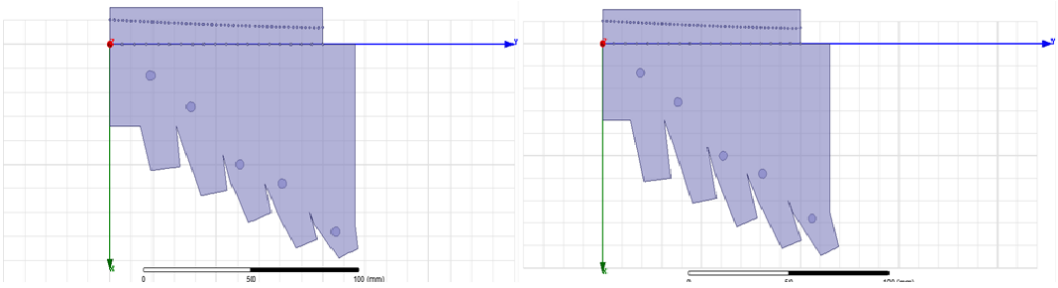

Figure 6.8: LOUTPUT for λ_0 and $1.5*\lambda_0$.

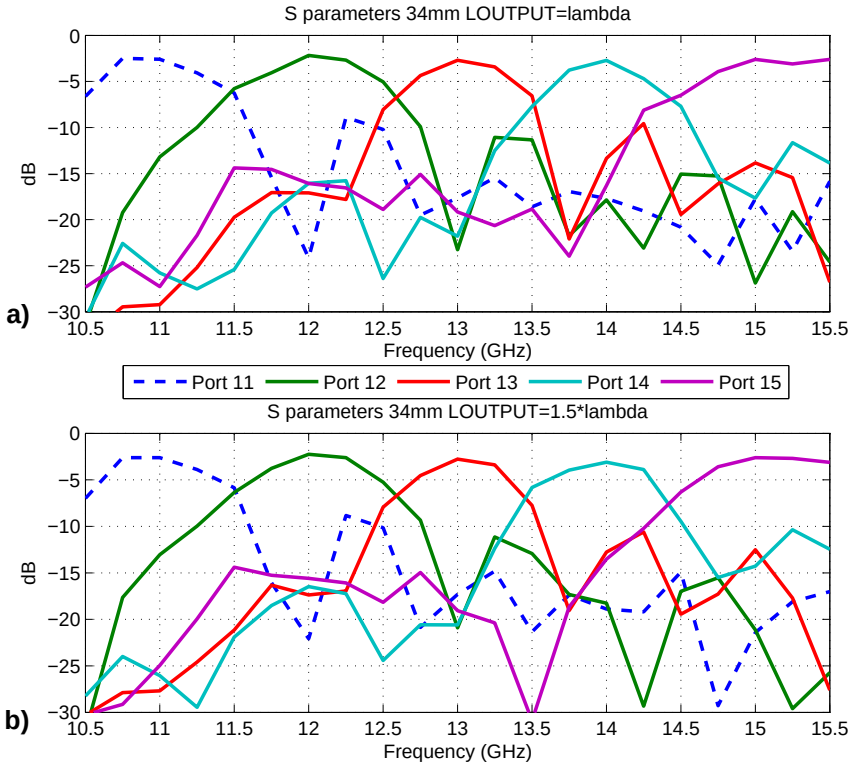

Figure 6.9: LOUTPUT for λ_0 and 1.5*λ_0 S parameters.

From 6.9 we can see some changes in somes levels, especially at the two last ports. From the results, it's difficult to decide between both of them, so to tip the balance we use the size criterion, preferring a smaller structure. So we keep a), the LOUPUT parameter at λ_0.

6.3.3 Changing the walls between ports

The walls of the actual structure (WOUTPUT changed) could be difficult to manufacture because of the gaps between them. They can be united to avoid this gaps, with PEC walls separating them 6.10 . In the future, we'll replaced these new walls by via-holes.

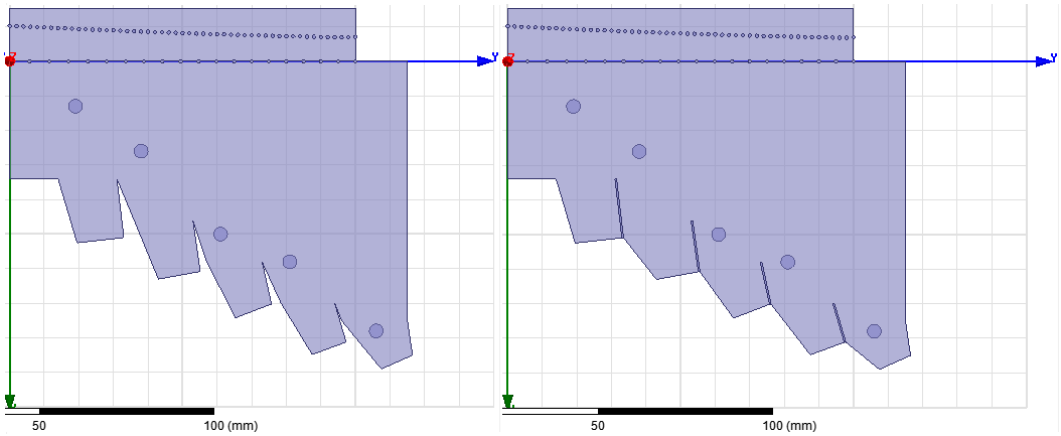

Figure 6.10: Gaps between walls and united walls structures.

These new walls introduce some modification to the defined parameters. Doing this union we are changing the length and inclination for WINPUT. We can see in 6.11 the re-definition of this parameter for the port 11, 12 and 13, compared with the previous design. Because port 11 is the first one, it doesn't need this change. To design this new polyhedron, we design it firstly as before. Once we have all the polyhedrons we unite theirs left walls with the right walls of theirs left ports. And finally, we introduce the PEC walls.

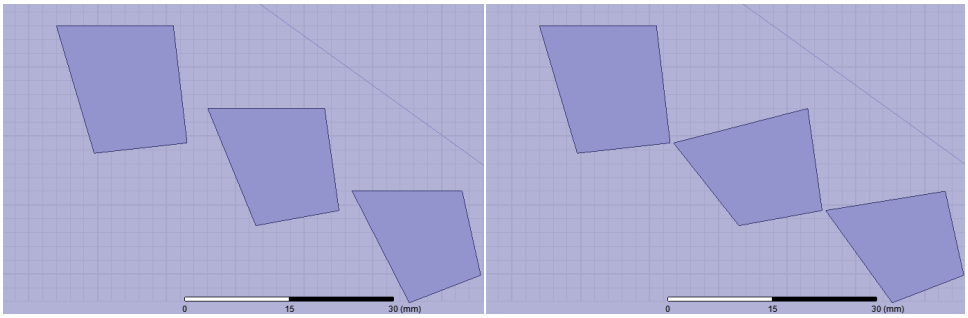

Figure 6.11: Old and new polyhedron design.

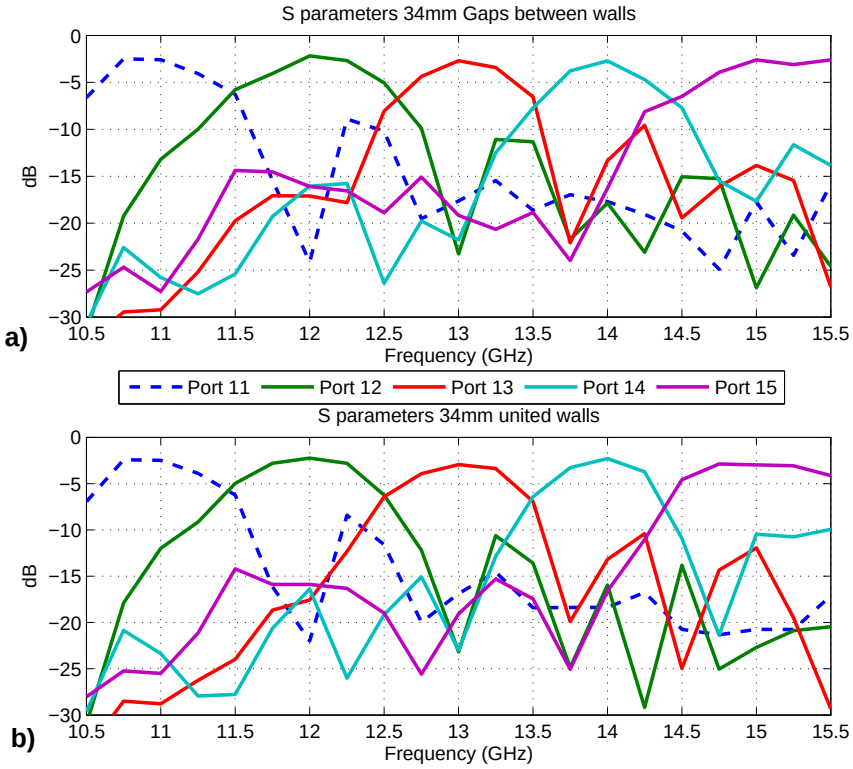

Figure 6.12: Gaps between walls and united walls S parameters.

As we see in 6.12 it's difficult to say which of both S parameter representations is better. Some levels go up, others go down. In some cases we increase the rejection between channels, in others it goes worse,... but all in quite small variations. So we can choose b) for its more compact design.

6.3.4 Changing the external walls orientation

We are been keeping untouchable till now the external walls orientation. We may think that oriented external walls from the antenna to the ports should help to guide the energy to the ports. It's true we are using PML for the external walls. But even with the PML, not the 100% of the leftover energy will be absorb. So, with oriented walls we can facilitate the energy path. So we try to orient right and left external walls like in 6.13 .

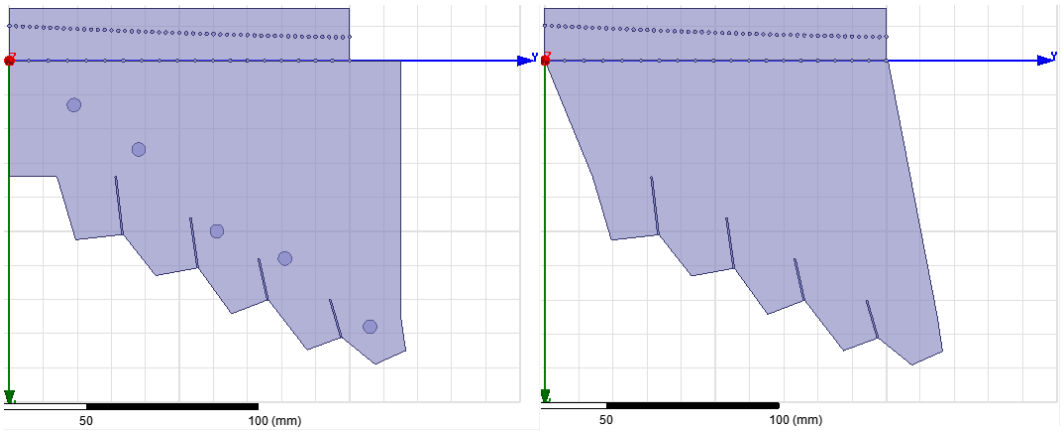

Figure 6.13: Original and 2-walls oriented structures.

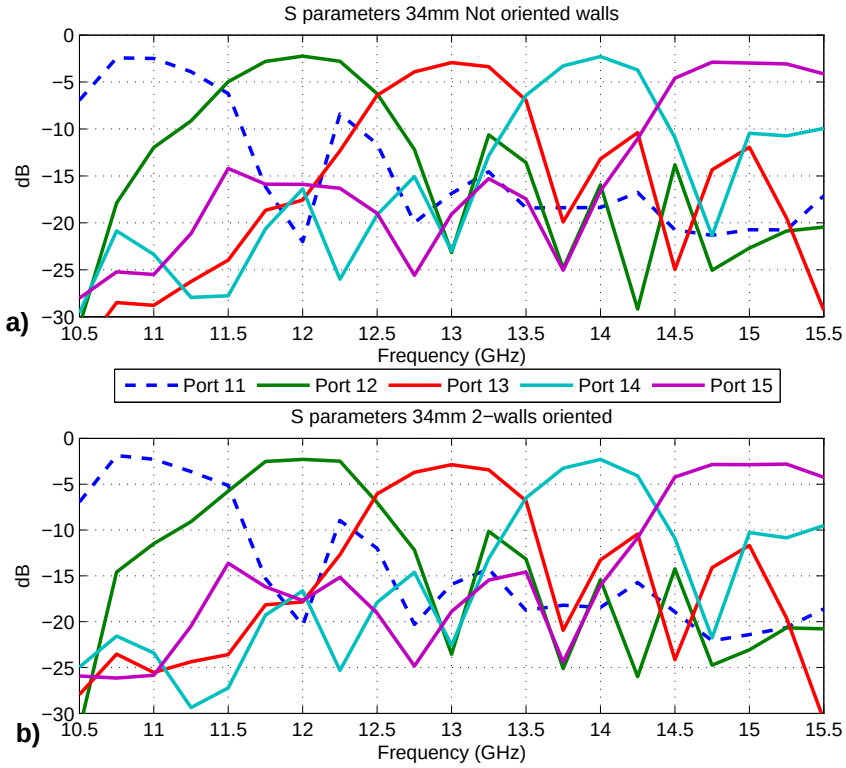

Figure 6.14: Not oriented and 2-walls oriented S parameters.

It can be seen from 6.14 that both responses are very similar. Maybe the walls help the energy to reach the ports, and, since there are no abrupt corners, the reflections are less dispersive. The 2-walls-oriented b) is a more compact structure, so we keep this last one.

6.3.5 Changing the orientation of the walls between ports

The idea is to avoid the possible reflections caused by these walls. Due to the original definition of the WINPUT parameter ,they are not perpendicular to the output ports and this could be causing some extra reflections. On the other hand, we will be decreasing the WINPUT parameter, having less energy entering through the port. We will have to compare 6.15 both results to find the best response.

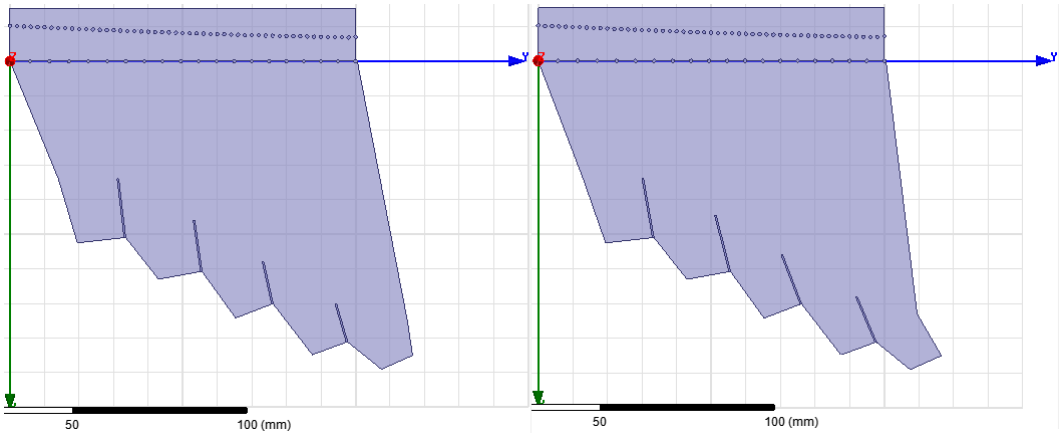

Figure 6.15: Normal and oriented walls between ports.

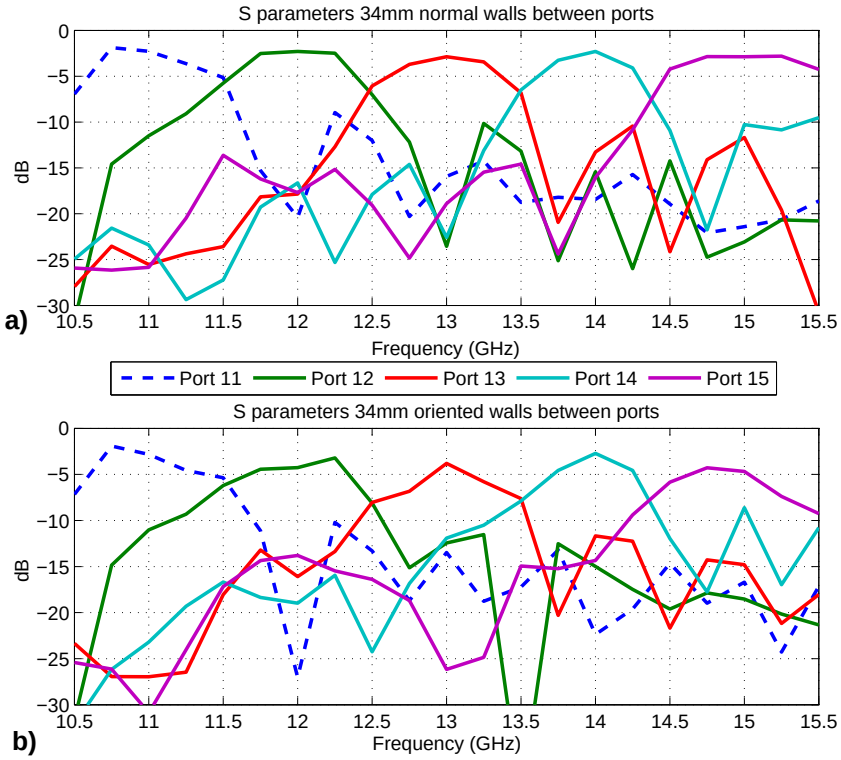

Figure 6.16: Normal and oriented walls between ports S parameters.

Seen the comparison between the two S parameters representation 6.16 it can be seen that some ports behaviour have worsened in b). Perhaps, with the new orientation we are discriminating an important quantity of energy, due to the decrease in the WINPUT parameter. We should remember we saw that it's more important not making shadowing to the next port that having a widely WINPUT parameter to collect as much energy as we can. So we already have a diminish WINPUT, we can't further decrease its size. We keep a).

6.3.6 Changing distance from the antenna

Since the first design till now we've kept the same distance from the antenna for all ports. The most critical distance of all is the first one, port 11. We settled to SF=21.29mm, or in other words, 34mm from the antenna. Now, we are going to try two more distances, nearer (27mm) and further (40mm).

34mm Vs. 27mm

There is no need to change all the ports location. We bring forward port 11 from 34mm to 27mm. We move a little its neighbour, port 12, because of the shadowing. Due to this slightly change we don't need to move port 13. And for the same reason, there is no need to move port 14, as well as port 15 6.17 . The main reason for this is to not move the last one, port 15, because it is already before its focus. If we move it forward to the antenna we'll move it away from its focus, entering this way in a more opened energy footprint. Due to the closeness between port 14 and 15 we can't enlarge theirs apertures. We can see in the next table the new SF setting.

Port	SF (mm)
11	14.19
12	18.63
13	8.96
14	13.108
15	-3.2

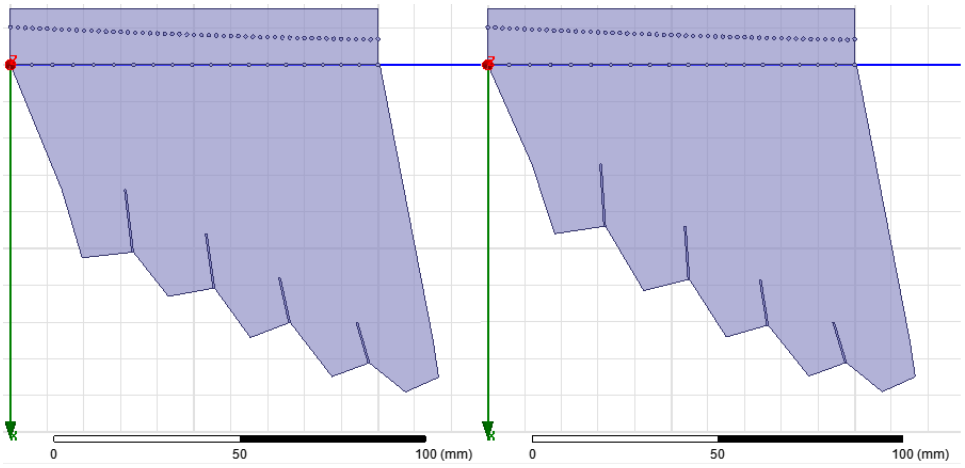

Figure 6.17: 34mm and 27mm port 11 distances.

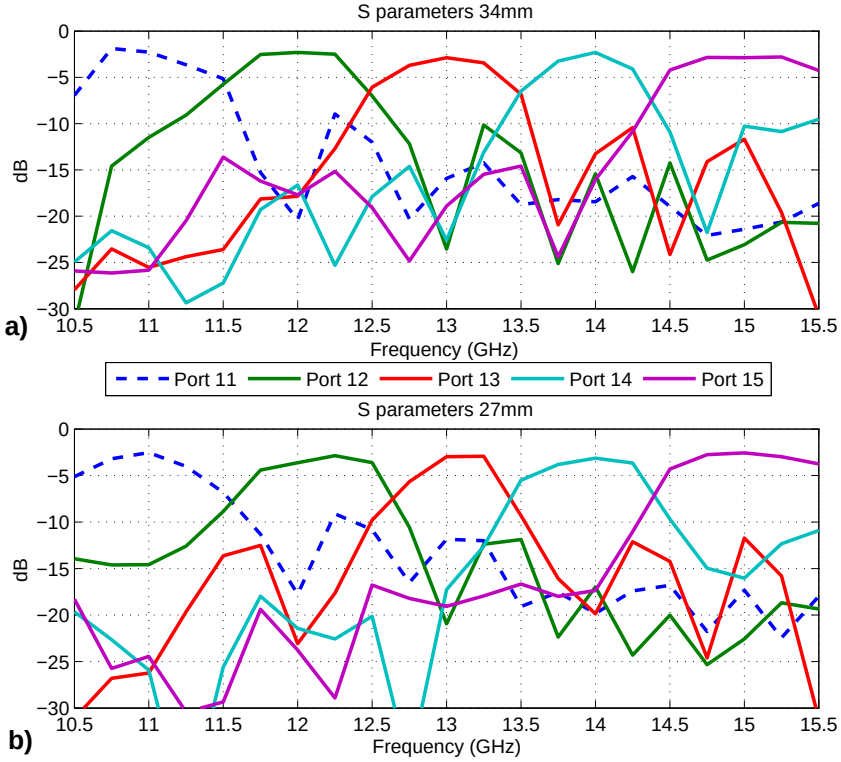

Figure 6.18: 34mm and 27mm S parameters.

It's difficult to choose one of them 6.18. For the new distance b) there are indeed some improvements, but we can't say so about port 12. The reason of the deterioration for this port may be due to the new shadowing caused by port 11. And this is something we can't change. For other ports deterioration for the 34mm case, however, we can act on them. But first, we need to see their behaviour without the PMLs. So for now, we maintain a), the 34mm distance.

34mm Vs. 40mm

For the same reason, we don't have again the necessity of changing all ports location 6.19 . Only 11's and 12's. The next table shows the new SF parameters.

Port	SF (mm)
11	27.66
12	25.15
13	8.96
14	13.108
15	-3.2

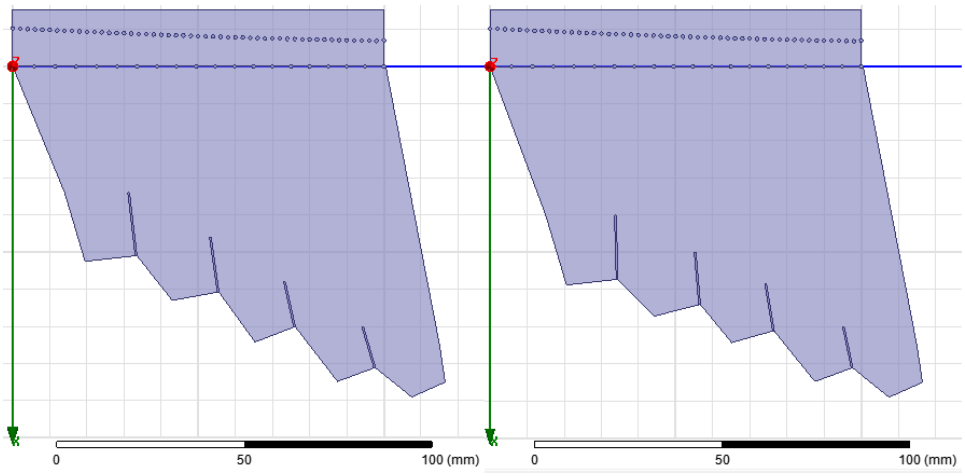

Figure 6.19: 34mm and 40mm port 11 distances.

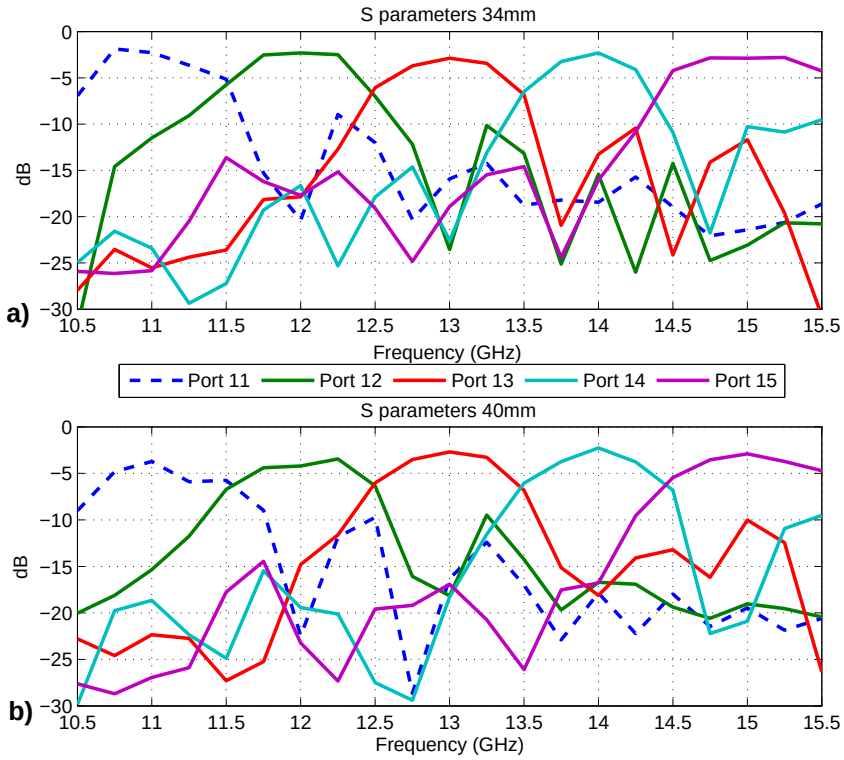

Figure 6.20: 34mm and 40mm S parameters.

Now 6.20 it's easier to see some deteriorations in ports 11 and 12 in b). They are too far from theirs focus. We keep a), the 34mm distance.

6.3.7 What we keep

A summary with all the changes made is presented here 6.21 :

- From section 6.3.1 we keep the middle point between $\lambda_1/2$ and λ_2 for the WOUTPUT parameter.
- From section 6.3.2 we keep λ_0 for the LOUTPUT parameter.
- From section 6.3.3 we keep the united-PEC walls.
- From section 6.3.4 we keep the two oriented walls structure.
- From section 6.3.5 we keep the same two oriented walls structure.
- From section 6.3.6 we keep the 34mm distance for port 11.

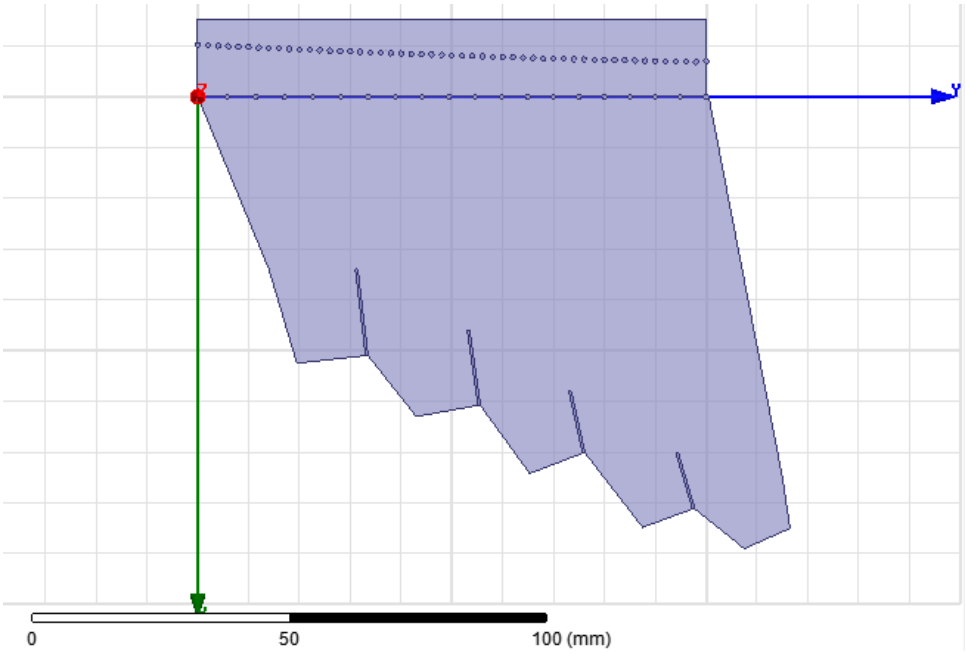

Figure 6.21: Structure after changes.

The next table shows all the ports parameters of the final structure.

Port	ΔW_{5dB} (mm)	WINPUT (mm)	LOUTPUT (mm)	WOUTPUT (mm)	SF (mm)
11	18.25	17	18.39	13.61	21.29
12	13.35	20.13	16.85	12.49	21.036
13	15.53	17.62	15.56	11.53	8.96
14	15.24	17.8	14.45	10.72	13.108
15	16.13	18.28	13.5	10.01	-3.2

There is no need to represent angle α, because as we said, it always has the same value. For WINPUT there are changes due to the new walls. Now, except ports 11 and 15, there has been an increase in the value due to the removal of the holes between ports. WOUTPUT has now other value (bigger) due to the changes explained. LOUTPUT and SF remain unchanged.

6.4 Adding ports 10 and 16

We've been introducing big-scale changes to the first design. It's true we've left some imperfect details. But we need to move on, because it's preferable to find first a big-scale design and then introduce later small-scale details than find for every change, the perfect match. The reason for this is that in this design we have a huge quantity of different parameters that affect the structure. Some new change could deteriorate the previous.

Therefore, the next step is to introduce the Dummy Ports (DP). Originally we use frequencies from 11GHz to 15GHz. Beneath 11GHz it's difficult to concentrate the energy in a focus, and above 15GHz it may have too shadowing due to all the other ports and to the closeness between the bigger frequencies, as seen in figure 3.6 c). But we can introduce one port beneath and one port above and use them as dummy ports 6.22 .

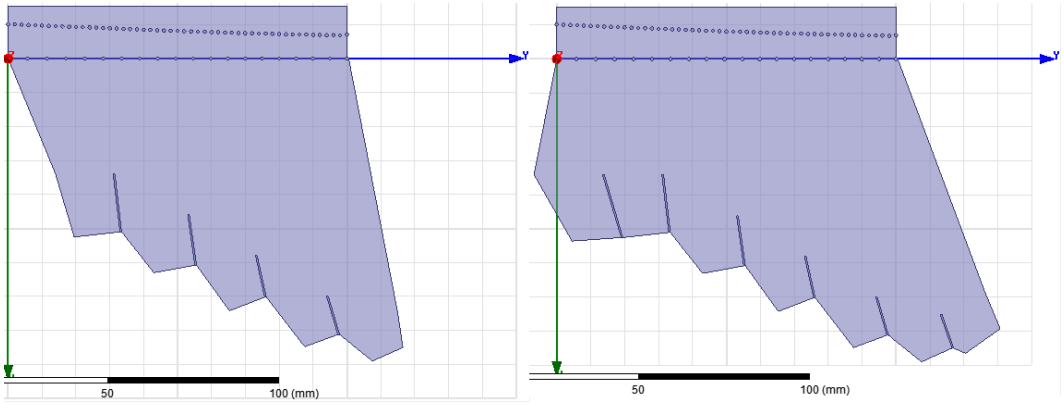

Figure 6.22: Introducing ports 10 and 16.

For port 10 WOUTPUT setting we've use the same criterion. But not for the port 16. If we use the same criterion, it'll be 9.39mm, and with this length we'll be rejecting some smaller wavelengths because they will be at cut-off. We've used a bigger value. At this zone there are wasted energy from almost all ports, but a minimum quantity from ports 11 and 12. We choose a length similar to port 13 so it will be collecting energy from all the other frequencies. Next table shows the selected values to both ports.

Port	WOUTPUT (mm)
10	14.95
16	12.48

Until now we've been using PML's at the walls. With them, we've been seeing the best possible behaviour for each structure. If we continue using PLM's, as we introduce Dummys we'll see a progressive deterioration in the response of the multiplexer, because we will be introducing reflective PEC walls and "wave ports". We need first to remove the PMLs, keeping this way the worse possible response with all the PEC walls, and check, as we introduce the Dummys if we obtain improvements in the response.

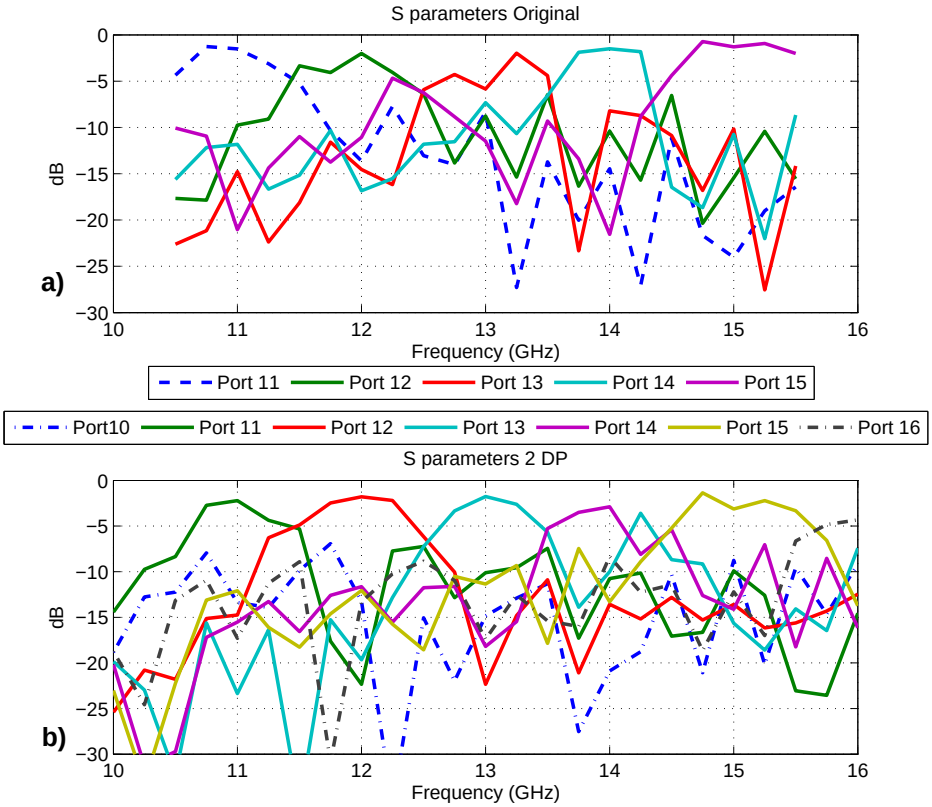

Figure 6.23: Original and 2 DP S parameters.

As we can see in the original structure representation 6.23 , it has been a deterioration in the multiplexer's response. Specially with the central ports (12, 13 and 14). Port 11 and port 15 are helped by the oriented walls, but not the others. We have now all the energy transmitted by the antenna spreading around the substrate, being reflected by all the walls.

However, in b), with ports 10 and 16 as dummys 6.23 , we can appreciate an improvement in all ports except 14's. With this two new ports we are collecting a good quantity of leftover energy, which won't be reflected to other places. There has been nevertheless some deterioration in port 14. Port 13 swallows now part of that energy, probably caused by some new reflection. We'll see how to improve that with the other dummys.

6.5 Dummy Ports of the left wall

We have to introduce Dummy Ports in both external walls. Left wall is smaller so it needs only a few ports. This wall is outside the energy propagation direction. So the energy that will reach this ports will be due to reflections. Furthermore, the most of this reflected energy will be from the lowest frequencies, i.e., the first ports, so they have to be capable to collect this frequencies (bigger wavelengths). Keeping this in mind, with two ports it will be capable to collect a reasonable quantity of leftover energy, being their WOUTPUT around 15mm 6.24 . The PEC wall between them has a little inclination so that it follows the direction of the reflected energy.

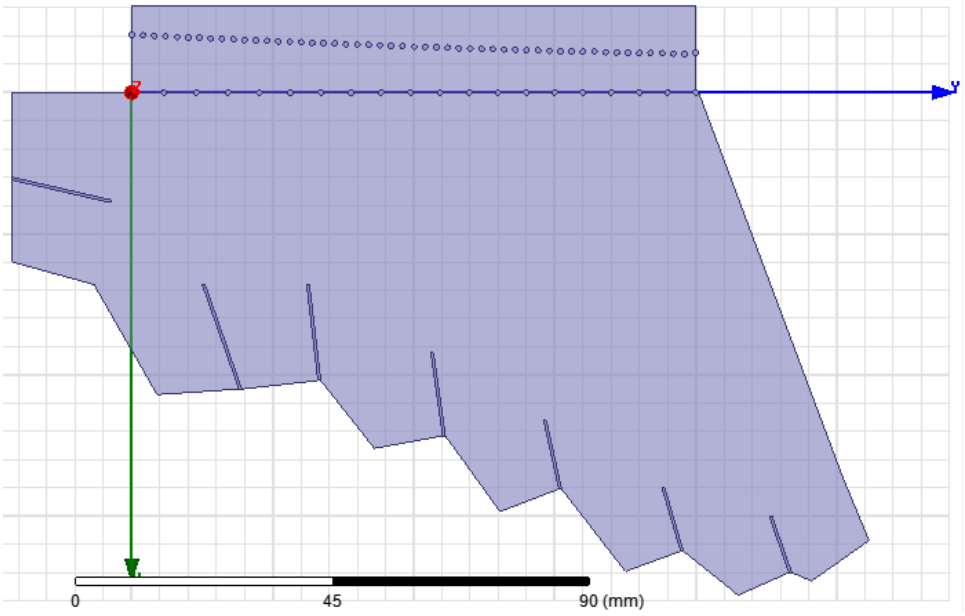

Figure 6.24: Structure with 4 DP.

As we see in 6.25 b), respect the previous structure, we've improved the previous worst port response, port 14. Port 13 takes away less energy from port 14 at 14.25GHz, due to the removal of the original oriented wall. Now, in that zone, the only element that affect the reflection is the wall between Dummy Port 1 and 2. The other ports have a similar response.

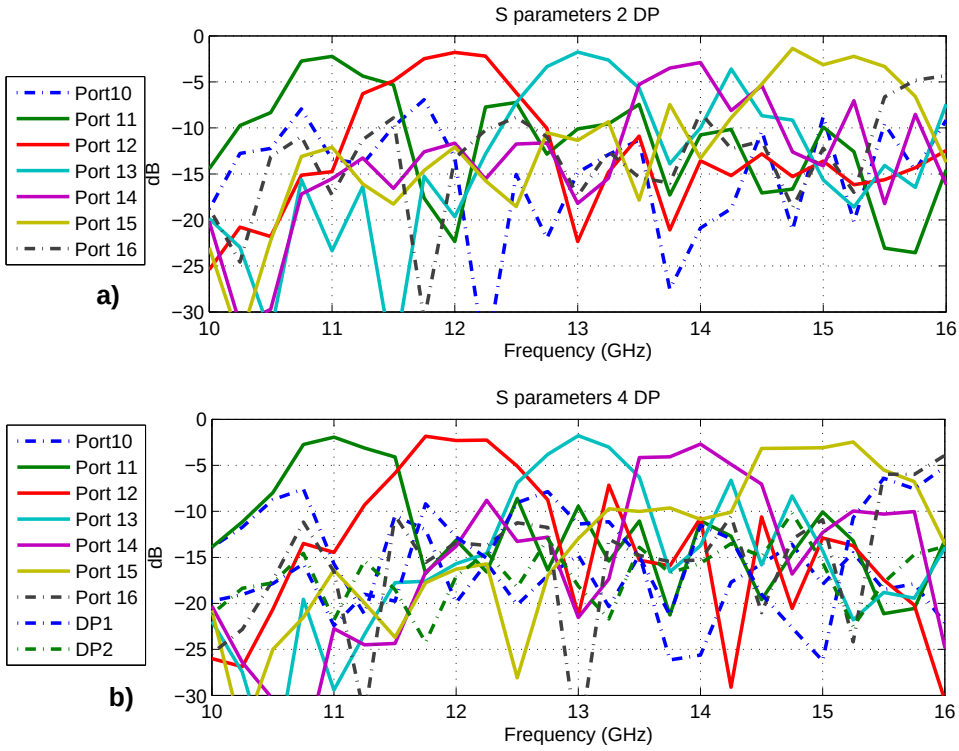

Figure 6.25: 2 DP and 4 DP S parameters.

6.6 Dummy Ports of the right wall

Now it is the turn of the right wall. Here there is a longer wall, so we need more Dummy Ports. The first thing to discuss is the orientation of the ports. We are going to test two orientations: oriented along the energy orientation from the antenna, and oriented along the reflections caused by the walls between walls.

6.6.1 Oriented along the energy from the antenna

As we already know, we are using focus prints to collect the energy. But it isn't a perfect design, so it could be energy escaping the focus and reaching other parts of

the structure. For this reason we orient the Dummy Ports along this energy, to catch all this leftover energy, and of course, other energy reflected by the walls between ports 6.26.

The first election is to choose the number of ports and theirs width. As we know the most restrictive port is 11, because its highest width. Its $\lambda_0/2$ is 10.12mm. So if we design the Dummys width above this value we ensure every frequency may enter them. With a value around 12mm or 13mm we can set 4 Dummys in this wall.

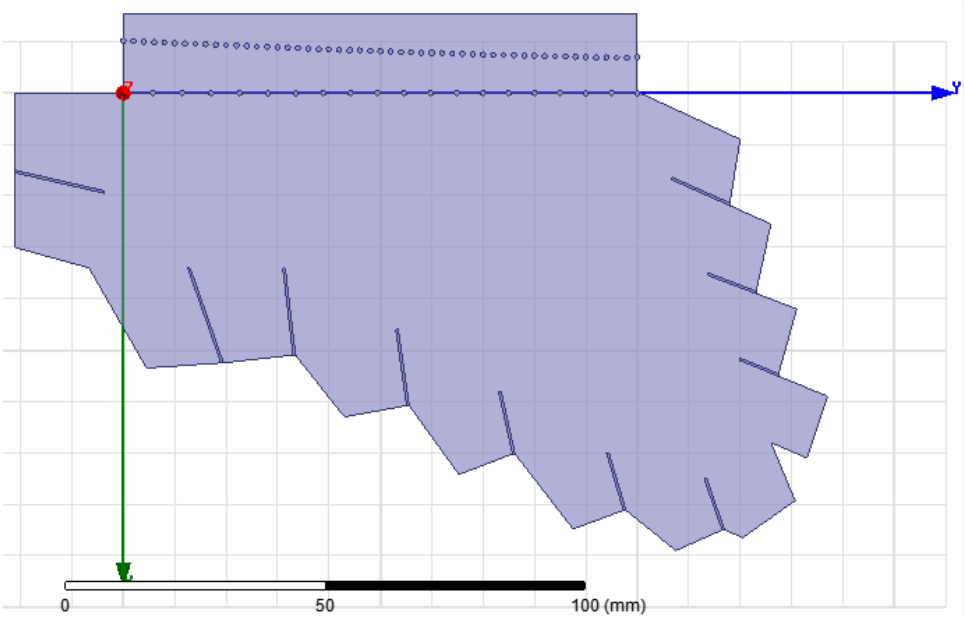

Figure 6.26: 8 DP antenna's orientation.

We can compare its S parameter representation with the previous, to see the role of these new ports 6.27 . These are the Dummy Ports of the right zone, so they will absorb mainly energy from the higher ports. This is exactly what it can be seen in b), comparing with a). In the 8 DP version b), ports 14 and 15 absorb more energy. Even port 13 has an improvement. All the new Dummy Ports are absorbing a significant quantity of energy. This is what they are made for, and this is what is decreasing the reflecting energy travelling across the substrate.

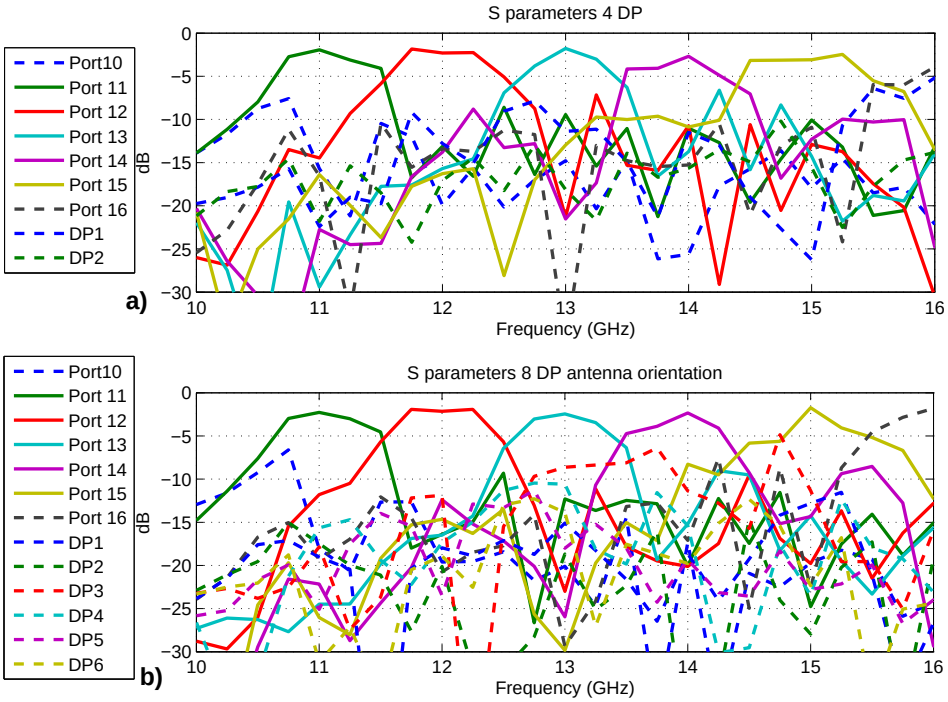

Figure 6.27: 2 DP and 8 DP with antenna's radiation orientation S parameters.

6.6.2 Oriented along the reflected energy from the ports

Now we try to mainly collect the reflected energy from the ports walls 6.28 . To compare with the previous design we keep the number of Dummy Ports at 8.

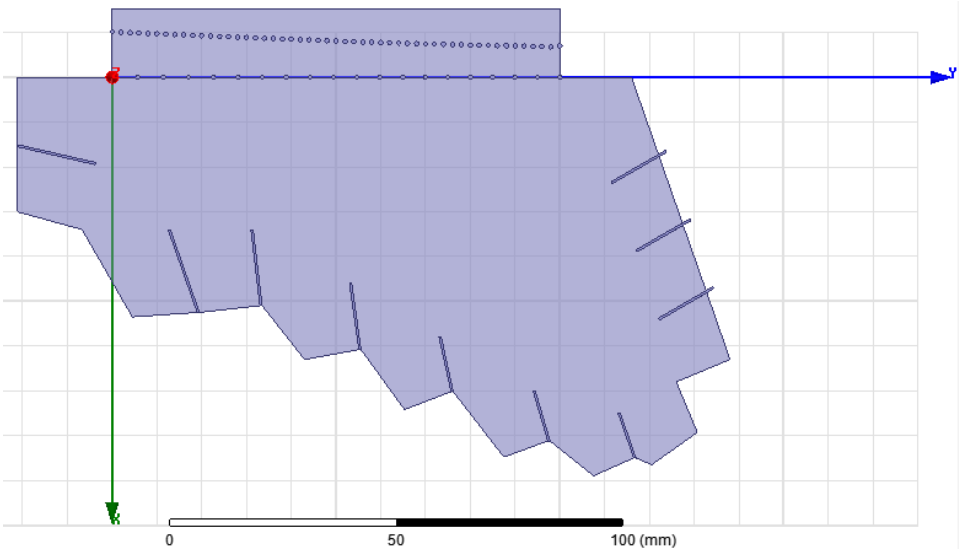

Figure 6.28: 8 DP RE's orientation.

The ports widths haven't been chosen, they are given by the number of ports (8) and theirs walls position. We present the S-parameters representation with the previous structure to compare and find the better solution 6.29 .

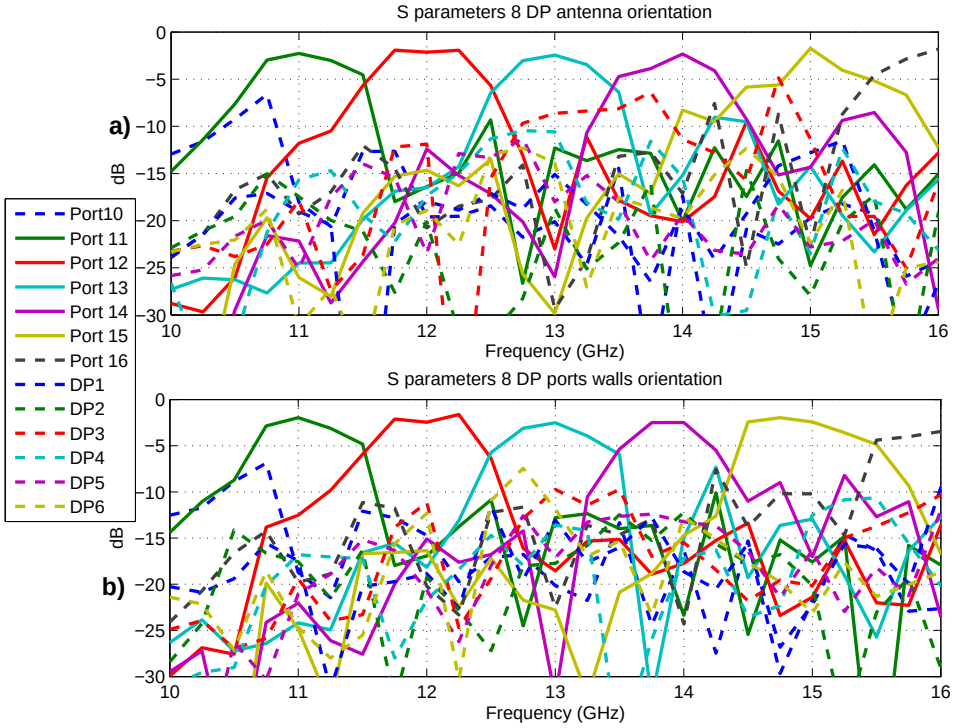

Figure 6.29: 8 DP with antenna's radiation and ports walls orientation S parameters.

Some levels have increased in b), but on the contrary, port 13 takes more energy at 14.25GHz. This absorption existed before, maybe caused by the second lobe of 13GHz. But now it has increased due to the new DP setting. In future works we can be interested in minimize second lobes. Anyway, we are not finished yet. We can prove two new options: put the dummy ports of the right wall further, or use 9 ports instead of 8.

So, even with this amplified bother, we are going to choose b) because we have new modifications to prove, and with the a) option we have no more odds.

Setting ports further

When the right wall dummy ports position was settled, the left side of theirs walls was placed in the line of the original right wall, and the ports in the other side of the walls. Now we try to set a little further these positions from the antenna, and observed the changes.

We only represent the S parameters 6.30 because the structure is the same but with the DP about 0.5mm further, so it can't be appreciate in the image.

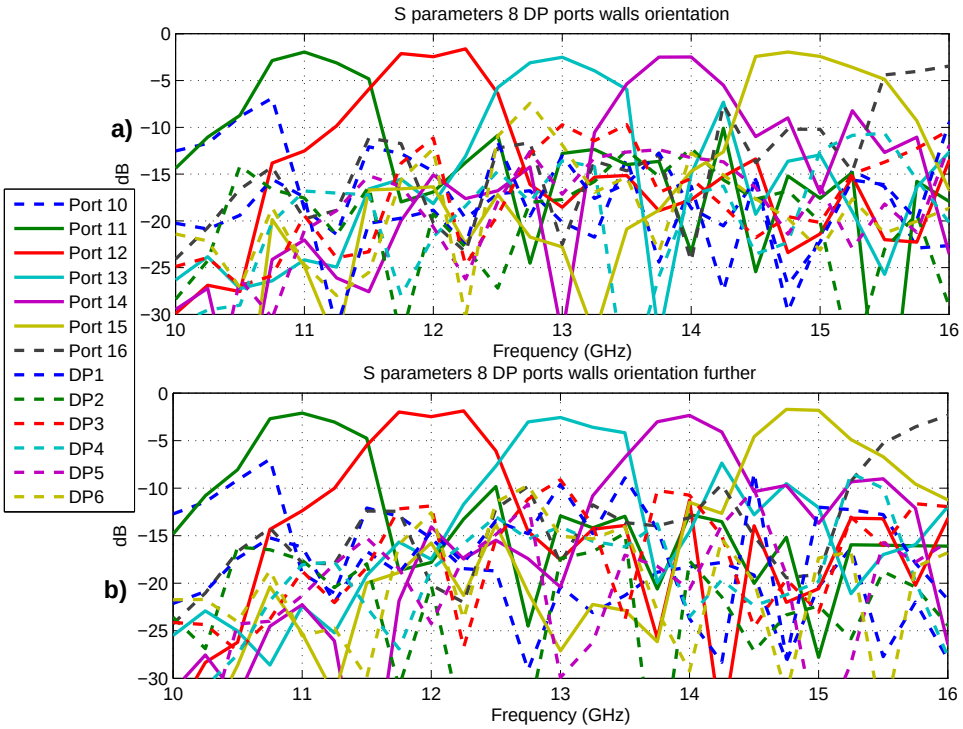

Figure 6.30: 8 DP ports walls orientation with further position S parameters.

As it can be seen in b), there is no attenuation of the second lobe of 13GHz. Anyway, there is no improvements in any other port. In fact, port 15 have a worse general response, so we discard this option.

Adding one more port

The other available option is to add a ninth port. In this case, we represent both structures 6.31 to appreciate the new port and how the dummy ports width has been decrease.

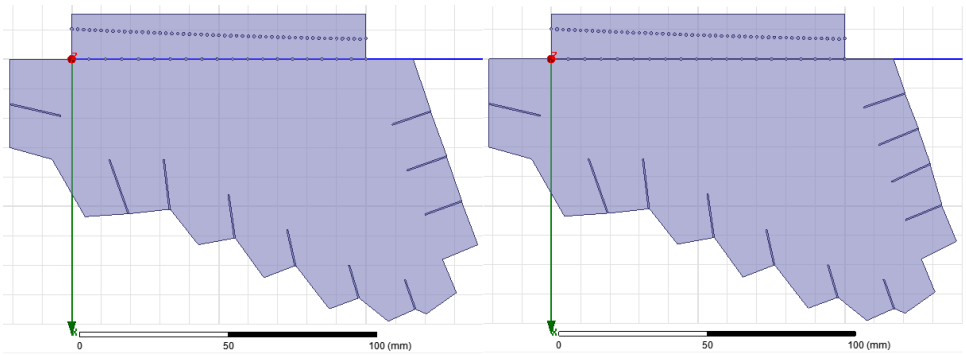

Figure 6.31: 8 and 9 DP.

Now, as usual, it has been presented the S parameters of both structures 6.32 .

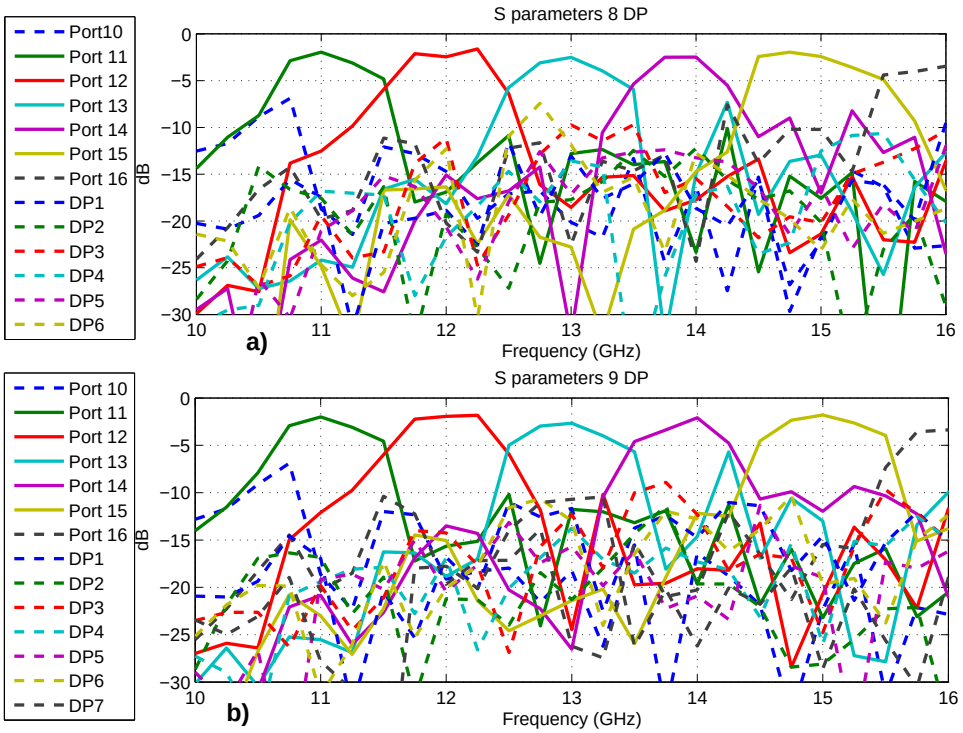

Figure 6.32: 8 and 9 DP S parameters.

The situation with the 13GHz's second lobe has worsened even more. Anyway, there is no easy solution here. If we choose the 8DP solution there could be problems in the future with the real microstrip ports, due to theirs unusual big width. It seems logical to use the 9 DP option, and search for a solution with this anomaly attenuated.

Moving the walls orientation

The problem with the 13GHz's second lobe may has been attenuated with the orientation of some walls. The first modification should be to change the orientation of the walls and see if the problem can be attenuated at least to the 8DP's value.

For this case, there has been some changes in the design process of the walls. Now they have been created as HFSS's "Draw box", and with the "rotate" label we change the orientation. The next image 6.33 presents the three chosen modifications.

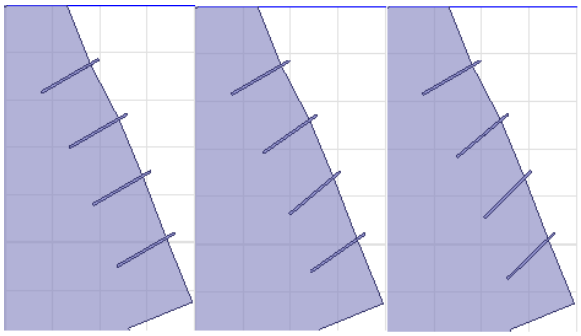

Figure 6.33: 9DP rotating walls.

As it can be seen, mainly the ports near the higher frequencies have been moved. The first one is like the previous case (but with the new "Draw box"'s design), the second one has some walls more inclined, and the third case has them even more.

In the next figure 6.34 it has been presented the S parameters of ports from 11 to 15GHz of the three structures. For a cleaner view, we only present levels from -10dB to 0dB.

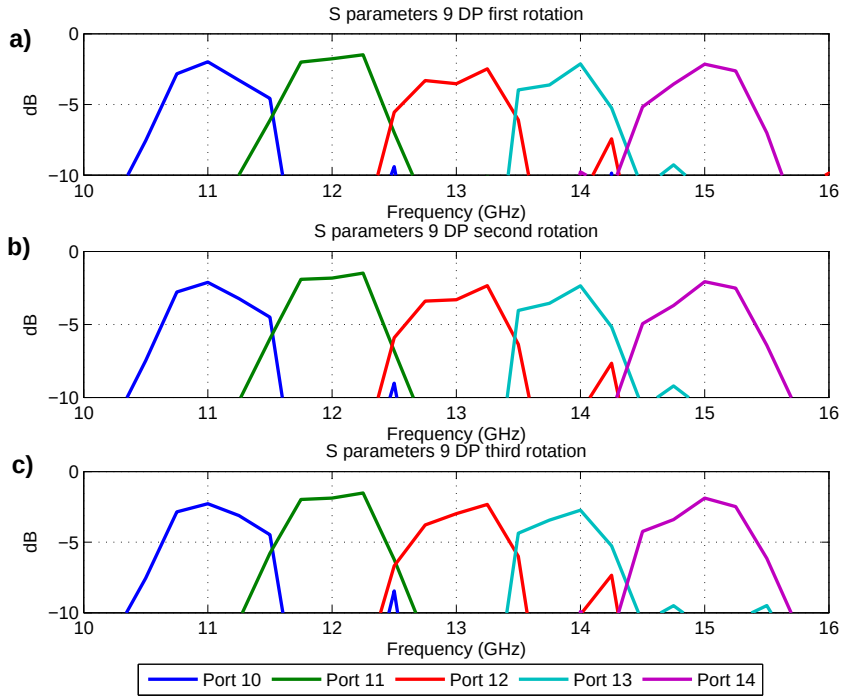

Figure 6.34: 9 DP rotating walls S parameters.

Thanks to this new presentation it can be appreciated that other frequencies, not only 13GHz, have the same second lobe, but more attenuated. Comparing the three options the one with the 13GHz's second lobe more attenuated is b).

Now, we check if option b) is better than the 8DP case 6.35 .

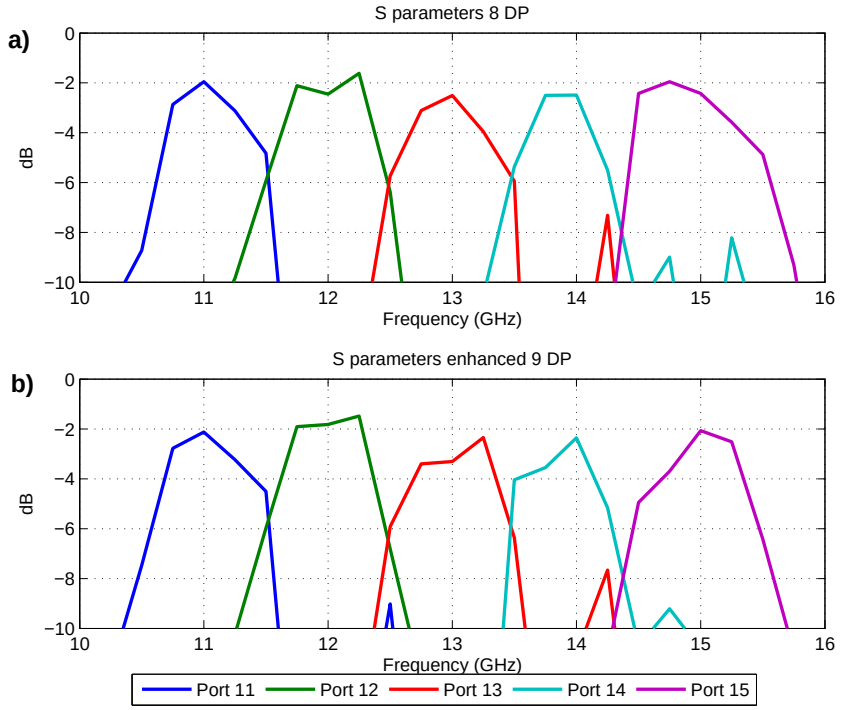

Figure 6.35: 8 DP and enhanced 9 DP S parameters.

Once again they have been represented from port 11 to 15, with levels between -10dB and 0dB. It can be seen that b) is better. So, for all the reasons presented in the previous points, this enhanced 9DP structure will be the final version 6.36 .

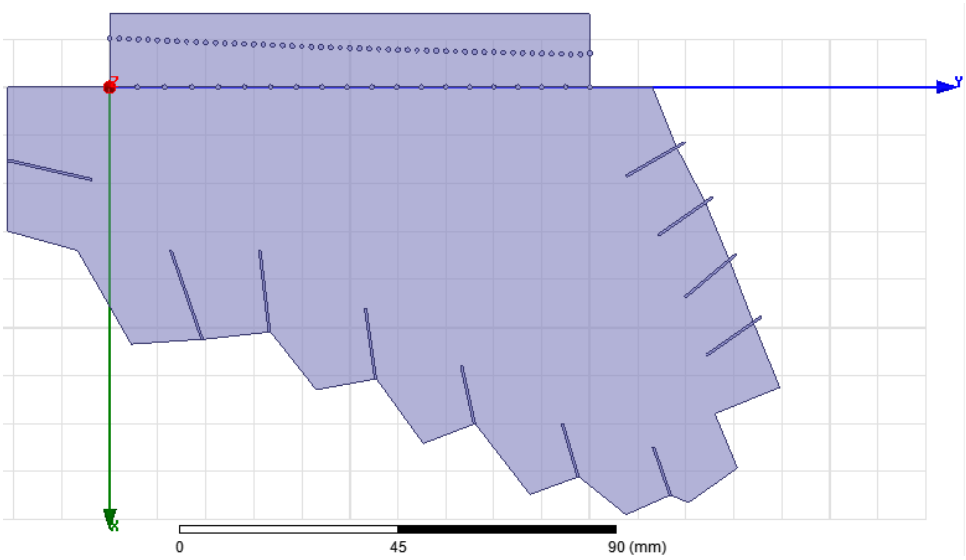

Figure 6.36: Final 9 DP.

Based on this design, we have to reach to a manufacturable design. The next steps are:

- Design the adaptive ports using microstrip technology.
- Replace PEC walls by via holes.
- Introduce losses to the design.

Chapter 7

Ports design in Microstrip Technology

We have reached to a final design of the quasi-optical space multiplexer. Until now all ports have been defined as "Wave Port". We have used this port's type because, in HFSS, this port's type gives a close response to a real case. But now, it is time to choose a real port's type in a specific technology.

In the first chapters, when it was discussed how the energy should be collected, we talked about coaxial and microstrip technology. For this project, we are going to use as a final design the ports in the frequency focus, and for this design the easiest designable option is the microstrip ports.

There is a lot of published work about microstrip transitions. For this project, we use the design developed by Deslades in [12]. As it can be seen in 7.1 b), there are two distinct parts: the initial microstrip and the taper. Some times it can be used a third SIW zone right before the antenna, but it can be despised here.

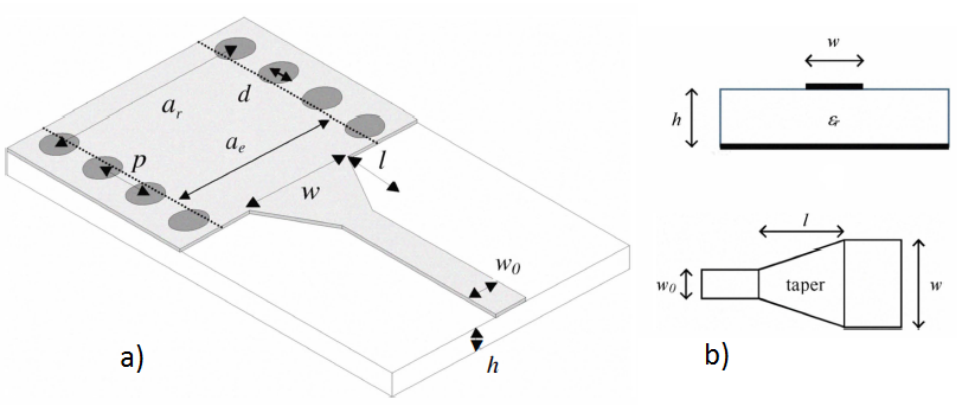

Figure 7.1: Deslades Microstrip transition.

From the image, we know that we have to obtain the following parameters:

- w: width of the taper in the antenna side.
- $w0$: width of the input microstrip.
- l: length of the taper.
- The length of the initial microstrip lu.

To obtain $w0$ there are two ways: using formulas, or using some specific software. We are going to obtain it with the free software TXLINE 2003. The length of the initial microstrip is a secure length, and it always has the same value. So we have chosen to set it at 5mm to have enough space for the connector. To obtain the other two parameters we use HFSS: a parametric sweep from the Optimetrics option.

7.1 Antenna's Input adaptation Port Design

The final design is a very complex structure with a high number of variables affecting the result, so it is very hard to use it to find a final ports type. We reduce the complexity of the structure to a scenario 7.2 with the antenna and a small substrate zone.

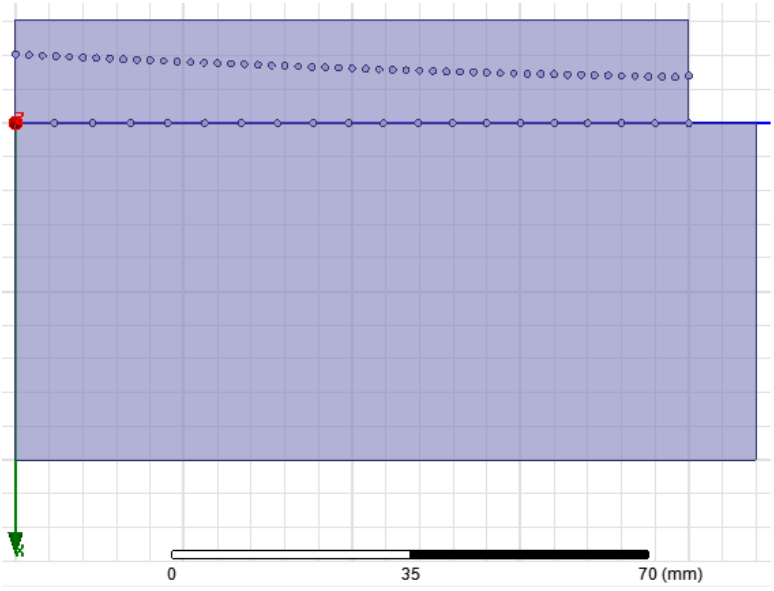

Figure 7.2: Only antenna structure.

We firstly obtain the S parameters S_{11} and S_{21} with the only antenna structure to set the ideal case 7.3 . And then, we try to obtain the different parameters of the adaptation port trying to maintain the same S parameters.

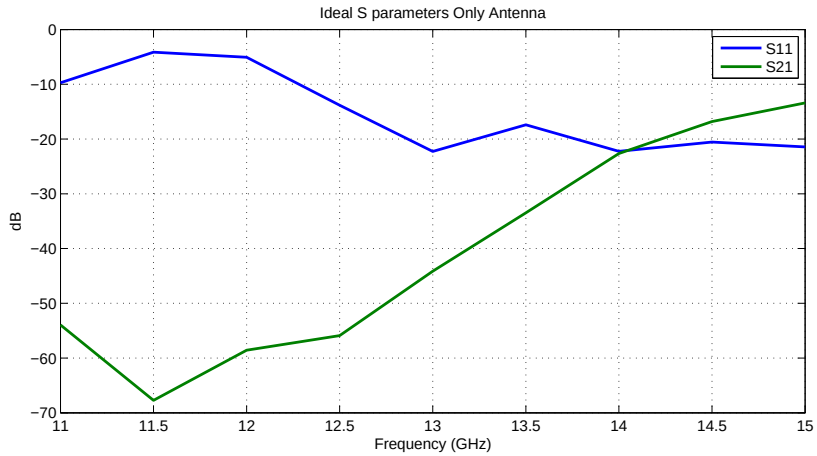

Figure 7.3: Ideal S parameters.

As we said before, we use the free software TXLINE 2003 to obtain *w0*. In 7.4 it can be seen a capture of the software. We use GaAs (Gallium Arsenide semiconductor) for the dielectric, with a dielectric constant of 2.2 and a loss tangent of 0.0002. For the conductor we use copper with a conductivity of $5.88 * 10^7$ S/m. For the thickness of the microstrip T we use a height of 35μm , and for the height H we use the height of the substrate, 1.57mm. We want a typical impedance of 50 Ω. The calculus will change with the bandwidth, but we need a unique value for all the frequencies, specially for the input and the output ports. Between all the values, we choose that one that gives the bigger value and can contain all the others: the lower bandwidth (15GHz).

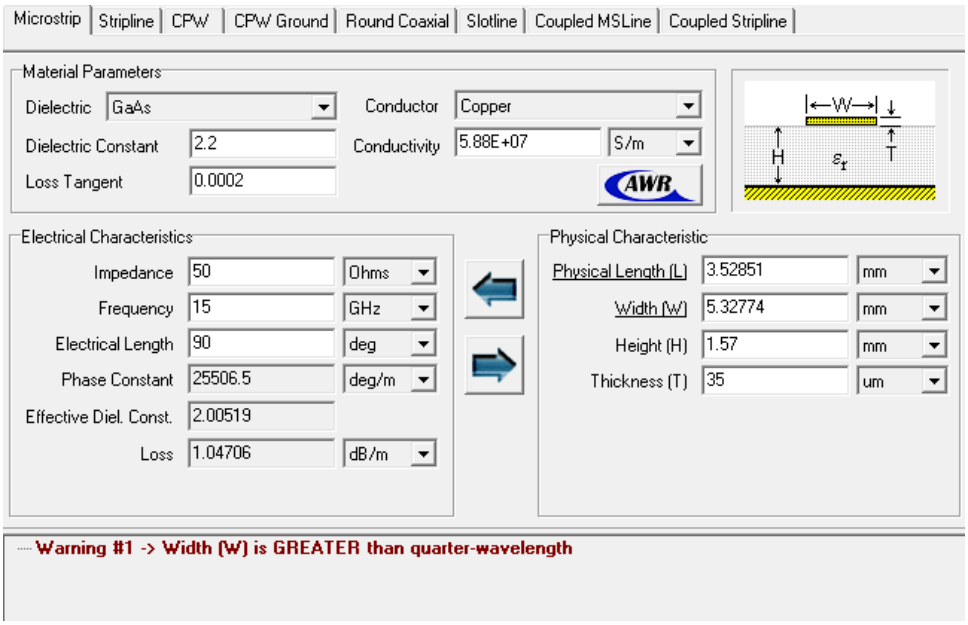

Figure 7.4: TXLINE software h=1.57mm 15GHz.

The calculated value for the *w0* parameter is 5.32774mm. It appears a warning because this width is bigger than a quarter of the wavelength (0.02/4=5mm), and there may be other modes besides the fundamental TE_{10}. Another problem related with the width of the ports appears. If this width is too extensive, the microstrip will be too close to some walls and this can cause overlapping with them, starting to behave like a Coplanar Waveguide.

There are two ways to avoid this problem: using a smaller value, losing adaptation, or changing the substrate's hight. It seems more logical to try using another hight for the substrate to not loose adaptation. Looking forward to the manufacturing of the multiplexer, we have to choose a value typically used in the industry. There is two possible highs broadly used that fulfil our necessities: 0.787mm and 0.508mm. In chapter 3.4 we already discuss the election between two given highs. Using the same criterion we choose the bigger one, 0.787mm. Using the same values for the other parameters we obtain a value for *w0* of 2.4415mm 7.5 . We avoid the warning this time.

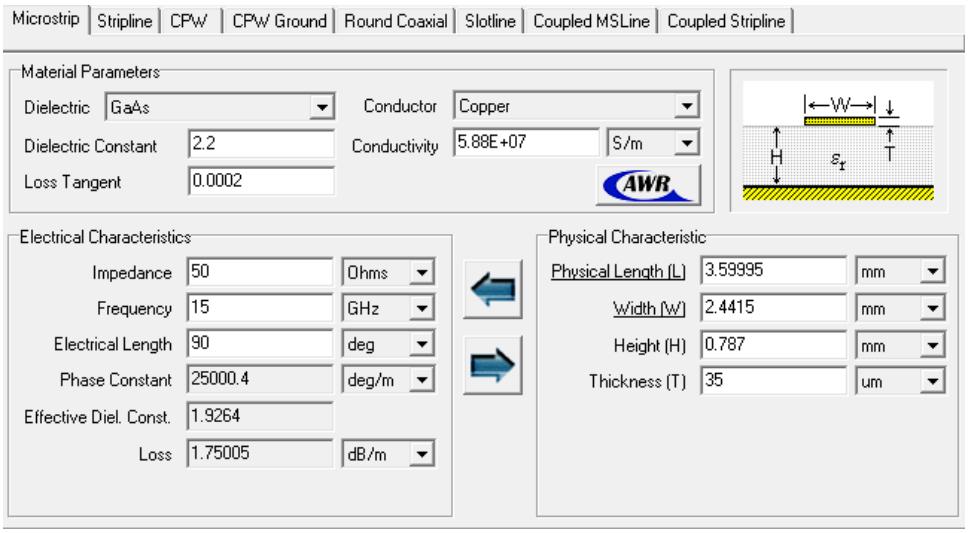

Figure 7.5: TXLINE software h=0.787mm 15GHz.

Now, with all the calculated parameters, it is time to find the better solution for parameters w and l using the parametric sweep of HFSS. Figure 7.6 shows both sweeps.

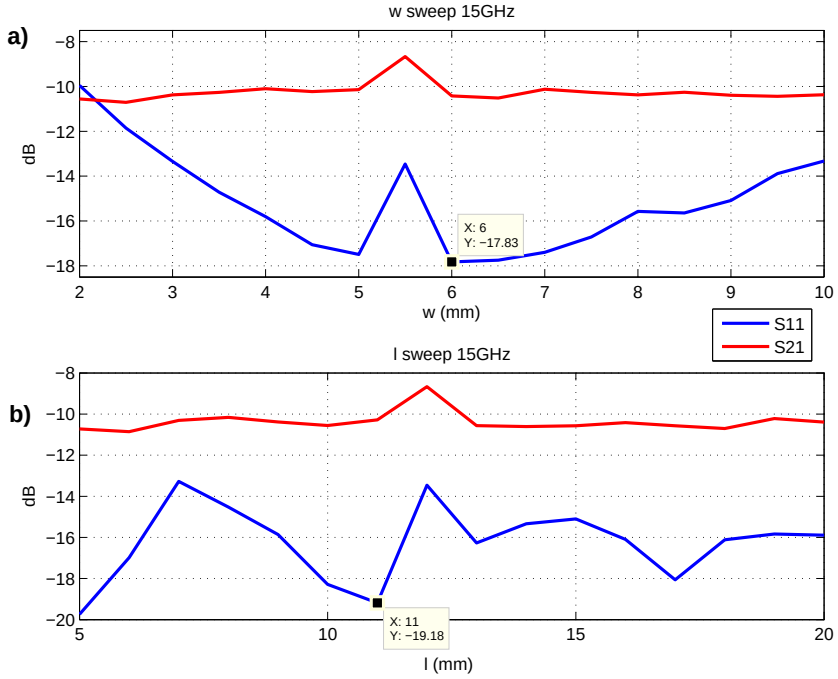

Figure 7.6: w and l sweep 15GHz h=0.787mm.

We firstly execute the parametric sweep shown in a) with a given value for parameter l, for example 12mm. From the text box we see that the value that gives the lower S11 is 6mm. Later, with this value, we execute the parametric sweep shown in b) to find the value of l that gives the lower S11. And from the box we see that it is 11mm.

In 7.7 figure we can see the final design for the input port. There is an extra wall. This extra wall is needed because the original was too close from the microstrip, and on the other hand, the Dummy ports of the left wall were wide enough to remove some millimetres and give them to the input port.

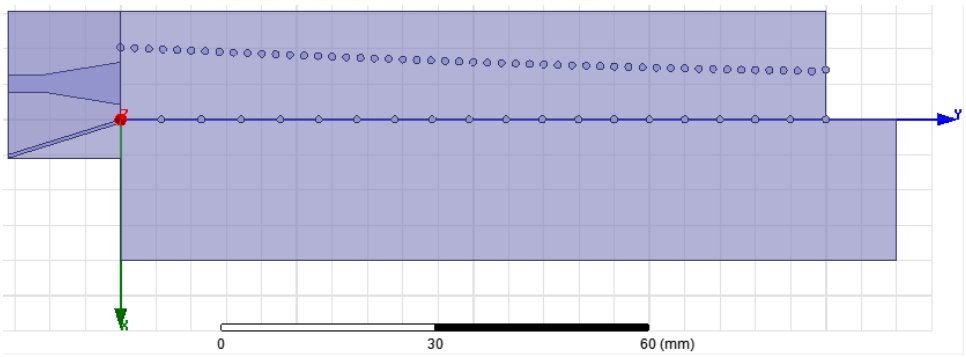

Figure 7.7: Adaptation input port.

HFFS use by default a PEC layer when a dielectric face is left naked. This is why until now, we have left free the upper and lower face. But now, with the introduction of the microstrip we need to specify when there is a PEC face or when there is dielectric in the open air. Once again, we use the options of HFSS. If we draw a structure defined as air on the dielectric, HFSS process it as an open dielectric. So, above the input port we draw a box defined as vacuum with a secure height of 4*h=3.148mm as shown in 7.8 . Zones with dielectric will be processed as open dielectric and the micostrip will be processed as PEC.

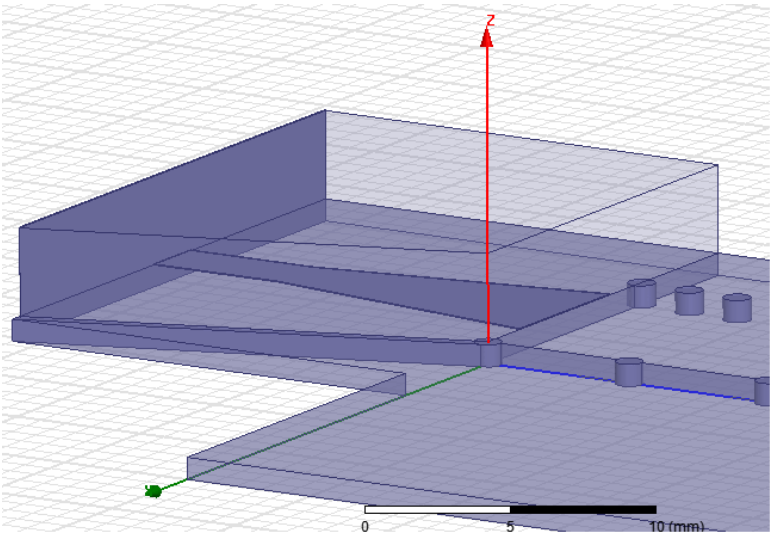

Figure 7.8: Air definition.

Now we can present 7.9 S parameters S_{11} and S_{21} of the new adaptation port with the ideal wave port structure.

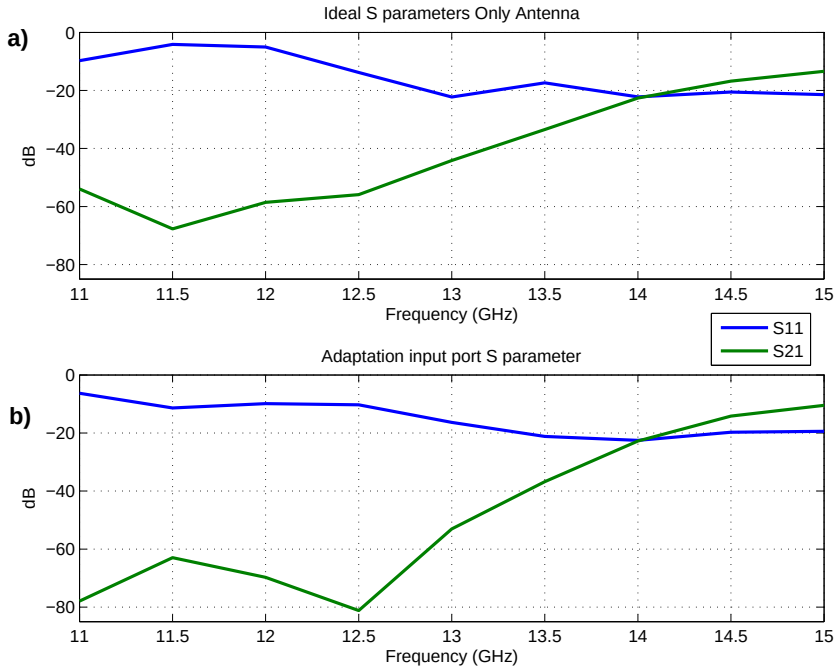

Figure 7.9: Only antenna and adaptation input port S parameters.

As we pretend from the beginning we have obtain a very similar response to the ideal case. In fact, some levels in b) for S_{11} are lower than the ideal case. So, we have designed our adaptation input port. For a general point of view it is hopeful to summarize all the parameters values:

- w = 6mm.
- $w0$ = 2.4415mm.
- l = 11mm.
- lu = 5mm.
- h = 0.787mm.

7.2 Rest of the adaptation ports design

For all the Dummy Ports it seems logical to use again only one value for the microstrip parameters, the higher (higher frequency, 15GHz), because these ports collect energy from almost all frequencies. And for the multiplexer's output ports there are two

options: use the corresponding parameters for each port, or use again the bigger values for all of them.

If we try to use the corresponding value for each parameter and frequency there will be a problem. The parameter $w0$ is easy to estimate with TXLINE 2003, for each frequency. But we estimated w and l with a parametric sweep. It would be necessary two sweeps for each frequency with the complete structure. This will consume too much time and computational work. At the end, there are these two options:

- All ports with the same values (higher frequency 15GHz).
- Estimation of $w0$ with TXLINE 2003 for each frequency and 15GHz's values for all w and l.

7.2.1 Values of 15GHz for all the other ports parameters

We use the calculated values for all ports: $w0 = 2.4415$mm, $w = 6$mm and $l = 11$mm. Figure 7.10 shows the structure.

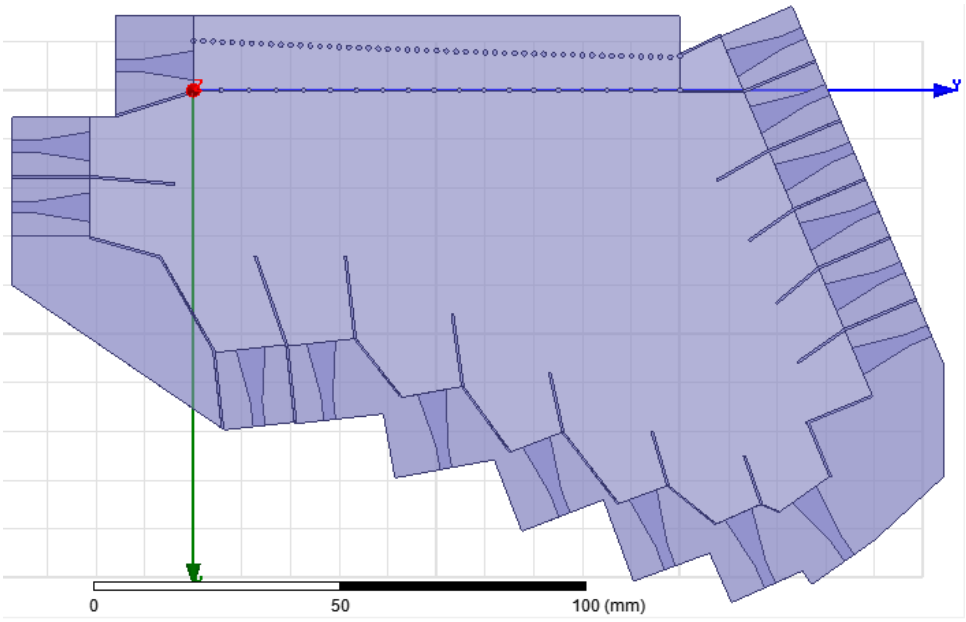

Figure 7.10: Adaptation ports with 15GHz's values.

Thinking of the manufacturable design, there have been added extra parts to the substrate between ports. And as it can be appreciated (other tone of transparency), above all these extra parts and all ports has been added the air boxes to simulate the naked dielectric zones. Figure 7.11 shows its S parameters along with the structure with the ideal "wave ports".

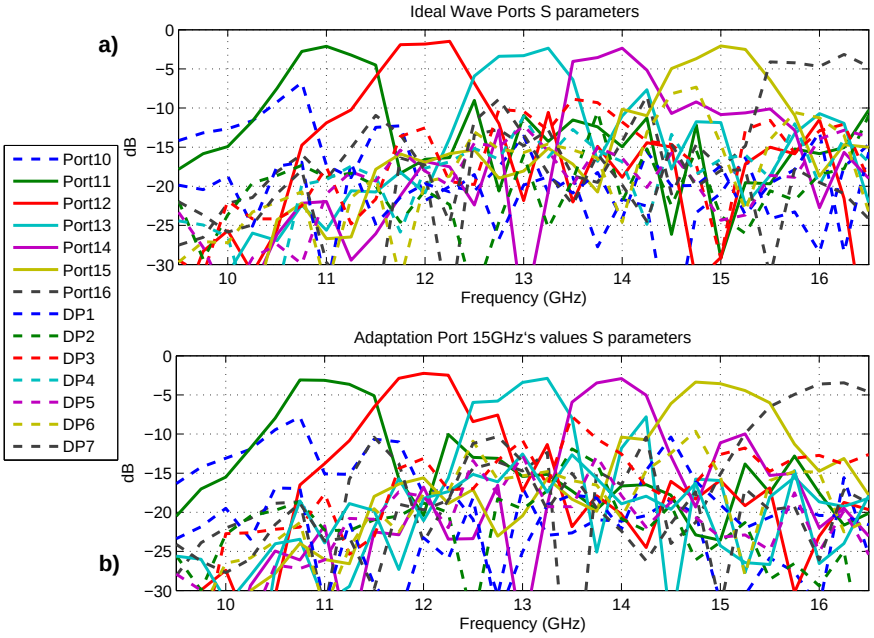

Figure 7.11: Adaptation ports with 15GHz's values and ideal wave port S parameters.

The results shown in b) are very similar to the ideal case a). Adding the microstrip ports, there are no deterioration of the ports collecting capacity.

7.2.2 Using TXLINE 2003 to calculate each multiplexer output port's *w0*

As we said before we use the software to calculate every *w0*. The next table shows the values for each frequency:

f(GHz)	*w0* (mm)
11	2.40687
12	2.41425
13	2.4225
14	2.43159
15	2.4415

It has been presented 7.12 directly the S parameters along with the previous case because the dimensions are too small to appreciate the difference between both structures.

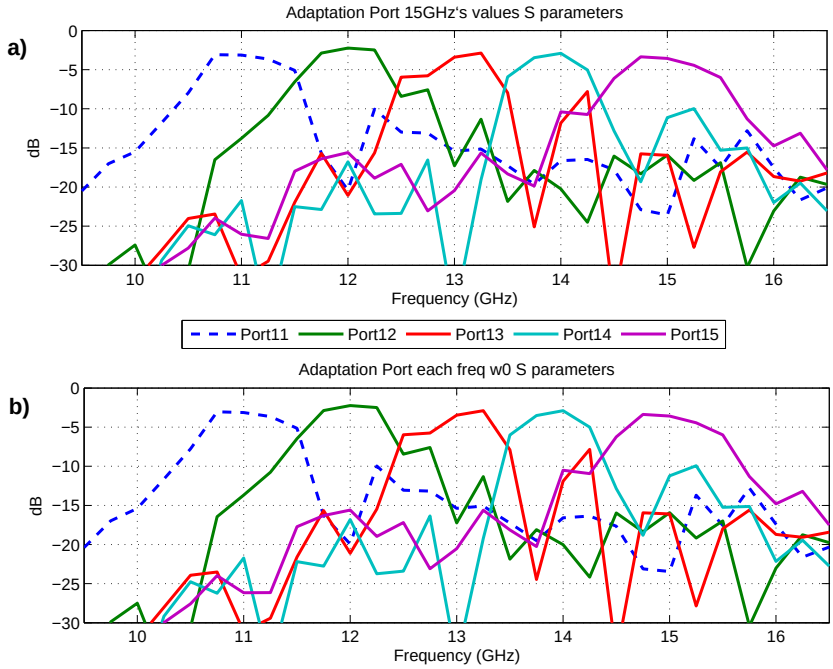

Figure 7.12: Adaptation ports with 15GHz's values and using TXLINE S parameters.

For an easier view we only present ports from 11 to 15. The differences between a) and b) are insignificant. We could use both of them to continue the design. But choosing one, it seems more appropriate to maintain the previous one. The only reason is to maintain parameters w and l with theirs adapted $w0$, 15GHz's.

Chapter 8

Replacing PEC walls by via holes

Until now we have been designing all the structures with PEC walls. It has been easier to work with these walls because their easy design and simulation. But, as we said at the beginning of this project, we are working with Leaky-Wave technology, so now we have the final design, it is time to replace PEC walls by via holes.

To create them, it has been used a script provided by this project's co-director. To define the parameters needed we use the parameters description from [5], like it shows figure 1.3 .

As we know from [13], the period of the cylinders P must be lower than twice their diameter to behave as a lossless wall. In this project we have chosen from the diameter of the cylinders d the value used in the lens designed by this project's co-director (and used in this own project), d=1mm.

To build the via-holes wall there are two possible scenarios: a wall given by two points, or a wall given by a point and an angle. In the first scenario we find the slope to obtain the associated line. Then we find the length of the line (easier with HFSS), and with the length and the maximum cylinders period P=2mm we find the numbers of cylinders needed:

$$n = \frac{l + P}{P} \tag{8.1}$$

Where l is the length of the wall, P is the cylinders period and n is the number of cylinders. Mathematically speaking these are the number of points of the line, so now we have the complete line with the number of points needed. We can do this calculus automatically for all this type of wall with Matlab, and with the known function *fprint(.,.,.,.)* we write all the cylinders location in a ".txt" file. We put this file's location in the given script and we run the complete script with HFSS to obtain the via-holes wall.

We do the same with the second scenario, but we find the line with basic trigonometry given one point, the angle and the length (obtained again with HFSS). The rest is the same.

In figure 8.1 it can be seen the final structure with all PEC walls replaced by via-holes walls.

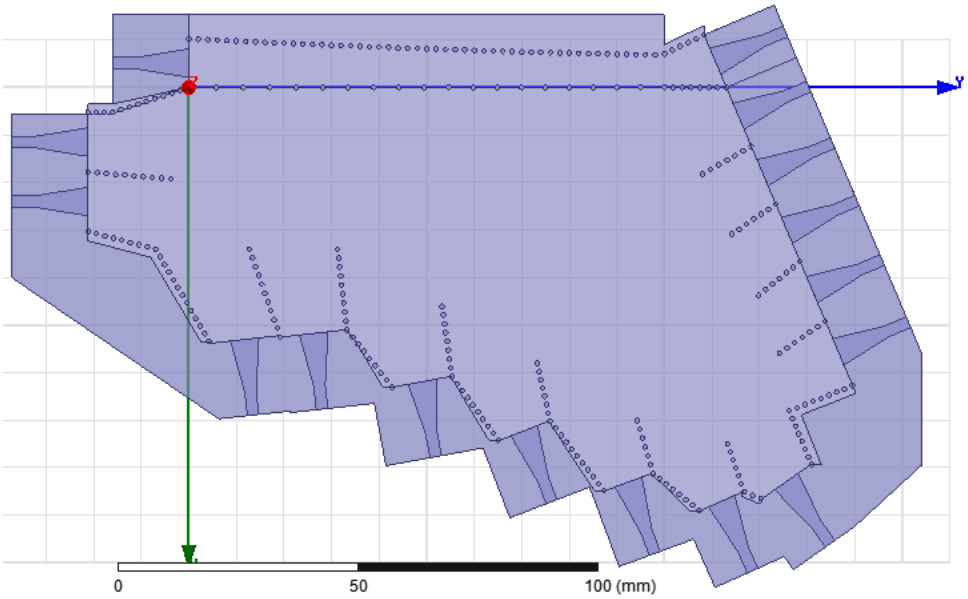

Figure 8.1: Final structure with via-holes walls.

Apart from the via-holes, there are two differences with the previous structure 7.10 . The walls between microstrip ports have been removed to obtain a closer model to a manufacturable structure. As it can be appreciate in 8.1 , in some places there are some extra space between the cylinders position and the air (extra metal layer length). In a manufacturable Leaky-Wave structure, the via-holes can't be the edges of the metal layer, because it can cause some undesired effects like leaks from the structure. This extra metal length is often twice of the cylinders diameter (in this case, 2*1mm).

Figure 8.2 shows the S parameters of this structure and 7.10 .

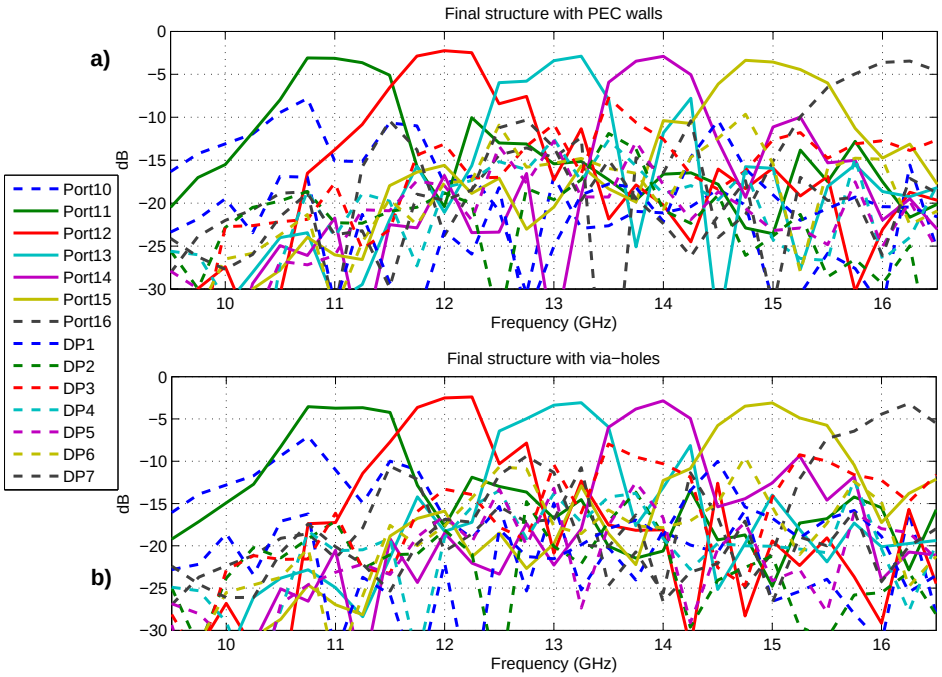

Figure 8.2: PEC walls and Via-holes S parameters.

As it can be seen in b) all levels remain almost equal. Port 11 has gone down a bit, but port 13 has improved its form and its second lobe has gone down. So in a general point of view we have replaced successfully the PEC walls by via-holes and we can say that this is the final structure.

Now it only remains to add losses to the design. And as a extra point, stratify the structure in layers to obtain the manufacturable design.

Chapter 9

Adding Losses

Until now we have been considering the dielectric ideal, i.e., without losses. But we are interested in a manufacturable design, so we need a simulation as realistic as possible.

We have to consider a real dielectric that will cause losses as the energy goes moving through it. From the microwave theory we know that theses losses (for a given frequency) will result in the appearance of a negative imaginary part in the electric permittivity:

$$\epsilon = \epsilon_0(\epsilon^{'} - j\epsilon^{''}) = \epsilon_0\epsilon^{'}(1 - j\frac{\epsilon^{''}}{\epsilon^{'}}) = \epsilon_0\epsilon^{'}(1 - jtan\delta) \tag{9.1}$$

and

$$\epsilon_r = \epsilon^{'}(1 - jtan\delta) \tag{9.2}$$

where

- ϵ': dielectric constant.
- ϵ": losses factor.
- $tan\delta$: losses tangent.

So we can represent the Dielectric Losses Tangent as:

$$tan\delta = \frac{\epsilon^{''}}{\epsilon^{'}} \tag{9.3}$$

HFSS allows the user to introduce many parameters such as this Dielectric Loss Tangent 9.1 in the properties of a given material. For the calculus of the microstrip's input length *w0* we used a loss tangent of 0.0002. We use in this case the same value.

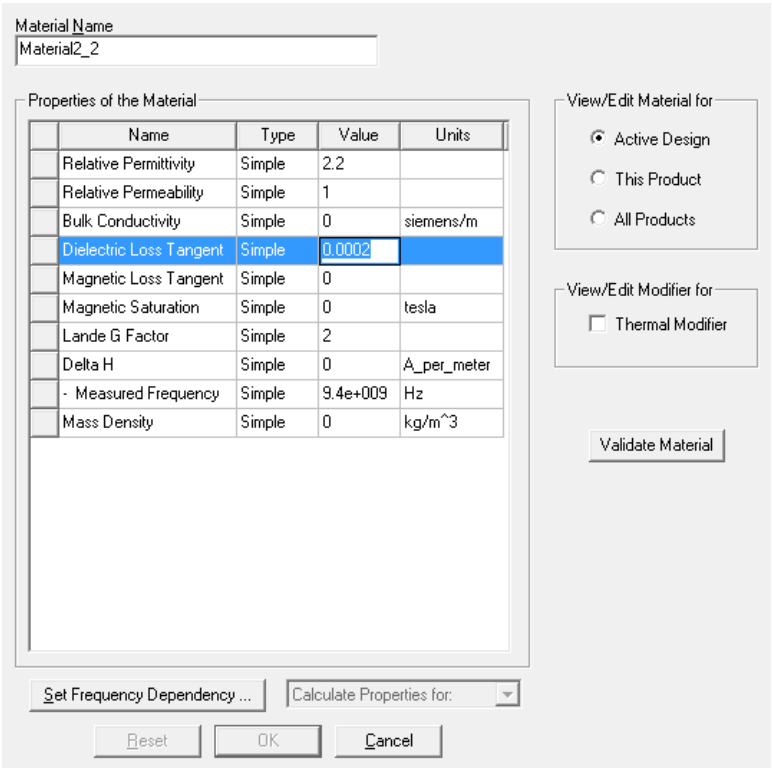

Figure 9.1: Dielectric's parameters.

Now we compare 9.2 the S parameters of the final structure without losses and with losses.

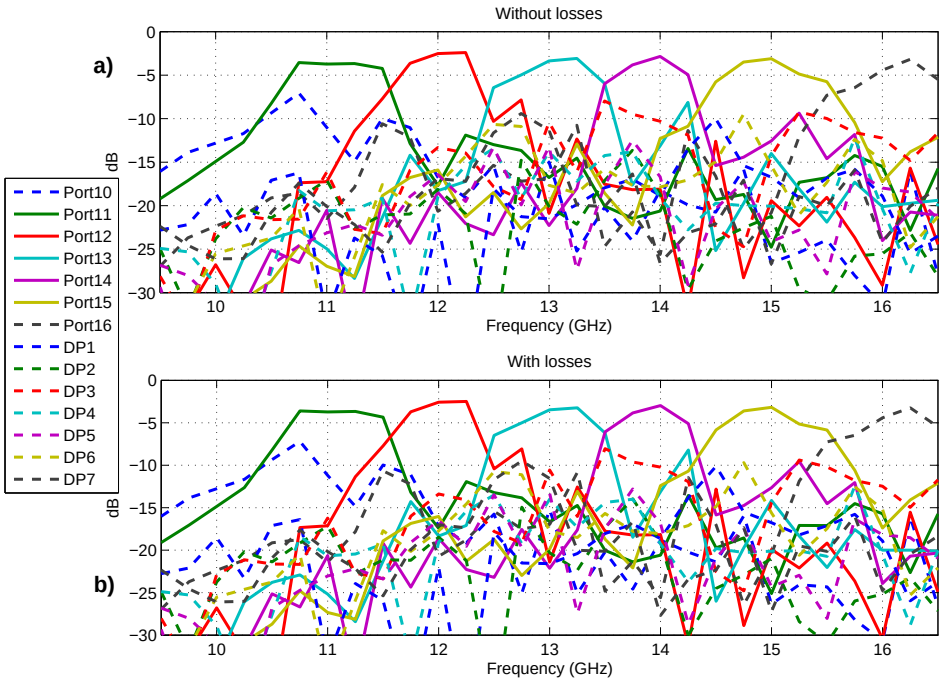

Figure 9.2: Without and with Losses S parameters.

Sawing both a) (without losses) and b) (with losses) it can't be appreciated any difference between both cases. This is a very good issue, and tell us that the introduction of losses have a very tiny variation in the results. We can assert at least that losses affect all ports the same way, so we can represent a zoom of one port (Port 14) 9.3 for both cases to appreciate the real difference.

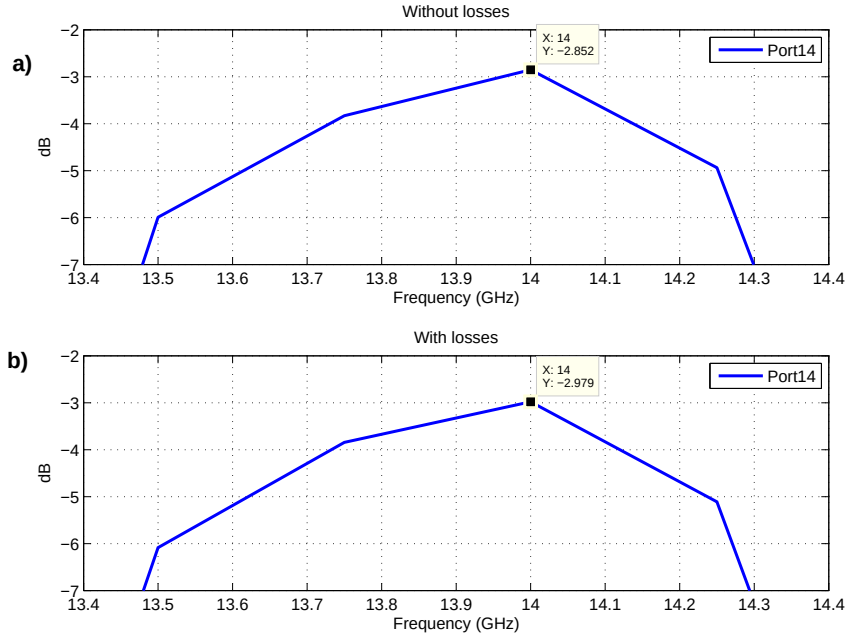

Figure 9.3: Without and with Losses port 14 zoom.

Comparing Port 14 maximum (14GHz) for case a) (without losses) and case b) (with losses) it can be seen the difference between them, 0.127dB. This difference is almost negligible. But now we have reached to a realistic and manufacturable structure.

Chapter 10

Layering of the structure

What we have reached in the previous chapter is the final structure. But to manufacture a structure integrated in a substrate it is used a milling machine. We introduce in the machine the original substrate and we load the design (metal layer, substrate and metal layer). Now, we need to define this four layers:

- Bottom metal: the bottom layer will be the ground of the structure 10.1 . Because the substrate in HFSS is free of any other material, the substrate itself behave as the metal on this face. The via-holes in the real structure won't be visible from the bottom (this view) because the metal will cover them.
- Substrate and via-holes: the final structure will have the dimension of the substrate. Given its dimension, it will be needed a original substrate of (vertical x horizontal) 122.412mm x 191.4mm 10.2 . Once the holes are made with the machine, they will behave has the expected PEC walls.
- Up metal layer: the layer formed by the up metal face and the microstrip ports 10.3 . For this HFSS's design it has been created as an object without hight to accelerate the simulation. Once created, we assigned it a Perfect E Boundary condition to recreate the PEC face.
- Air layer: the last layer is the object created as an Radiation Boundary condition to simulated the naked substrate in those parts not covered by metal 10.4 .

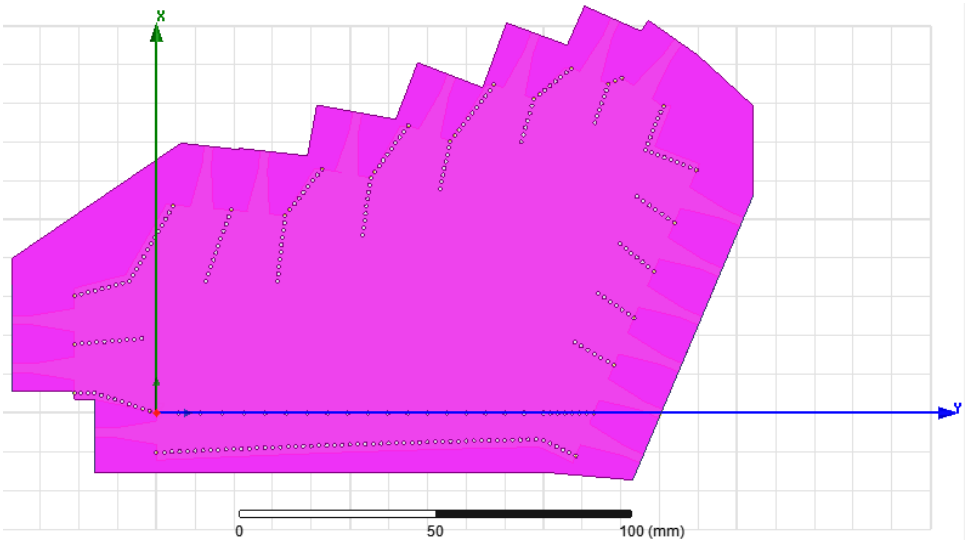

Figure 10.1: Bottom view: single metal layer.

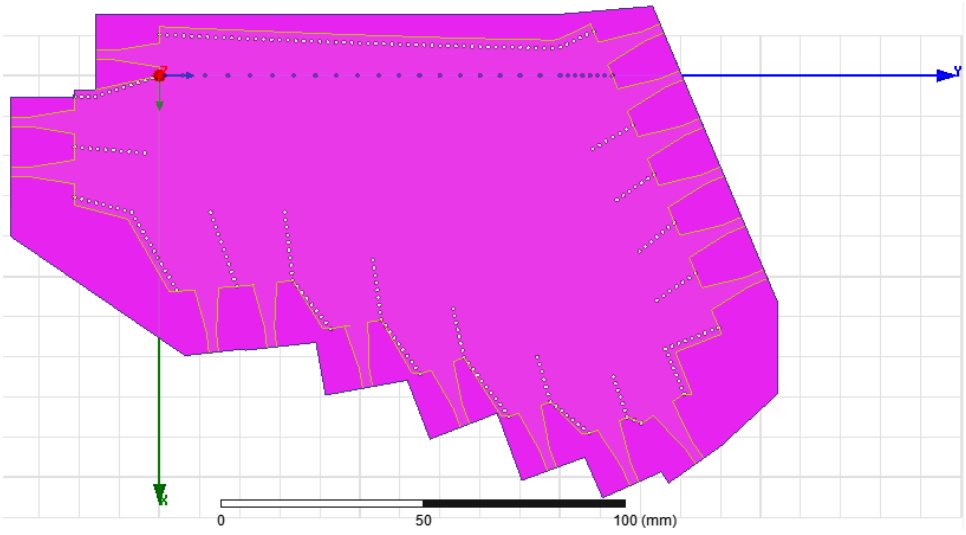

Figure 10.2: Substrate layer.

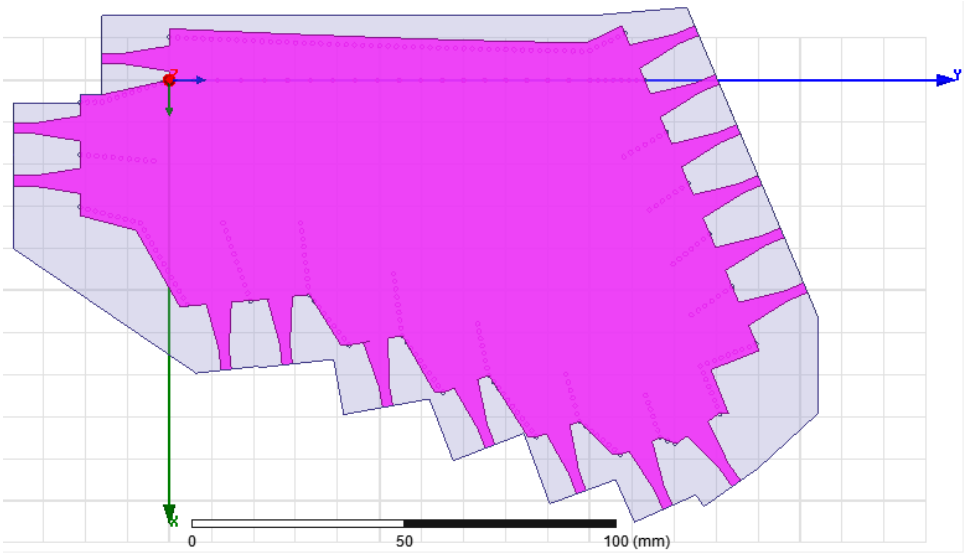

Figure 10.3: Up metal layer.

Figure 10.4: Air layer.

It only remains on last presentation: the S parameters of this ultimate structure along with the final structure with losses 10.5 .

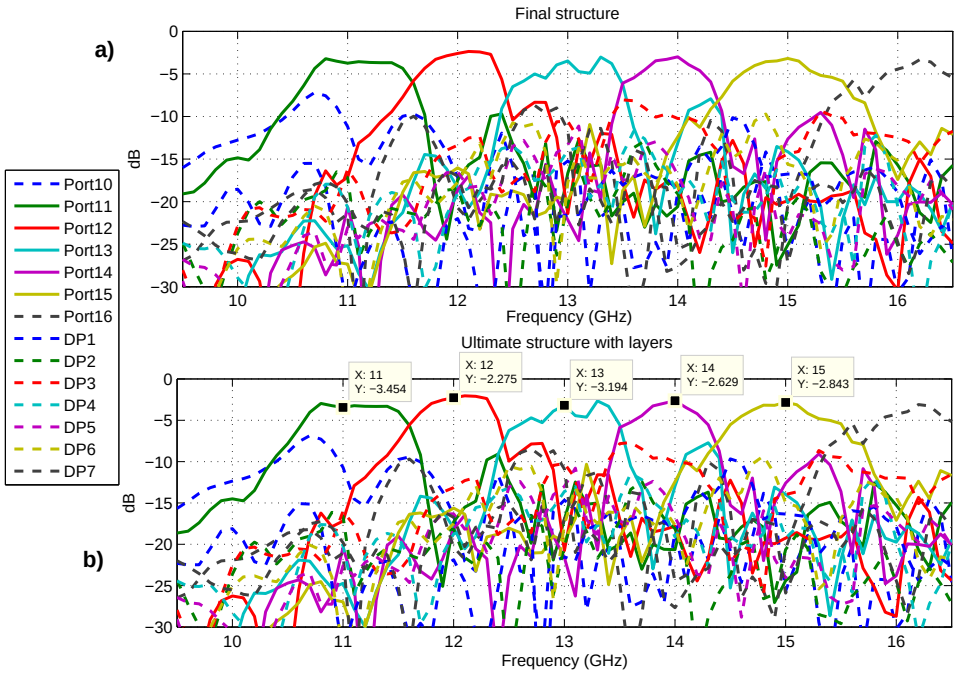

Figure 10.5: Final structure with losses and Ultimate structure S parameters.

As we expected, both figures are quite similar. This representation has been done with more resolution: 0.1GHz. With this resolution appears some falls in 13GHz's channel, but at least, at any point of any channel, within a bandwidth of 0.5GHz, we can ensure a value above -5dB.

Now we have the final design of the multiplexer, it is appropriate to represent the E-field for each frequency 10.6 .

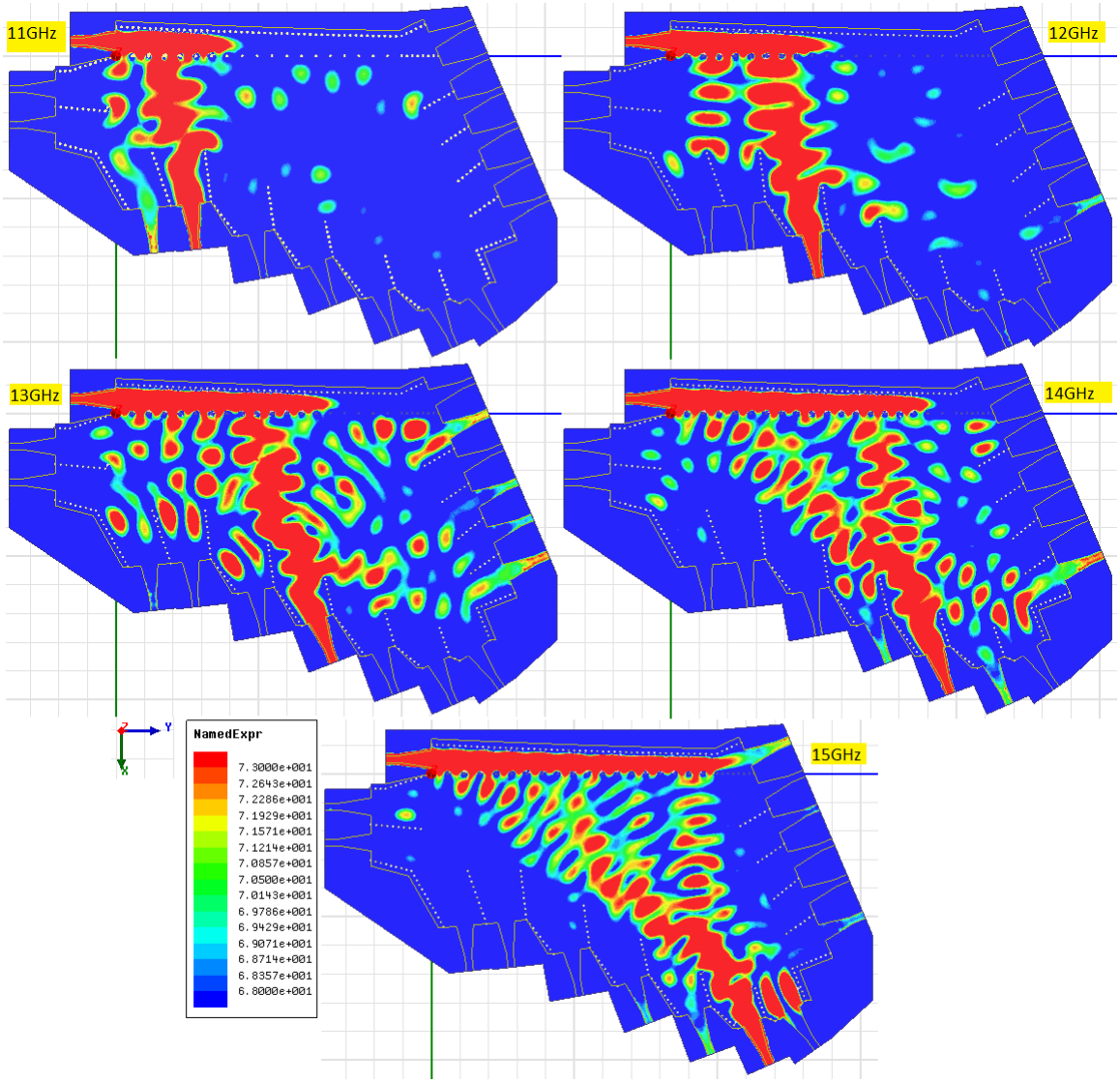

Figure 10.6: Layered structure: E-field for each frequency.

Other way to show the device's behaviour is the Real Poynting Vector representation 10.7 , and see the energy's direction with the aid of the arrows.

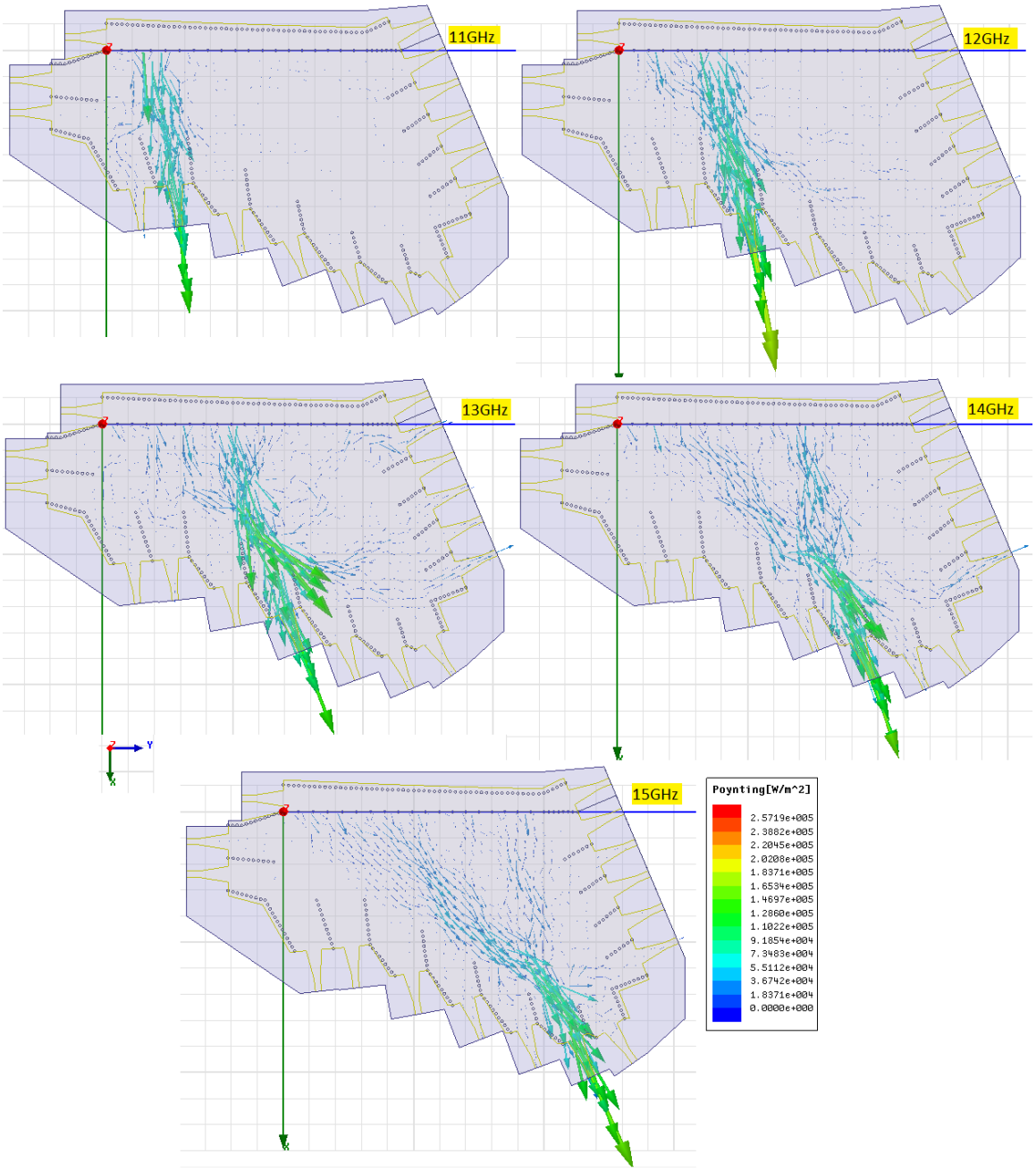

Figure 10.7: Layered structure: Real Poynting Vector for each frequency.

As the S parameters, E-field and Real Poynting Vector representations have shown, the required multiplexer's behaviour is achieved. For each frequency we have the well defined path to the desired output port.

To conclude the design of the multiplexer we can say that we have achieved our objectives: we have a manufacturable design of a space multiplexer based on Substrate-Integrated Waveguide antennas with five usable ports from 11GHz to 15GHz. We have achieved insertion losses less than 3.5dB (10.5) in the worst case for a minimum bandwidth of 0.5GHz approximately.

In the last chapter we'll see some techniques (for future works) to improve some quality parameters and obtain not only a manufacturable device but an attractive device for the industry.

Chapter 11

Conclusions and Future Lines

Our main objective was to reach to a manufacturable multiplexer built in a new technology as the Substrate Integrated Waveguide Antennas. And the steps to get this device have been:

- Get the desirable modulated leaky SIW with near-field focusing, with well defined focus.
- Define all the parameters of the antenna, useful to the design of the multiplexer.
- To familiarize with the concept we tried some ideas like using coaxial output ports (at the focus and aligned) and aligned SIW ports.
- Once the idea worked, we tried what we thought was the best option: SIW ports at each frequency's focus, but using PEC walls instead to simplify the design.
- Design the real ports in microstrip technology.
- Replace all the PEC walls by via-holes.
- Introduce losses to the device.
- Layering of the structure.

At the end, we have ensured the well performance of the device, with well defined channels for each frequency, ensuring for a 0.5GHz-bandwidth insertion losses below 3.5dB, and of course, ensuring all the SIW properties, as high Q factor, high power capacity, low cost, mass production, low weight.

But, as we said, the multiplexer needs some improvements to compete with other devices in the real market. We present here some ideas for future lines of work:

1 Develop the coaxial output ports idea.

2 Decrease the bandwidth using the ΔW_{5dB} parameter.

3 Decrease the bandwidth using the Scanning Ratio.

In chapter 4 we started to design the multiplexer with coaxial output ports (1). We tried two designs: locating ports in the focus and in a previously calculated line. The two options gave some initial good results, but in the E-field representation we saw energy passing through the ports due to the ports impossibility of taking such quantity of energy.

For this problem we saw two combined solutions. In the first place, we have to try to collect more energy, so a possible answer is to put some reflectors after the ports to redirect this energy again to them. But even with these reflectors, there will be energy wasted. So we will need some Dummy Ports to collect this wasted energy. These Dummys need to be coaxial ports to maintain rigour in the work. And, for the same reason we have to try to design the antenna's input and output ports in the coaxial technology.

This is the only open point in the project, but there are more open lines. As we know, we reached to a manufacturable design for the multiplexer. And this is a very interesting device because of its low insertion losses (S parameter for output ports above -5dB) and its well defined channels for each frequency mixed with all the advantages of the SIW technology named in chapter 2 . But there are other properties such as the bandwidth that makes our device weak against other multiplexers in other technologies. And if we want to make the multiplexer attractive for entities like the European Space Agency (ESA) we need to improve these points.

We can define the bandwidth for a SIW antenna as the following ratio:

$$BW(GHz) = \frac{\Delta W_{5dB}(mm)}{SR(mm/GHz)} \tag{11.1}$$

Where BW is the bandwidth, ΔW_{5dB} (2) is the 5dB-width of the beam and SR (3) is the antenna's scanning ratio. We can define ΔW_{5dB} from the focus distance and the antenna's length, as:

$$\Delta W_{5dB}(mm) = \lambda_0(mm)\frac{F(mm)}{L(mm)} \tag{11.2}$$

Where λ_0 is the wavelength, F is the focus distance from the antenna and L is antenna's length. If we increase L we decrease ΔW_{5dB}, therefore we will be increasing the antenna's resolution. Decreasing ΔW_{5dB} means, in (11.1), decreasing also the bandwidth. We obtain the same result decreasing the focus distance F.

Seeing (11.1), another way to decrease the bandwidth is increasing the Scanning Ratio SR. The Scanning Ratio (mm/GHz) depends on the angular-frequency-scanning sensitivity (deg/GHz) of the modulated SIW line. Higher scanning sensitivities would produce a higher change in the focus position for the same frequency increment, or alternatively, lower increment in the frequency for the same change in the focus location. The scanning sensitivity can be controlled in multiple ways. By simply choosing the SIW dielectric permittivity one can strongly control the scanning ratio as demonstrated in [14]. Also, the addition of high impedance surface (HIS)

sheets [15] can further increase the SR to reduce the filter BW. The use of meander lines can also increase the Scanning Ratio. Conversely, the SR can be decreased by means of novel passive [16], [17] or active [18] artificial transmission lines with reduced beam squint, so that the resulting BW could be notably increased. Therefore, by using frequency dispersion enginnering techniques, we can modify the scanning ratio of the SIW line to control the channels bandwidth.

Specifically for the ESA, some of the typical specifications are:

- Ku-band: 12-18GHz
- 6-12 channels (up to 20 channels)
- 36MHz bandwidth
- 40MHz separation
- Insertion losses in excess of 10dB are acceptable

For now, we only have 5 channels. But, during the project we saw how Port 16 works. We can perfectly treat it like other channel instead of a Dummy Port. But firstly, we need to redesign it to obtain its appropriate parameters. To obtain more channels we will need some other changes in the antenna, such as improving the Scanning Ratio obtaining more channels in the same space.

The bandwidth and separation required are quite difficult to achieve with the actual design. We are talking about values around 0.036GHz (bandwidth) and 0.04GHz (separation), and for now, we have values around 0.5GHz. We need, in other words, to reduce drastically the bandwidth (BW). So, we need to work with the mentioned equation (11.1) to achieve this demand.

The last point, the insertion losses required, are amply achieved. They require all channels above -10dB, and we have all of them already above -5dB.

So, to achieve all the required specifications we need to work more in the multiplexer's design, but with the achieved device we have obtained a new multiplexer in a new technology, with a lot of improvements over other technologies used to the date.

Bibliography

[1] Xu F., Wu K., *"Guided-Wave and leakage characteristics of Substrate Integrated Waveguide"* in *IEEE MTT-S Trans., vol. 53, no. 1, pp. 66-73*, 2005.

[2] Eleftheriades G.V., Siddiqui O.F., *"Negative refraction and focusing in hyperbolic transmission-line periodic grids"*, in *IEEE MTT-S Trans., vol. 53 no. 1, pp. 396-403*, 2005.

[3] Wong J.K.H., Balmain K.G., Eleftheriades G.V., *"A diplexer based on the spatial filtering property of planar anisotropic transmission-line metamaterials"*, in *IEEE ATSANM Trans.,pp. 241-244*, 2006.

[4] Momeni O., Afshari E., *"Electrical Prisms: a high quality factor filter for millimeter-wave and teraherz frequencies"*, in *IEEE MTT-S Trans., vol. 57 no. 11, pp. 2790-2799*, 2009.

[5] Martinez-Ros A.J., Gomez-Tornero J.L., Goussetis G., *"Planar leaky-wave antenna with flexible control of the complex propagation constant"*, in *IEEE Trans. Antennas Propag., vol. 60, no. 3, pp. 1625-1630*, Mar. 2012.

[6] Bozzi M., Xu F., Deslades D., *"Modeling and design considerations for substrate integrated waveguide circuits and components"*, in *TELSIKS, pp. VII-XVI*, 2007.

[7] Wu K., Deslades D., Cassivi Y., *"The substrate integrated circuits: a new concept for high-frequency electronics and optoelectronics"* in *TELSIKS, vol. 1, pp. III-X*, 2003.

[8] Gómez-Tornero J.L., Quesada-Pereira F., Álvarez-Melcón A., Goussetis G., Weilly Andrew R., Guo Y.J., *"Frequency steerable two dimensional focusing using rectilinear leaky-wave lenses"*, in *IEEE Trans. Antennas Propag., vol. 59, no.2, pp. 407-415*, Feb. 2011.

[9] A.J. Martínez-Ros, J.L. Gómez-Tornero, and F. Quesada-Pereira, *"Efficient analysis and design of novel SIW leaky-wave antenna"*, IEEE Antennas and Wireless Propagat. Lett., vol.12, pp.496-499, March 2013.

[10] Y.LI and E.Wolf, *"Focal shifts in diffracted converging spherical waves"*, Optics Communications, vol. 39, no. 4, 15 Oct. 1981.

[11] Martínez-Ros A.J., Gómez-Tornero J.L., *"Quasi-optical multiplexing using leaky-wave near-field focusing techniques in substrate integrated waveguide technology"*, in *Proc. of the IEEE Int. Microwave Symp.* (IMS), Seattle, WA, USA, June 2013, in press.

[12] Deslades D., *"Design equations for tapered microstrip-to-Substrate Integrated Waveguide Transitions"*, in *IEEE MTT-S Int.*, 2010.

[13] Deslades D., Wu K., *"Substrate Integrated Waveguide Leaky-Wave antenna: concept and design considerations"*, in *IEEE APMC2005 Proceedings*, 2005.

[14] A. Martinez-Ros, J. Gomez-Tornero, and G. Goussetisy, *"Frequency scanning leaky-wave antenna for positioning and identification of RFID tags"* in 2011 IEEE Int. Conf. on RFID-Technologies and Applications (RFID-TA), sept. 2011, pp. 451-456.

[15] M. Garcia-Vigueras, J. Gomez-Tornero, G. Goussetis, A. Weily, and Y. Guo, *"Enhancing frequency-scanning response of leaky-wave antennas using high-impedance surfaces"*, IEEE Antennas Wireless Propag. Lett., vol. 10, pp. 7-10, 2011.

[16] M. Antoniades and G. Eleftheriades, *"A CPS leaky-wave antenna with reduced beam squinting using NRI-TL metamaterials"*, IEEE Trans. Antennas Propag., vol. 56, no. 3, pp. 708-721, 2008.

[17] C. Caloz, S. Abielmona, H. Van Nguyen, and A. Rennings, *"Dual composite right/left-handed (D-CRLH) leaky-wave antenna with low beam squinting and tunable group velocity"*, Phys. Status Solidi B, vol.244, no. 4, pp. 1219-1226, 2007.

[18] D. Sievenpiper, *"Superluminal waveguides based on non-foster circuits for broadband leaky-wave antennas"*, IEEE Antennas Wireless Propag. Lett., vol. 10, pp. 231-234, 2011.